CHARACTERISATION AND RECOVERY OF METAL VALUES FROM SPENT LITHIUM-ION BATTERIES

by

MOHAMMAD AL HOSSAINI SHUVA

A thesis submitted in partial fulfillment of
the requirements for the award of

MASTER OF SCIENCE IN
MATERIALS AND METALLURGICAL ENGINEERING

Department of Materials and Metallurgical Engineering
BANGLADESH UNIVERSITY OF ENGINEERING AND TECHNOLOGY
Dhaka-1000, Bangladesh

January, 2013

CANDIDATE'S DECLARATION

This is to certify that the work presenceed in this thesis is original and this thesis or any part of it has not been submitted elsewhere for the award of any degree or diploma

MOHAMMAD AL HOSSAINI SHUVA

CERTIFICATE OF RESEARCH

This is to certify that the work presenceed in this thesis is carried out by the author under the supervision of Dr. ASW Kurny, Professor of the Department of Materials and Metallurgical Engineering, Bangladesh University of Engineering & Technology, Dhaka.

Dr. ASW KURNY

MOHAMMAD AL HOSSAINI SHUVA

This thesis titled "Characterisation and recovery of metal values from spent lithium-ion batteries.", submitted by Mohammad Al Hossaini Shuva, Student No. 1009112009, Session October 2009 has been accepted as satisfactory in partial fulfillment of the requirement for the degree of MASTER OF SCIENCE IN MATERIALS AND METALLURGICAL ENGINEERING on January 2013.

BOARD OF EXAMINERS

1. ---------- Chairman

Dr. ASW Kurny
Professor
Department of Materials and Metallurgical Engineering
Bangladesh University of Engineering & Technology
Dhaka-1000, Bangladesh.

2. ---------- Member
Dr. Md. Mohor Ali
Professor & Head
Department of Materials and Metallurgical Engineering
Bangladesh University of Engineering & Technology
Dhaka-1000, Bangladesh

3. ---------- Member
Dr. Md. Ahmed Sharif
Associate Professor
Department of Materials and Metallurgical Engineering
Bangladesh University of Engineering & Technology
Dhaka-1000, Bangladesh

4. ---------- Member
Dr. M. Abdul Gafur
Project Director
Development of Materials for Tools and Bio-metallic Implants
PP and PDC, BCSIR Laboratories, Dhaka-1205

ACKNOWLEDGEMENTS

Firstly, thanks to Allah for giving me the strength and patience, for completing this thesis work.

It was a long journey (starting in October, 2010) to finish the work. During this journey I got encouragement from a wide range of people. I want to express my utmost gratitude to my supervisor, Prof. Dr. ASW Kurny for his continuous support, invaluable advice, understanding and keeping faith on me. I was never set back in this work due to my supervisor's inspiration and appreciation.

This M.Sc thesis work could not be completed without the contribution from my parents, my brother and sister. They continuously encouraged me for getting the higher degree. Their mental support and advice helped me the most for finishing this thesis.

At this moment, I want to acknowledge the Director and the stuff members of Institute of Mining, Mineralogy and Metallurgy, BCSIR for their tremendous support in using different facilities of the institute and also, for their helpful attitude. The Analytical Chemistry department of BCSIR helped me with Atomic Absorption Spectroscopic analysis. I gratefully acknowledge their sincere cooperation.

I am especially indebted to Dr. Abdul Gafur, Project Director, "Development of Materials for Tools and Biometallic implant", PP & PDC, BCSIR. He had given me the freedom to use his lab and equipments anytime and on any days in the week. I found a great deal of inspiration, from his relentless hard working ability and remarkable personality.

I want to thank Mr. Md. Ashiqur Rahman, Sr. Lab Technician of "Chemical Analysis Lab, MME, BUET" for acquainting me with a wide range of equipments and helping me in time of need. I am also thankful to my research collegues in the "Minerals Processing Lab, MME, BUET", for their friendly attitude and helpful suggestions throughout the period of this work.

Dedicated to My Parents

ABSTRACT

Lithium ion batteries were characterized to identify the potential of recovering metal values from these batteries. Different component parts of spent batteries of two types (M 660 and V83) were examined. The outer casings were found to be of aluminum alloy. Aluminum , lithium , copper and cobalt consisted were 45.99 percent of the total weight of the spent batteries. The rest was electrolyte solvent, adhesive and other impurity elements. In cathode electrode, lithium and cobalt constituted 7.09 and 60.24 percent respectively. $LiCoO_2$ was the prominent phases in cathode of the spent batteries. Graphite was presence in anode of spent lithium ion battery. The proportion of aluminum in aluminum foil current conductor was determined by Atomic Absorption Spectroscopy (AAS). In the M 660 and V 83 batteries aluminum was found to be 98.90% and 98.66 % respectively and thickness of foil was 25µm. The proportion of copper in copper foil current conductor was determined by Chemical Analysis. In the M 660 and V83 LIB copper was found to be 99.06% and 98.86 % respectively and thickness of foil was 25µm

In order to determine the presence of lithium and cobalt, the active cathode with foil was leached in sulfuric acid. During leaching the process parameters were kept fixed at acid concentration = 2.5M, temperature = room temperature (due to exothermic reaction), solid-liquid ratio = 1: 30 (gm/ml), time=2-5 min, and percentage of hydrogen peroxide = 5. After completion of leaching the solution was filtered this will separate the aluminum foil. Then this leach out sample was analyzed in Flame Photometer (AFP) and UV- Spectroscopy (UVS) to determine the presence of lithium and cobalt. To analyze the lithium in AFP and cobalt in UVS we had to calibrate the machine with analytical reagent lithium carbonate and analytical reagent cobalt sulfate powder according to the standard procedure. With respect to that calibration curve the presence of lithium and cobalt of spent lithium ion battery was determined. The effect of process variables, such as concentration of sulfuric acid and hydrogen peroxide and solid/liquid ratio were studied to determine the optimum conditions for this purpose.

Leaching of the cathode paste was also carried out in hydrochloric acid media in presence of hydrogen peroxide as a reducing agent. Effect of process variables, such as concentration of hydrochloric acid and hydrogen peroxide, temperature, time and solid/liquid ratio were studied to determine the optimum conditions. It was found that the dissolution of $LiCoO_2$ increased with increasing temperature, concentration of HCl, time and solid/liquid ratio (S/L) ratio. Li and Co from $LiCoO_2$ were leached around 89% with addition of 3.5 Vol% of H_2O_2 as a reducing agent.

Kinetic parameters were established from the time versus dissolution curve using temperature as variable and keeping the other parameters fixed. Dissolution reached up to 81% for lithium and 79% for cobalt at 80^0C temperature within 40 minutes. Leaching behavior for both lithium and cobalt were found to follow the chemical reaction controlled process. Activation energy of lithium and cobalt were found to be 23.83KJ/mol and 27.72 KJ/mol respectively; which again justified the appropriateness of the model.

The recovery products lithium carbonate and cobalt hydroxide were got by chemical precipitation with 2M NaOH at P^H value 11-12. X-ray diffraction results ensure the presence of lithium carbonate and cobalt hydroxide in recovery product.

TABLE OF CONTENTS

CHAPTER 3: EXPERIMENTAL

CHAPTER 4: RESULTS AND DISCUSSIONS

NOMENCLATURE

Notation	Definition
XRD	X-ray Diffraction
AAS	Atomic Absorption spectroscopy
OES	Optical Emission Spectroscopy
k	Reaction rate constant
E	Activation energy
R	Universal gas constant
A	Pre-exponential factor
K	Kelvin, unit of temperature
X	Fraction of reacted particle
A	Arrhenius constant
Kc	Experimental rate constant
T	Temperature
t	Time

LIST OF TABLES

LIST OF FIGURES

Chapter 1

INTRODUCTION

1.1 Motivation behind this work

Use of high power lithium-containing batteries as electrochemical power sources in modern-life equipments is increasing rapidly [1]. In 2003, primary lithium batteries, and lithium-ion secondary rechargeable batteries (LIBs) constituted about 28% of the total rechargeable batteries used in the world [2]. Primary lithium batteries use metallic lithium as cathode and contain no toxic metals; however, there is possibility of fire if metallic lithium is exposed to moisture while the cells are corroding. Lithium ion secondary rechargeable batteries (LIBs), on the other hand, do not contain metallic lithium [2]. Most lithium-ion systems use a material like Li_XMA_2 at the positive electrode and graphite at the negative electrode. Some materials used at the cathode include $LiCoO_2$, $LiNiO_2$ and $LiMn_2O_4$. The electrolyte is an organic liquid with dissolved substances like $LiClO_4$, $LiBF_4$ and $LiPF_6$. LiBs consist of heavy metals, organic chemicals and plastics in the proportion of 5–20% cobalt, 5–10% nickel, 5–7% lithium, 15% organic chemicals and 7%plastics. It is estimated that 200–500 MT of LiBs are discarded each year [3].

Recycling of LIBs has become important because their disposal may become a serious problem due to the presence of flammable and toxic elements or compounds in these batteries. At the same time, some economic benefits could be achieved through the recovery of major components from LIBs [4]. There are two problems to be solved; disposal of harmful waste and prevention of explosion during recycling of LIB waste. Since spent LIBs represent a valuable waste material for the recovery of metals present (Co, Li, Mn and Ni) or their compounds, recycling of spent batteries may result in economic benefits. A number of processes have been developed on the recycling technologies of LIBs, most of them, however, are still in pilot plant or laboratory scale [5]. Most of the proposed processes are based on hydrometallurgy chemistry [5, 6].

For hydrometallurgical recycling of spent lithium-ion batteries, the spent LIBs are subjected to some such of pre-treatment processes as skinning, removing of crust, crushing, sieving and separation of materials in order to separate the cathode materials from other materials. The separated cathode material is then used to recover cobalt and other metals through a series of chemical processes [7]. Early attempts for the recovery of metal values from the spent lithium ion battery concentrated on the

hydrometallurgy processes [6]. Leaching in various acidic and alkaline media and leaching in presence of hydrogen per oxide has been tried to extract lithium and cobalt from the spent batteries. Solvent extraction with D2EHPA and Cyanex 272 for the separation of lithium from cobalt in leach liquor has also been attempted [4]. Recycling rates for commonly used materials are growing in many industrial countries. In Bangladesh no work on the recovery of metal values from spent lithium ion batteries has so far been reported.

1.2 Outline of this thesis:

The primary aim of this work is to determine the quantity and the nature of metallic values contained in LIBs and to determine the optimum conditions for the extraction of metal values from these batteries. The successful completion of the work will help to reduce our dependence on the import of two useful metals or compound of lithium and cobalt and at the same time, help to reduce environmental pollution.

The academic interest of the work includes the study of the mechanism and kinetics of the various steps (leaching, chemical precipitation, etc) involved in the process of recovery of metal values from spent lithium ion batteries. The outline of this work is discussed below:

- Spent lithium ion batteries were collected from local scrap dealers and other sources. Different types of lithium ion batteries were collected and sorted.
- The spent batteries were dismantled for the physical identification and separation of the different component parts. The weight proportions of the different components were also determined.
- The phases present in spent lithium ion batteries were identified by x-ray diffraction analysis and the chemical composition of the different component parts were determined by OES, AAS, and conventional methods of wet chemical analysis.
- Leaching was carried out in sulfuric acid and hydrochloric acid. Hydrogen per oxide was used in both acids as reducing agent. The insoluble impurities were separated by filtration. The filtered solution was used for further investigation.
- The effects of process parameters like acid concentration; solid-liquid ratio, time and temperature, etc on the kinetics of leaching were investigated to determine the optimum condition of leaching.

- Cobalt was separated from the leach liquor as cobalt hydroxide by chemical precipitation techniques. The effects pH was investigated to determine the optimum condition for precipitation with addition of sodium hydroxide.
- The percentage of the extracted metal was determined by UV visible spectroscopy, atomic absorption spectroscopy and flame photometry.
- Lithium was separated from the leach liquor as lithium carbonate (Li_2CO3).

Chapter 2

LITERATURE REVIEW

2.0. The Battery

A battery is a device that converts the chemical energy contained in its active materials directly into electric energy by means of an electrochemical oxidation-reduction (redox) reaction. In the case of a rechargeable system, the battery is recharged by a reversal of the process [8]. While the term ‘‘battery’’ is often used, the basic electrochemical unit being referred to is the ‘‘cell.’’ The cell consists of three major components:

1. **The anode or negative electrode** — which gives up electrons to the external circuit and is oxidized during the electrochemical reaction.
2. **The cathode or positive electrode** — which accepts electrons from the external circuit and is reduced during the electrochemical reaction.
3. **The electrolyte**—the ionic conductor—which provides the medium for transfer of charge, as ions, inside the cell between the anode and cathode. The electrolyte is typically a liquid, such as water or other solvents, with dissolved salts, acids, or alkalis to impart ionic conductivity. Some batteries use solid electrolytes which are ionic conductors at the operating temperature of the cell

2.1. Classification of Batteries

Batteries can be classified into two broad sections, namely primary and secondary batteries depending on the recharging ability. Reserve battery and fuel cells are other classifications whose does not strictly limit to the primary and secondary batteries. All of these classifications are briefly described below. Depending on the nature of electrolyte, batteries can also be classified as wet cell and dry cell. Present day batteries are mostly dry cell types. The classification of batteries is shown at Table 2.1.

Table 2.1: Battery classification overview

Batteries			
Primary Batteries	**Secondary Batteries**		
Zinc-carbon	Lead acid automobile	**Reserve batteries**	**Fuel cell**
Alkaline	Non automobile lead-based		
Zinc-air	Lithium		
Silver oxide	Nickel Cadmium		
Etc.	Nickel Metal Hydride		
	Nickel Zinc etc.		

2.1.1. Primary batteries

Primary batteries irreversibly (within limits of practicality) transform chemical energy to electrical energy. When the initial supply of reactants is exhausted, energy cannot be readily restored to the battery by electrical means. Hence, primary batteries are not rechargeable and come gradually to the spent condition with time of use. Even if never taken out of the original package, primary (or “disposable") batteries can lose 8 to 20 percent of their original charge every year at a temperature of about 20°–30°C. This is known as the "self discharge" rate and is due to non-current-producing "side" chemical reactions, which occur within the cell even if no load is applied to it. The rate of the side reactions is reduced if the batteries are stored at low temperature, although some batteries can be damaged by freezing. High or low temperatures may reduce battery performance [8]. Different types of primary batteries are available of which zinc-carbon dry cell batteries are the most prominent. Alkaline zinc-carbon batteries however are currently replacing the old zinc-carbon type in many countries due to their higher life time and energy density. Common types of primary batteries are discussed here.

2.1.1.1. Zinc carbon batteries

Zinc carbon batteries are packaged in zinc can that serves as both a container and anode. Zinc carbon batteries are the least expensive batteries and thus a popular choice by manufacturers when devices are sold with batteries included. Nowadays the primary electrolyte in zinc carbon type battery is $ZnCl_2$ with a small amount of NH_4Cl. They can be used in remote controls, flashlights, toys, or transistor radios.

2.1.1.2. Alkaline batteries

Alkaline batteries are a type of power cell dependent upon the reaction between zinc and manganese dioxide (Zn/MnO2). Alkaline batteries have a higher energy density and longer shelf-life compare to the carbon zinc batteries. The primary electrolyte in alkaline batteries is KOH and this electrolyte type differentiates the primary and alkaline batteries. These batteries can be used in cassettes players, radios, or other appliances.

2.1.1.3. Zinc-air batteries

Zinc-air batteries are electro-chemical batteries powered by the oxidation of zinc with oxygen from the air. These batteries have high energy densities and are relatively inexpensive to produce. They are used in hearing aids and in experimental electric vehicles. These batteries may become an important contributor in the future high energy and long cycle battery designs.

2.1.1.4. Silver oxide batteries

Silver oxide batteries have a long life and very high energy/weight ratio, but a prohibitive cost for most applications due to the high price of silver. They are available in either very small sizes as button cells where the amount of silver used is small, or in large custom design batteries where the superior performance characteristics of the silver oxide chemistry outweigh cost considerations.

2.1.2. Secondary Batteries

Secondary batteries can be recharged; that is, they can have their chemical reactions reversed by supplying electrical energy to the cell, restoring their original composition. Rechargeable batteries, especially nickel-based batteries self-discharge more rapidly than primary batteries. A freshly charged Ni-Cd battery loses 10% of its charge in the first 24 hours, and thereafter discharges at a rate of about 10% a month. However, modern lithium ion battery designs have reduced the self-discharge rate to a relatively low level (but still high compared to the primary

batteries) [8]. Lithium ion batteries are now dominant in the mobile industry. Lead acid heavy duty batteries are very commonly used in transportation. Other batteries of rechargeable types are generally Nickel-cadmium (Ni-Cd) battery, Nickel-metal-hydride (Ni-MH) battery, Nickel-zinc (Ni-Zn) battery etc.

2.1.2.1. Lead-acid automobile batteries

Lead-Acid automobile batteries are types of rechargeable batteries usually used on the automobiles. Lead acid batteries are rechargeable batteries made of lead plates situated in a 'bath' of sulfuric acid within a plastic casing. Almost ninety percent of the lead acid batteries are recycled.

2.1.2.2. Non-automotive lead-based batteries

Gel cells and sealed lead-acid batteries are commonly used to power industrial equipment, emergency lighting, and alarm systems. The same recycling process applies as with automotive batteries. An automotive store or a local waste agency may accept the batteries for recycling.

2.1.2.3. Lithium batteries

In these types, lithium ions move from the negative electrode to the positive electrode during discharge and back when charging. During discharge, lithium ions Li^+ carry the current from the negative to the positive electrode, through the non-aqueous electrolyte and separator diaphragm. Lithium metal or lithium compounds are used as an anode in lithium batteries. Depending on the design and chemical compounds used, lithium cells can produce voltages from 1.5 V to about 3 V, twice the voltage of an ordinary zinc-carbon battery or alkaline cell. Lithium batteries are used in many portable consumer electronic devices, and are widely used in industry [8].

2.1.2.4. Nickel-cadmium batteries

The nickel-cadmium battery (commonly abbreviated NiCd) is a type of rechargeable battery using nickel oxyhydroxide and metallic cadmium as electrodes. However, due to the hazardous element cadmium, the uses of these batteries are banned in many countries and lithium ion batteries are currently replacing this type.

2.1.2.5. Nickel-metal-hydride batteries

The rechargeable sealed nickel-metal hydride battery is a relatively new technology with characteristics similar to those of the sealed nickel-cadmium battery. The principal difference is

that the nickel-metal hydride battery uses hydrogen, absorbed in a metal alloy, for the active negative material in place of the cadmium used in the nickel-cadmium battery [9]. A NiMH battery can have two to three times the capacity of an equivalent size nickel-cadmium battery. These batteries are used in electric vehicles, consumer electronics etc.

2.1.2.6. Nickel-zinc batteries

The nickel-zinc battery system uses the nickel/nickel oxide electrode (also known as the nickel-hydroxide/nickel oxyhydroxide electrode) as the positive and the zinc/zinc oxide electrode as the negative. This kind of batteries may be used in cordless power tools, cordless telephone, digital cameras, battery operated lawn and garden tools, professional photography, electric bike, and light electric vehicle sectors.

2.1.3. Reserve batteries

Also called deferred-action batteries, reserve batteries are special purpose primary batteries usually designed for emergency use. The electrolyte is usually stored separately from the electrodes which remain in a dry inactive state. The battery is only activated when it is actually needed by introducing the electrolyte into the active cell area. This has the double benefit of avoiding deterioration of the active materials during storage and at the same time it eliminates the loss of capacity due to self discharge until the battery is called into use. They can thus be stored for 10 years or more yet provide full power in an instant when it is required. The reserve batteries can be classified by the type of activating medium or mechanism that is involved in the activation [8].

Water-activated batteries: Activation by fresh- or seawater.

Electrolyte-activated batteries: Activation by the complete electrolyte or with the electrolyte solvent. The electrolyte solute is contained in or formed in the cell.

Gas-activated batteries: Activation by introducing a gas into the cell. The gas can be either the active cathode material or part of the electrolyte.

Heat-activated batteries: A solid salt electrolyte is heated to the molten condition and becomes ionically conductive, thus activating the cell. These are known as thermal batteries.

These batteries are used, for example, to deliver high power for relatively short periods of time, in missiles, torpedoes, projectiles and bomb fuses, and various weapon systems.

2.1.4. Fuel Cell

A fuel cell is a device that converts the chemical energy of a fuel (hydrogen, natural gas, methanol, gasoline, etc.) and an oxidant (air or oxygen) into electricity. In principle, a fuel cell operates like a battery. Unlike a battery however, a fuel cell does not run down or require recharging. It will produce electricity and heat as long as fuel and an oxidizer are supplied.
Fuel cell construction generally consists of a fuel electrode (anode) and an oxidant electrode (cathode) separated by an ion-conducting membrane. Oxygen passes over one electrode and hydrogen over the other, generating electricity, water and heat. Fuel cells chemically combine the molecules of a fuel and oxidizer without burning or having to dispense with the inefficiencies and pollution of traditional combustion [8].

2.2. Concept of the Secondary Lithium Ion Battery

Primary lithium ion batteries became commercial goods in 1970. They are, however, not rechargeable. In 1978, intercalating materials were introduced by Murphy et al [10]. They found that Li-ions could migrate into/out from $LiWO_4$ structure via intercalation/de-intercalation reactions. Intercalation and de-intercalation are considered as a guest material enters and leaves a host material without ruining the structure of host. For example, it is just similar to make water enter into and leave out a sponge by squeezing it, while the main structure of the sponge is not destroyed. As shown in Fig. 2.1 defined intercalation as LiyMnYm +AzBw → Li(y-x)MnYm + LixAzBw [11,12]. The idea of rocking chair for rechargeable batteries was proposed in associated papers and patents published and agreed during 1980~1984 [10,12,13].

Until 1990, the first rechargeable lithium cell with components of $LixC_6/LiClO_4$ in PC/EC/ $Li(1+x)CoO_2$ or $Li(1+x)YO_2$ (Y = Ni or Mn) to adopt the principle was made. The secondary lithium cells, consisting of $LiCoO_2$ as a cathode (positive electrode) and carbon as an anode (negative electrode), show good cycling performance and high energy density. They have been used as the major power sources for portable electric devices.

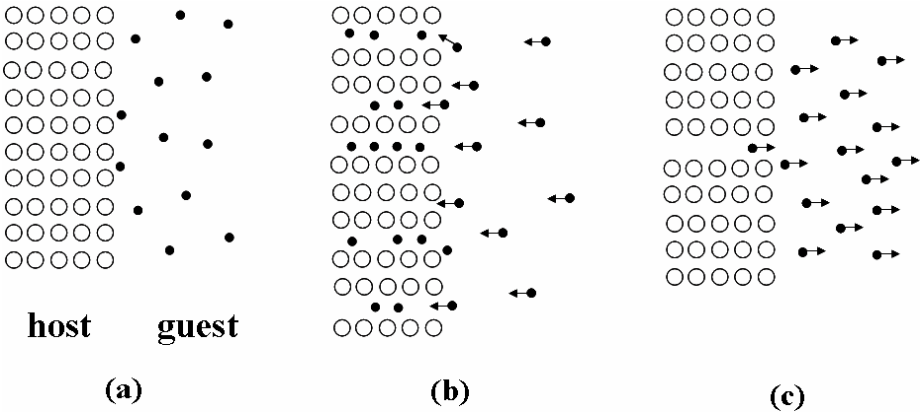

Fig. 2.1: Illustration of the intercalation reaction: (a) no reaction, (b) intercalation, (c) extraction reaction [11].

2.2.1. Cathode Materials

In recent years, tremendous researches have been done to find alternative cathode materials to replace $LiCoO_2$ for its high cost and limited availability. A lot of efforts have also been made to improve the electrochemical characteristics of the cathode materials, such as $LiCoO_2$ [14], $LiMn_2O_4$ [14], $LiNiO_2$ [15], LiNi1-x-yMxM'yO_2 [16], $LiFePO_4$ [17].

2.2.1.1. $LiCoO_2$ Cathode Material

Yoshio et al indicated that at present $LiCoO_2$ was the most commonly used cathode material for commercial rechargeable lithium ion batteries due to its easy preparation, high voltage (~ 3.9V), good reversibility (upon 500th), and high theoretical capacity (about 280 mah/g) [18]. $LiCoO_2$ is layered structure in which the Li^+ and Co^{3+} ions occupy alternating (1 1 1) layers of octahedral sites in a rock-salt structure. The typical reversible limit of delithiation for $LixCoO_2$ in commercial batteries is x = 0.5 at a voltage plateau of 3.8V [14], which corresponds to a discharge capacity of about 140 mah/g. However, layered $LiCoO_2$ often suffers from structure instability and safety programs. The charging reaction is [19]:

$$LiCoO2 \rightleftharpoons Li\ (1-x)CoO2 + xLi+ + xe- \qquad (2.1)$$

The delithiated phase of LiCoO2 contains Co(IV), a strong oxidant which can give a highly exothermic reaction upon contact with the electrolyte solvent. Caballero et al. , Kobayashi et al. and Ceder et al. used various strategies to avoid this drawback, like replacing cobalt with another transition metal [20, 21, 22].

2.2.1.2. $LiMn_2O_4$ Cathode Material

Wu et al. indicated that $LiMn_2O_4$ had the theoretical capacity about 147 mah/g, and the practical specific capacity is about 120 mah/g [23]. It means that almost about 80% of Li-ion can be d-intercalated from $LiMn_2O_4$. The $LiMn_2O_4$ material has many advantages including low material costs, low toxicity, high cell voltage and easy synthesis. However, it suffers two main issues: one is the poor cycle life induced by the John-Teller distortion as it is reduced into $LiMn_2O_4$, and the other is the Mn^{2+} ion dissolution into the electrolyte after cycling.

2.2.1.3. $LiMnO_2$ Cathode Material

$LiMnO_2$ may exist in the same layered structure as $LiCoO_2$ exists in orthorhombic phase. The o-$LiMnO_2$ has the high theoretical capacity of 285 mah/g based on the Mn^{3+}/Mn^{4+} redox couple, and Mn is cheaper and has lower toxicity than Ni and Co. It can be synthesized by a conventional solid state reaction methods, sol-gel, Pechini, ion-exchange, or hydrothermal methods [24]. Vitins and West indicated that $LiMnO_2$ was not thermodynamically stable as a layered structure, but as an orthorhombic phase of o-$LiMnO_2$ [25]. However, both the layered and orthorhombic $LiMnO_2$ were observed to undergo a detrimental phase transformation into a spinel-like phase through minor atomic rearrangements during the first removal and subsequent cycling of Li, leading to eventual degradation of electrode performance.

2.2.1.4. $LiNiO_2$ Cathode Material

Layered structure LiNiO2 cathode material was developed by Moli Energy Co. in 1990 in Canada after Sony introduced the $LiCoO_2$ cathode material [26]. Song et al. (2004) indicated that LiNiO2 with moderate cost and specific capacity of 190 mah/g was thought to be a good candidate for the cathode material of lithium ion batteries, but synthesized a pure compound was complex and difficult [27]. The ideal structure of $LiNiO_2$ is layered, the same structure as $LiCoO_2$, however, the Li-Ni-O system is characterized by existence of a Li1-xNi1+xO_2 ($0<x<1$) solid solution. At low x values ($0<x<0.2$), the presence of Ni2+ cation in the Li layers is found in the structure [28]. This result makes the preparation of $LiNiO_2$ powders without cation mixing be difficult.

2.3. Lithium Ion Secondary Battery of Recycling Processes

Xu et al. indicated that metallic scraps could be subject to different recycling processes, including the basic two classes of recycling processes: physical processes and chemical processes [2]. The principal flow-sheet shown in Fig. 2.2 was mainly adopted in

hydrometallurgical recycling processes of spent lithium-ion batteries. Firstly, the spent lithium ion secondary battery should be subjected to some types of physical processes as pre-treatment processes such as skinning, removing of crust, crushing, sieving and separation of materials in order to separate the cathode materials from other materials. Secondly, the separated cathode materials will be used to recovered cobalt and other metals through a series of chemical processes.

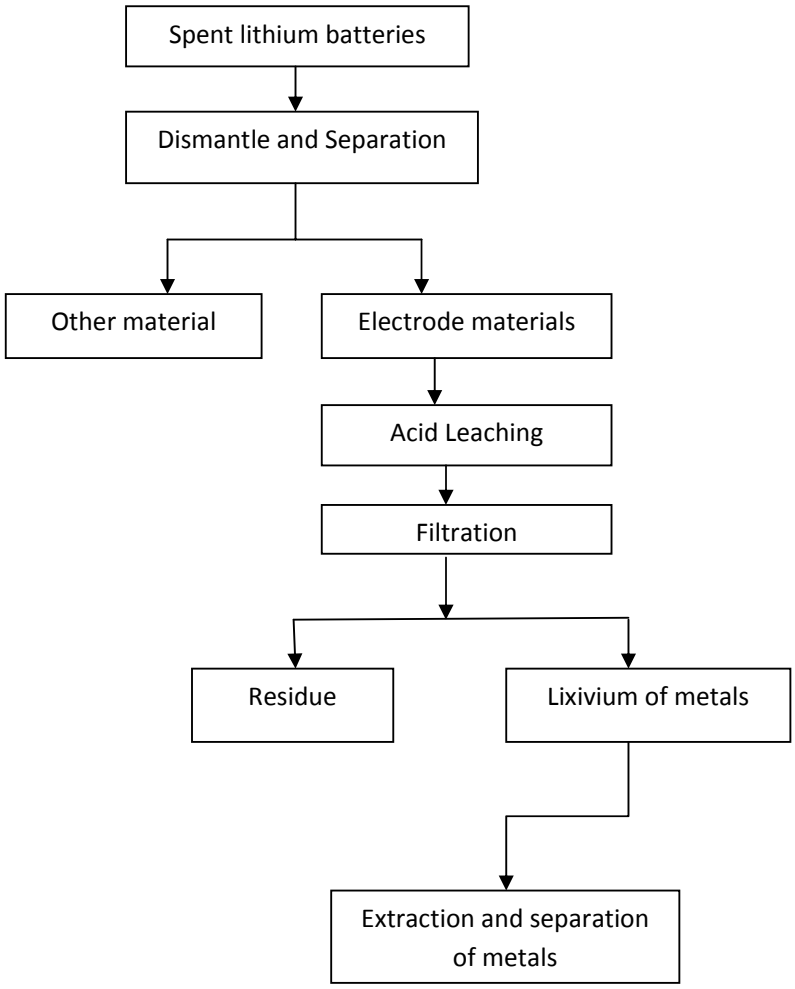

Fig.2.2: Flow sheet of the hydrometallurgical recycle process route of lithium ion rechargeable battery

Safety precautions should be taken and be emphasized when lithium ion secondary batteries are manually dismantled [1]. First, the plastic cases of the batteries were removed using a small knife and a screwdriver. Second, in order to remove the metallic shell that covered the battery, it was immersed into liquid nitrogen for 4 min and fixed in a lathe. Such a cryogenic method was adopted for safety precautions. Third, the metallic shell was then cut using a saw;

the ends of the metallic shell were removed firstly and a longitudinal cut was done aiming to access the internal material of the battery which was removed using pliers. Fourth, anode and cathode were uncurled manually, separated and dried for 24 h at 60^{o}C. All steps in the experimental procedure were carried out using glasses, gloves and gas masks for safe operation.

2.3.1. Physical Processes

Tenorio et al. noted that among the physical processes for recycling spent lithium ion secondary battery, mechanical separation techniques intend to separate materials according to different properties like density, conductivity, magnetic behavior, etc [29]. Thermal processes are usually associated with the production of steel, ferromanganese alloys or other metallic alloys. Mechanochemical (MC) process is to use a grinding technique that makes the crystal structure of the $LiCoO_2$, the positive electrode in the lithium ion secondary battery, into disordered system, enabling useful substances such as Co and Li easily extracted by acid leaching at room temperature from the lithium ion secondary battery scraps wastes. Dissolution process is to use special organic reagents to dissolve the adhesive substance (PVDF), which adheres the anode and cathode electrodes, and therefore this process can make $LiCoO_2$ get separated from their support substrate easily and recovered effectively [6].

2.3.1.1. Mechanical Separation Processes

Mechanical separation processes are usually applied as a pretreatment to treat the outer cases and shells and to concentrate the metallic fraction, which will be conducted to a hydrometallurgical or a pyrometallurgical recycling process in recycling of spent lithium ion secondary battery.

Shin et al. presented a process for the recovery of metal from spent lithium ion secondary battery for possible application to a commercial scale plant, including mechanical separation of lithium cobalt oxide particles and a hydrometallurgical procedure for lithium and cobalt recovery [4]. The experimental procedure is illustrated in Fig. 2.3. A series of mechanical processes involving crushing, sieving, magnetic separation, fine crushing and classification were carried out to yield enriched particles of lithium cobalt oxide in sequence. Two stages of crushing and sieving resulted in satisfactory separation of the metal bearing particles from the waste. A magnetic separator was used to remove pieces of steel casing. In order to eliminate small pieces of aluminum foil attaching to the particles of lithium cobalt oxide, a fine crushing was followed. The reason why mechanical separation is emphasized before the metal leaching

process here is that it improves the recovery efficiency of target metals and eliminates the need for a purification process of the leachate.

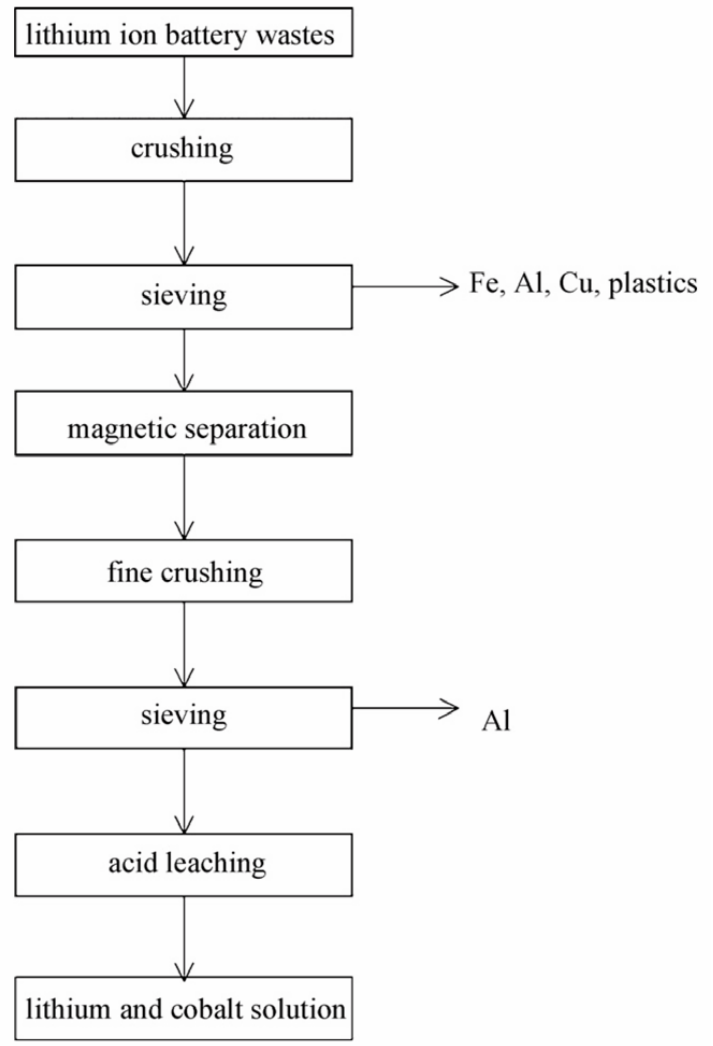

Fig. 2.3. Flow sheet of the metal recovery process [4].

Because PVDF binder does not dissolve in acid solution, it remains in the cake after filtration. Also, carbon does not dissolve in acid solution, and instead it floats on the solution; from filtration it is separated in the cake. The electrolyte lithium exafluorophosphate ($LiPF_6$) decomposes into lithium fluoride and phosphor pentafluoride in the crushing process, and the lithium dissolves in the acid solution during leaching. The organic solvents, propylene carbonate (PC) and diethyl carbonate (DEC) were evaporated in the crushing process.

2.3.1.2 Thermal Treatment

Lee and Rhee applied a recycling process involving mechanical, thermal, hydrometallurgical and sol–gel steps to recover cobalt and lithium from spent lithium ion secondary battery and to synthesize $LiCoO_2$ from leach liquor as cathode active materials [30]. Electrode materials containing lithium and cobalt can be concentrated with a two-step thermal treatment. First, lithium ion secondary battery samples were thermally treated in a muffle furnace at 100-150^oC for 1 h. The samples were disassembled with a high-speed shredder. Second, a two step thermal treatment was performed in a furnace, and electrode materials were liberated from the current-collectors by a vibrating screening. Next, the cathode active material, $LiCoO_2$, was obtained by burning off carbon and binder in the temperature range 500-900^oC for 0.5-2 h. Third, after $LiCoO_2$ in a nitric acid solution was leached in a reactor, the gel was placed inside a stainless steel crucible and calcined into powder in air for 2 h in the temperature range 500–1000^oC.

Castillo et al. reported that the solid residue coming from the operational step of the dilute HNO_3 acid leaching of spent lithium ion secondary battery and consisting of iron, cobalt and nickel hydroxides mixture and some traces of $Mn(OH)_3$, were introduced into a muffle furnace at 500^oC and held there for 2 h to eliminate carbon and organic compounds [31].

The alloy can then directly undergo beneficiation in metallurgical applications.

2.3.1.3. Mechanochemical Process

Zhang et al. reported that room temperature extraction of valuable substances from $LiCo0.2Ni0.8O_2$ scrap containing the PVDF has been carried out using 1N HNO_3 solution after mechanochemical treatment by a planetary mill with and without Al_2O_3 powder [19]. Crystalline $LiCo0.2Ni0.8O_2$ in the scrap was pulverized and became amorphous by mechanochemical treatment for 60 and 240 min, respectively, with and without Al_2O_3 power. This shows that the addition of Al_2O_3 is very effective for mechanochemical treatment. Accordingly, Co as well as Ni and Li were extracted at a high yield of more than 90% from the amorphous scrap sample. About 1% of fluorine in PVDF was dissolved in the filtrate when the Al_2O_3 powder was added to the scrap during the mechanochemical treatment, while no fluorine was detected in the filtrate obtained from the ground scrap sample without Al_2O_3 powder.

Saeki et al. developed an effective process for recovering Co and Li from lithium ion secondary battery wastes by using mechanochemical method [32]. The process consists of co-grinding $LiCoO_2$ with polyvinyl chloride (PVC) in planetary ball mill in air to form Li and Co chlorides, and subsequent leaching with water of the ground product, to extract Co and Li. In the grinding stage, mechanochemical reaction between $LiCoO_2$ and PVC takes place to form chlorides which are soluble in water. Therefore, grinding stage is important to improve the yield. PVC plays an important role as a chloride source for the mechanochemical reaction. The grinding facilitates mechanochemical reaction, and the extraction yields of both Co and Li are improved as the grinding progresses. The 30 min grinding makes the recoveries of Co and Li to reach over 90% and nearly 100%, respectively. Accordingly, about 90% of chlorine in the PVC sample has been transformed into the inorganic chlorides by the time. The concept of this process is to recycle useful materials from the both wastes of battery and PVC.

2.3.1.4. Dissolution Process

Contestabile et al. presented a laboratory-scale spent lithium ion secondary battery recycling process without the separation of anode and cathode electrodes [5]. The battery rolls were treated with N-methylpyrrolidone (NMP) at 100^{o}C for 1 h and $LiCoO_2$ was effectively separated from their support substrate and recovered. The recovery of both copper and aluminum in their metallic form was also achieved. Although this process was very convenient, the recovery effects of $LiCoO_2$ were demonstrated to be influenced by the used adhesive agent and rolling method of electrodes.

Xu et al. reported that this process has the advantage of making $LiCoO_2$ get separated from their support substrate and recovered easily, and therefore this process greatly simplifies the separation procedures of cobalt and aluminum [2]. It still has the disadvantage that the solvent for dissolving PVDF, N-methylpyrrolidone (NMP), is too expensive and consequently is not very suitable for scale up operation.

The further work to do in this respect is to develop much cheaper solvent and make it recycled and reused in order that this treatment cost could be decreased.

2.3.2. Chemical Processes

Chemical processes are connected to leaching steps in acid or alkaline medium and purification processes i order to dissolve the metallic fraction and to recover metal solutions that could be used by the chemical industry. Recycling through chemical processes basically

consists of acid leaching or base leaching, chemical precipitation, filtration, extraction or other processes.

2.3.2.1. Acid Leaching

The dust, which has been separated from plastic, iron scraps and paper residues in the sorting and dismantling preliminary treatment step, is leached by an acidic solution in order to transfer the metals of interest from it to the aqueous liquor.

The leaching of $LiCoO_2$ from spent lithium ion secondary battery is usually carried out by using inorganic acids such as H_2SO_4 [33], HCl [5] and HNO_3 [3] as leaching agents.

Zhang et al. studied the leaching of $LiCoO_2$ by the use of H_2SO_3, $NH_4OH{\cdot}HCl$ and HCl as leaching agents [19]. The experimental results are shown in Table 2.2. The experimental results indicated that the leaching efficiency of Co is highest in hydrochloric acid among these three leaching agents and higher the temperature, higher the leaching efficiency of Co.

Mantuano et al. and Lee and Rhee studied the leaching of $LiCoO_2$ by the use of H_2SO_4 and HNO_3 to substitute HCl with the addition of hydrogen peroxide as a reducing agent respectively [33,3].

Lee and Rhee indicated that in the process of reductive leaching with the addition of hydrogen peroxide as a reducing agent, the leaching efficiency increased by 45% for Co and 10% for Li compared with that in only nitric acid leaching [3]. This behavior seems to be due to the reduction of Co^{3+} to Co^{2+}, which is readily dissolved. The leaching efficiency of Co and Li increased with increasing HNO_3 concentration, temperature, and hydrogen peroxide concentration and with decreasing S/L ratio. An effective condition for the leaching would be 1M HNO_3, 10-20 g/L initial S/L ratio, 75^{o}C, and 1.7 vol.% H_2O_2 addition.

Table 2. 2. Effect of solid-to-liquid ratio (S:L) on leaching of cobalt and lithium with various leachants [19]

Leachant	S:L (g: ml)	Leach efficiency (%)	
		Co	Li
6% H_2SO_3	1:200	84.5	81.1
6% H_2SO_3	1:150	69.3	61.9
6% H_2SO_3	1:100	65.2	62.6
6% H_2SO_3	1:50	33.3	29.7
1 M $NH_2OH.HCl$	1:100	95.6	92.7
1 M $NH_2OH.HCl$	1:50	89.3	92.2
1 M $NH_2OH.HCl$	1:25	76.4	74.8
1 M $NH_2OH.HCl$	1:12.5	46.4	38.8
4 M HCl	1:100	89.9	92.8
4 M HCl	1:60	89.8	92.7
4 M HCl	1:40	88.2	92.7
4 M HCl	1:20	90.6	93.1

2.3.2.2. Bioleaching

It has been reported that bio-hydrometallurgical processes have been gradually replacing the hydrometallurgical one due to their higher efficiency, lower costs and few industrial requirements [34]. Bio-hydrometallurgical processing of solid waste is similar to natural biogeochemical metal cycles and reduces the demand of resources, such as ores, energy and landfill space [35].

The study of Mishra et al. was carried out on bioleaching method for the extraction of cobalt and lithium from spent lithium ion secondary batteries containing LiCoO2, using chemolithotrophic and acidophilic bacteria, acidithiobacillus ferrooxidans, which utilized and ferric ion in the leaching medium.

The current technologies of bio-hydrometallurgical processes have not gotten mature in their applications for recycling lithium-ion secondary batteries and are still in the research stage until now [2].

2.3.2.3. Solvent Extraction

Such extractants as di-(2-ethylhexyl) phosphoric acid (D2EHPA),Trioctylamine (TOA), diethylhexyl phosphoric acid (DEHPA) or 2-ethylhexyl phosphonic acid mono-2-ethylhexyl ester (PC-88A) were usually used as extractants to separate the metals in some hydrometallurgical process, in which Co, Li and Cu are usually recovered from spent lithium ion secondary batteries [19,30].

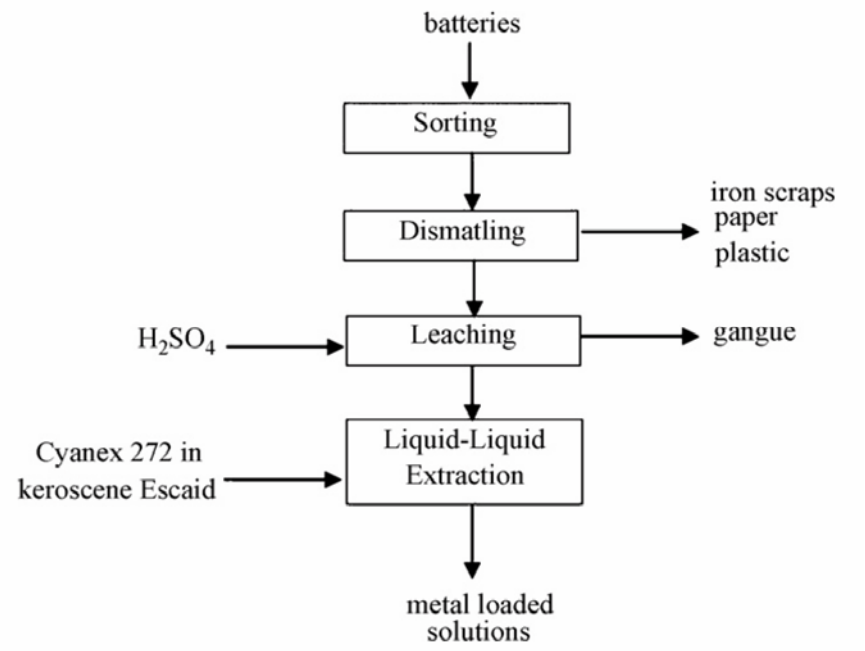

Fig.2.4: Scheme of the hydrometallurgical route evaluated in this paper to treat NiCd, NiMH and lithium-ion secondary rechargeable batteries [33].

Mantuano et al noted that a hydrometallurgical plant involving metal purification/ separation by liquid–liquid extraction with Cyanex 272 (bis-2,4,4-trimethylpentyl phosphinic acid) as extractant, was technically viable to separate base metals from NiCd, NiMH and lithium ion secondary battery of spent mobile phone [33]. The route comprises the main steps schematically shown in Fig. 2.4: preliminary treatment of batteries, followed by leaching with sulphuric acid and metal purification/separation by liquid–liquid extraction with Cyanex 272 (bis-2,4,4-trimethylpentyl phosphinic acid) as extractant. Metal separation by liquid–liquid extraction with Cyanex 272 must be carried out in two sequential steps: firstly to extract aluminium at pH 2.5-3.0 and secondly to remove cobalt at pH 4.5, thus leaving lithium in
Zhang et al. (1998) discussed the separation of cobalt from lithium from the hydrochloric acid leach liquor by employing solvent extraction [19]. Fig. 2.5 gives the pH dependence of the

extraction of cobalt and lithium from the leach solution containing 17.25 g/L Co and 1.73 g/L Li with 0.29 M di-(2-ethylhexyl) phosphoric acid (D2EHPA) and 0.30 M 2-ethylhexyl phosphonic acid mono-2-ethylhexyl ester (PC-88A) in kerosene. It is found that the extraction of cobalt increases rapidly with the increase of pH in the region of pH < 5 and essentially complete extraction occurs when the pH is higher than 6.5. On the other hand, lithium is not extracted at all at pH < 5.5 in all cases. Above pH 5.5, lithium begins to extract slightly into the organic phase. It appears that the extraction ability of D2EHPA for lithium is greater than that of PC-88A.

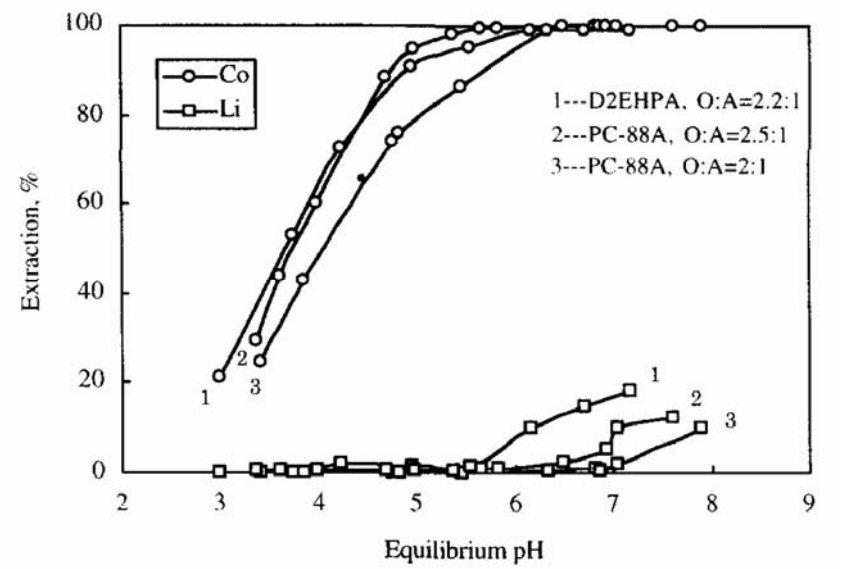

Fig. 2.5: pH dependence of extraction of cobalt and lithium with 0.29 M D2EHPA and 0.30 M PC-88A in kerosene (feed solution: [Co])

2.3.2.4. Chemical Precipitation

Contestabile et al. studied a laboratory process aiming to the treatment and recycling of spent lithium ion secondary batteries [5]. The process consisted of sorting, crushing and riddling, selective separation of the active materials, lithium cobalt dissolution and cobalt hydroxide precipitation. The flow sheet of the recycling process is shown in Fig. 2.6. The cobalt dissolved in the hydrochloric solution was recovered as 0.29 M D2EHPA and 0.30 M PC-88A in kerosene (feed solution: [Co] = 17.25, [Li] = 1.73 (g /L); pH = 0.6) [5,19]. cobalt hydroxide $Co(OH)_2$ by addition of one equivalent volume of a 4M NaOH solution. The precipitation of cobalt hydroxide begins at a pH value of 6 and can be considered to be completed at pH 8.

Castillo et al. studied the separation of lithium and manganese by the addition of sodium hydroxide solution [31]. The operating conditions and separation results are reported in Table 2.3. The selective precipitation separation process was applied on spent Li ion batteries, after preliminary dissolution in acidic medium. The choice of the acid is reported hereafter.

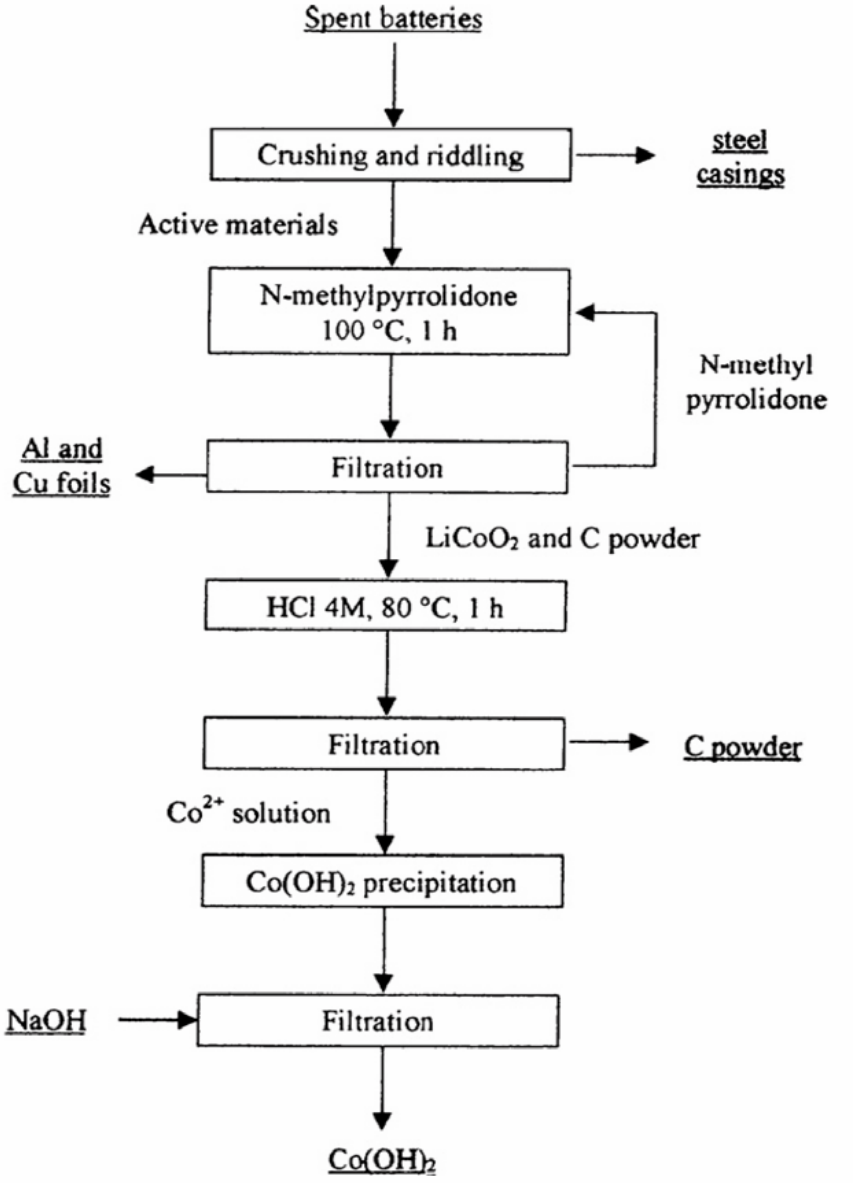

Figure2.6. Flow-sheet of the recycling process for spent lithium-ion batteries [5].

Table 2.3. Experimental conditions with standardized solution

Sl.no.	Metal content of the standardized solution (molar ratio)	Initial pH	NaOH[a] (ml)	Results	
				Filtrate content	Precipitate Content
1	Li-Mn (0.08-0.1)	3.8	30	Li (100%)	Mn (100%)
2	Li-Mn-Ni (0.08-0.1-0.02)	2.9		Li and Mn (100%) for further separation see solution (1)	Ni[b] (100%)
3	Li-Mn-Fe (0.08-0.1-0.2)	0.71	16	Li (100%) and Mn (70%) for further separation see solution(1)	Fe(100%) Mn(10%)

[a]Volume (ml) of NaOH solution (10 $molL^{-1}$) added to 200 ml nitrate solution to reach the pH of metal hydroxide precipitation
[b]Ni extracted from the solution after complexation with dimethylglyoxime

2.3.2.5. Electrochemical Process

Cobalt ions, extracted from waste $LiCoO_2$ by using a nitric acid leaching solution, are potentiostatically transformed into cobalt hydroxide on a titanium electrode and cobalt oxide is then obtained via a dehydration procedure [22]. In linear sweep voltammetry, distinct cathodic current peak is observed and indicates that hydroxide ions are formed near the electrode via the electro-reduction of dissolved oxygen and nitrate ions give rise to an increase in the local surface pH of the titanium. Under appropriate pH conditions, island-shaped cobalt hydroxide is precipitated on the titanium substrate and heat treatment of

the cobalt hydroxide results in the formation of cobalt oxide. The detailed reaction mechanisms are considered to be:

$$2H_2O + O_2 + 4e- = 4OH- \quad (2.2)$$

$$NO_3- + H_2O + 2e- = NO_2 + 2OH- \quad (2.3)$$

$$Co^{3+} + e- = Co^{2+} \quad (2.4)$$

$$Co^{2+} + 2OH^- / Ti = Co(OH)_2 / Ti \quad (2.5)$$

The reduction of dissolved O_2 and nitrate ion, i.e., reactions (2.2) and (2.3), could increase the local pH of the electrode. Thus, the precipitation of hydroxide films of $Co(OH)_2$ (Eq. 2.5) under appropriate pH condition could be possible. Therefore, this process provides a good way for recovering cobalt oxide from $LiCoO_2$. Finally, the differences of the lithium-ion secondary batteries of recycling processes depicted from different precursors have been studied as shown in Table 2.4.

Table 2.4. Recovery process for lithium-ion secondary batteries by different investigators.

References	**Sample**	**Leach conditions**	**Separate method**	**Additive**
Zhang et al.	$LiCoO_2$ batteries	4M HCl, 80ºC, 1h	Solvent extraction methods	PC-88A
Contestabile et al.	$LiCoO_2$ cell (cylindrical 1850 size)	4M HCl, 80ºC, 1h	Change pH value	NaOH
Castillo et al.	Li Mn Ni (cylindrical spent battery)	HNO_3 2M, 80ºC, 2h	Change pH value	NaOH
Lee and Rhee	$LiCoO_2$ cell (cylindrical 1850 size)	HNO_3 1M + 1.7 vol.% H_2O_2, 75ºC, 1h	Amorphous citrate precursor method	--
Lee and Rhee	$LiCoO_2$ batteries	HNO_3 1M + 1.7 vol.% H_2O_2, 75ºC, 1h	Amorphous citrate precursor method	--
Shin et al.	$LiCoO_2$ batteries	H_2SO_4 + 15 vol.% H_2O_2, 75ºC, 10 min	--	--
Nan et al.	$LiCoO_2$ batteries	3M H_2SO_4, 75ºC, 4h	Chemical deposition and solvent extraction methods	AcorgaM5640 Cyanex 272
Aktas et al.	$LiCoO_2$ batteries	4M H_2SO_4 + H_2O_2, 80ºC, 4h	Precipitation technique using ethanol	C_2H_5OH
Nan et al.	$LiCoO_2$ batteries and NiMH batteries	3M H_2SO_4 + 3 wt.% H_2O_2, 70ºC, 5h	Solvent extraction methods	AcorgaM5640 Cyanex 272

2.4. Effect of Reaction Operating Conditions

2.4.1. Effect of Leaching Process

Some reaction conditions such as acid concentration of leaching agent, leaching reaction temperature (T), leaching reaction time (t) and solid-to-liquid ratio (S/L) can affect the leaching efficiency; the different operating conditions are described as follows.

2.4.1.1. Effect of Acid Concentration

Lee and Rhee et at. reported the effects of HNO_3 concentration in the presence of 0.8 vol.% H_2O_2 on the leaching of $LiCoO_2$ at a S/L ratio of 20 g/Land 75°C for 30 min (Fig. 2.7) [3]. The efficiencies of both Co and Li increase with increasing HNO_3 concentration. Over 80% Co and 80% Li were readily extracted within 30 min at 1 M HNO_3.

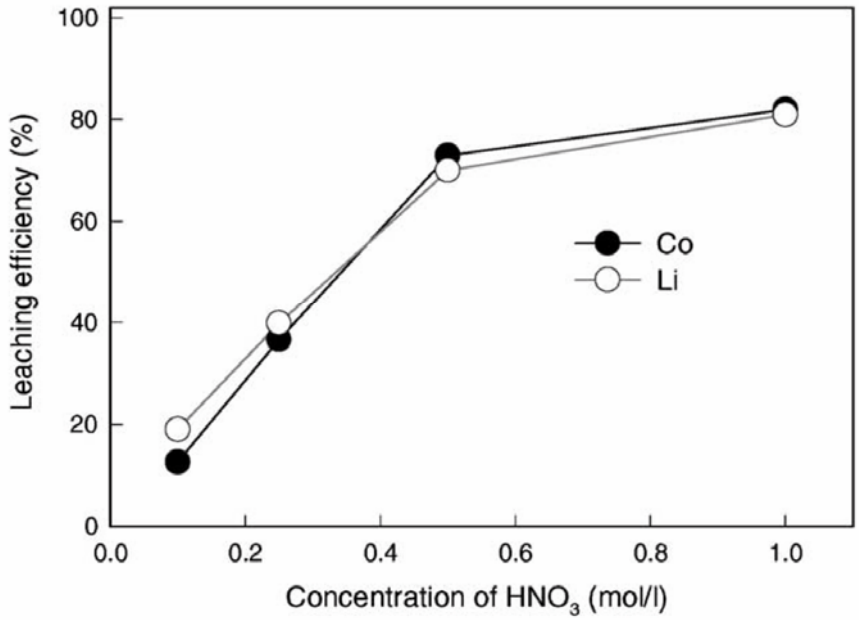

Figure 2.7. Effect of HNO_3 concentration on $LiCoO_2$ leaching (20 g /L, 75 °C, 400 rpm, 30 min, 0.8 vol.% H_2O_2)

Castillo et al. carried out tests with nitric acid under the same conditions but concentration varying from 0.5 to 5 M [31]. The spectrophotometric analyses results show that approximately 100% lithium could be recovered when the concentration was in the range 1 and 2M (Fig. 2.8). At the same time, samples have been analyzed at different times by ionic chromatography to quantify manganese. Results prove that manganese is even present for very

dilute acid (Fig. 2.9). On the other hand, the filtrate does not contain other ions than Fe^{3+}, Ni^{2+} and Co^{2+} if the nitric acid concentration does not reach 5 M.

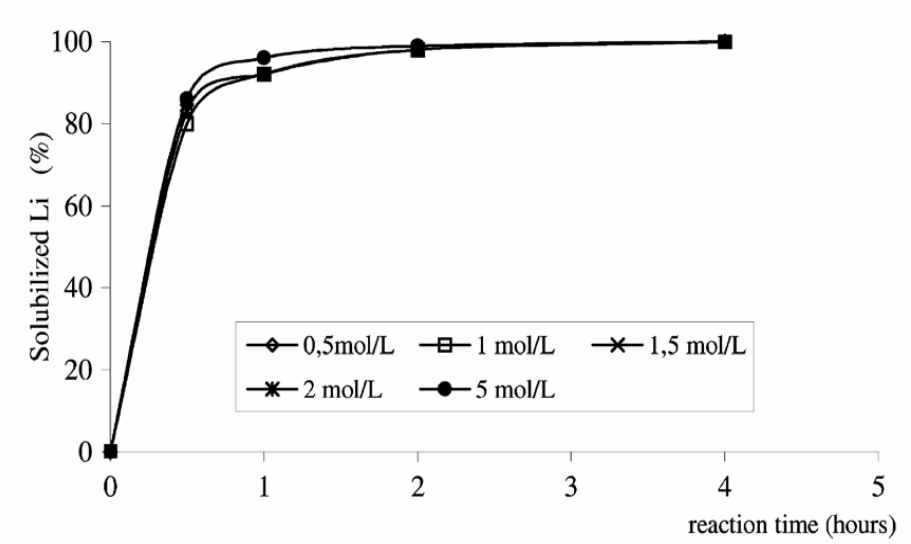

Figure 2.8. Lithium recovery (%) vs. dissolution time in nitric acid at various concentrations

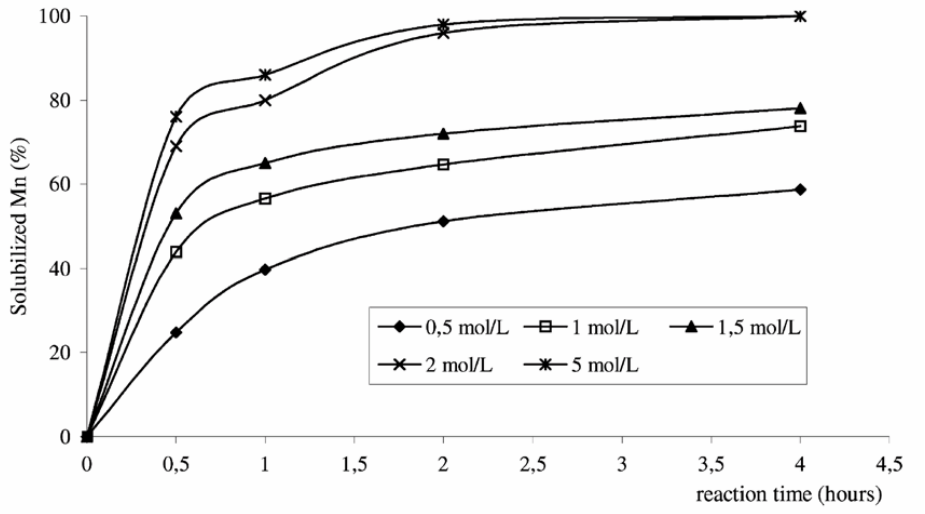

Figure 2.9. Manganese recovery (%) vs. dissolution time in nitric acid at various concentration

2.4.1.2. Effect of Reaction Temperature

Zhang et al. showed that metal leaching is significantly affected by temperature (Fig. 2.10) [19]. An increase in temperature remarkably enhanced the leaching of the metals. However, in the case of sulfurous acid, when the temperature was raised from 60 to 80°C, the percentages of cobalt and lithium leached decreased. This likely resulted from the evaporation of SO_2 in the sulfurous acid at high temperature.

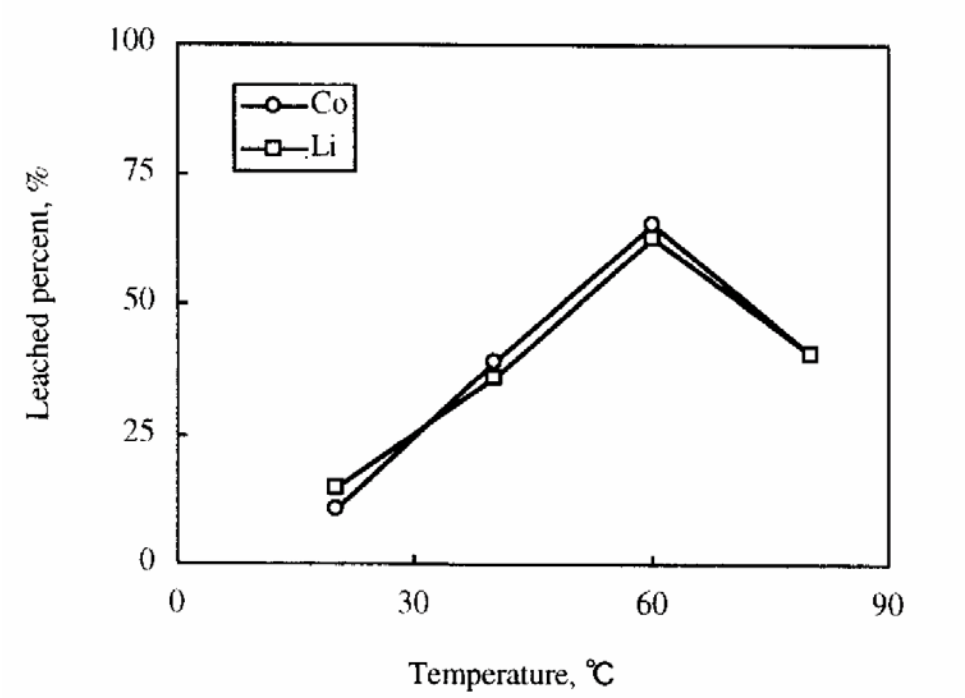

Figure 2.10. Effect of temperature on leaching of cobalt and lithium with 6% sulfurous acid solution.

Nan et al. showed that the efficiency of leaching of Co was relatively low at lower reaction temperature and acid concentration [37]. With the increasing of H_2SO_4 concentration and temperature from 2 to 4 M and 50–90°C, respectively, the leaching efficiency increased. More than 95% Co was leached within 4 h when the temperature approached 90°C. Figs. 2.11 and 2.12 show the effect of H_2SO_4 concentration and reaction time on the leaching percentages of cobalt at 50 and 90°C, respectively. At higher acid concentration and reaction temperature, the leaching efficiency of cobalt in a 6% sulfurous acid solution (t = 30 min, S:L = 1:100) (Zhang et al., 1998) was favorable [19].

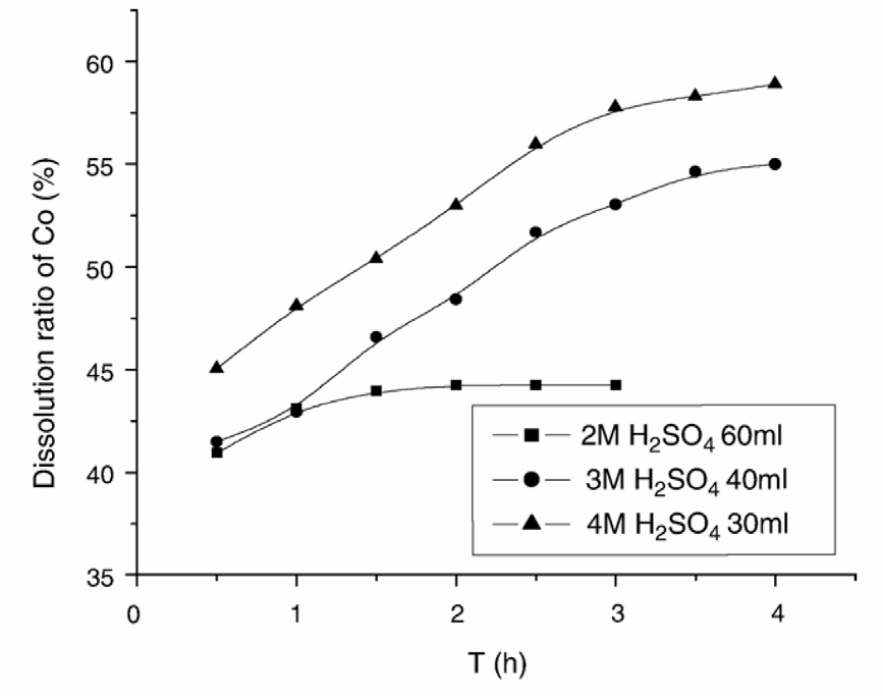

Figure 2.11.Effect of H_2SO_4 concentration and reaction time on the dissolution of $LiCoO_2$ at 50 ^oC

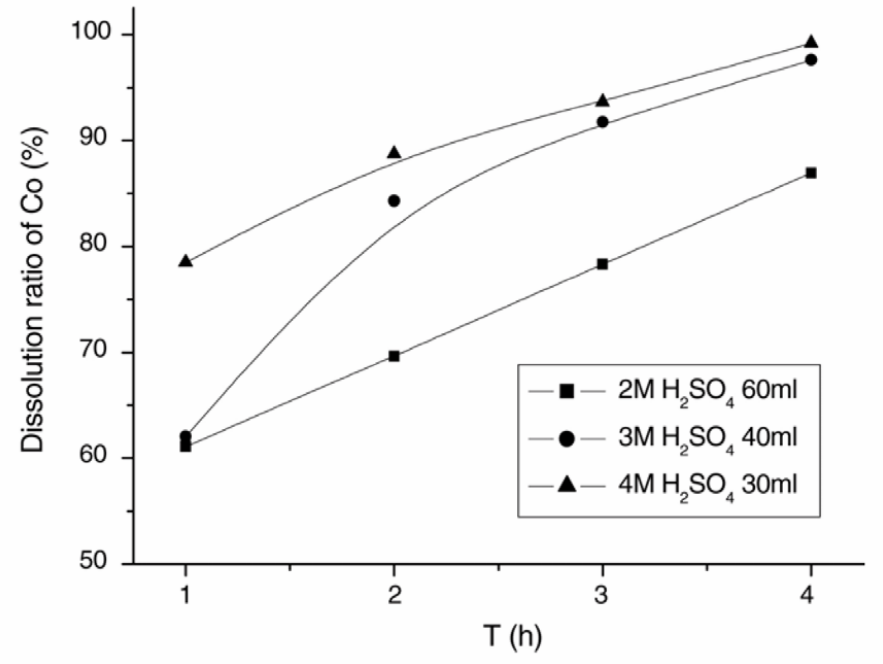

Figure 2.12. Effect of H_2SO_4 concentration and reaction time on the dissolution of $LiCoO_2$ at 90 ^oC

2.4.1.3. Effect of Reaction Time

The effect of reaction time on the dissolution of Co, Ni, and Co is presented in Fig. 2.13 [37]. It is seen that the dissolution of powder residues is enhanced with the increase of dissolving time, and about 90% Co, Ni, and Co could be leached out after 5 h. In addition, it was also found that the dissolution of mixed RE was over 99.5% in 5 h under such dissolution conditions. The insoluble material could be put in the posterior batch. So, the dissolving time of 5 h was chosen in the given process.

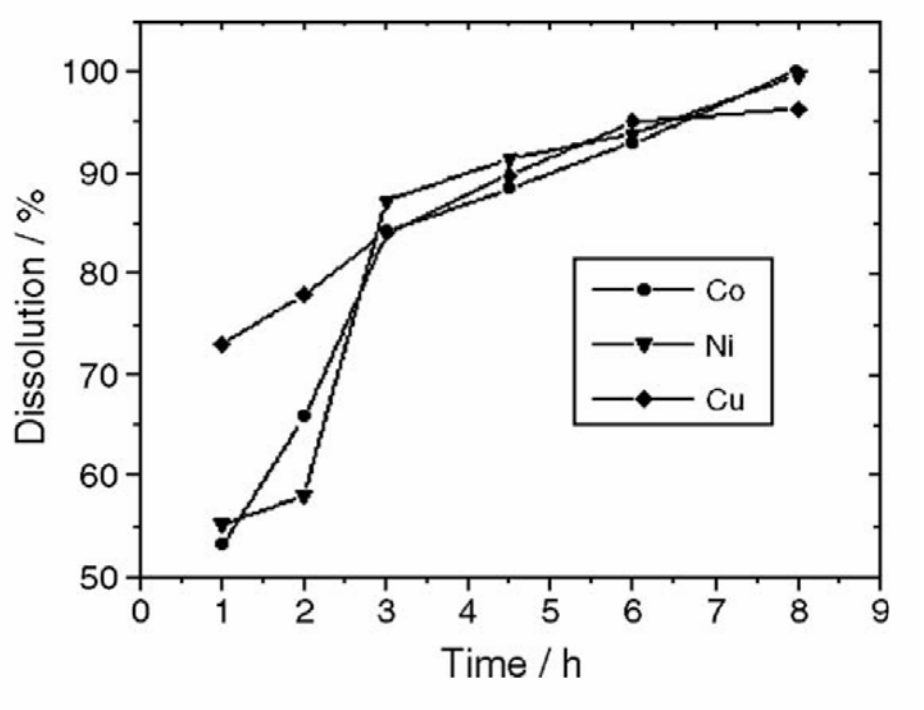

Figure 2.13. Effect of reaction time on the dissolution of Co, Ni, and Cu using 3 mol L^{-1} H_2SO_4 and 3 wt.% H_2O_2 at 70 °C and S/L=1:15

Fig. 2.14 gives the time dependency of the leaching of cobalt and lithium with hydroxylamine hydrochloride solution (NH_2OH•HC1) [19]. It is apparent that increasing the reaction time is beneficial to metal leaching. About 92% of cobalt and lithium can be leached within 30 min in the case of hydroxylamine hydrochloride solution (NH_2OH•HC1).

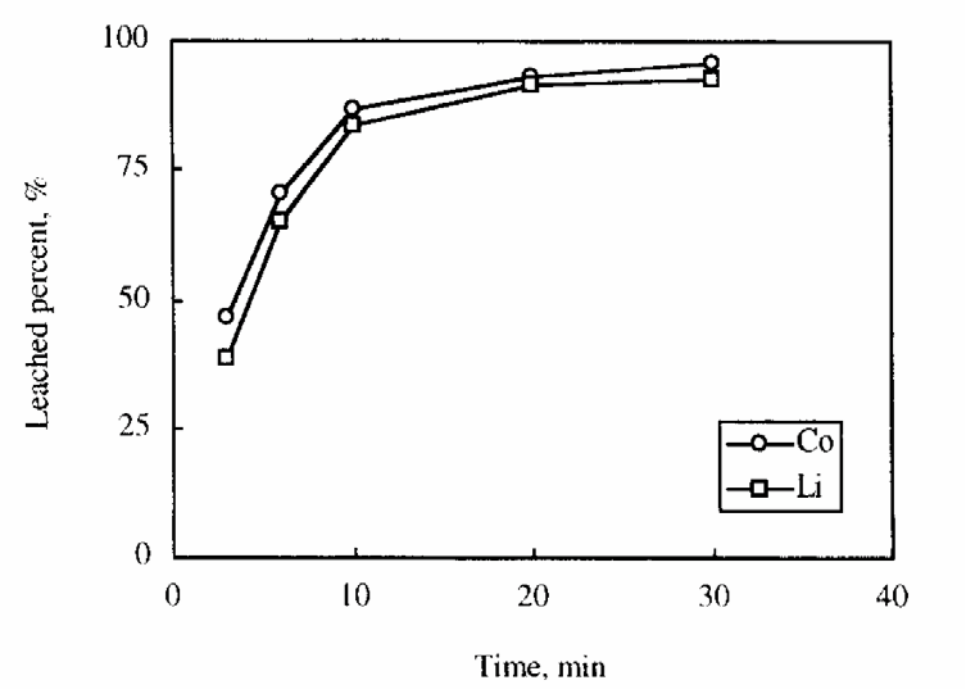

Figure 2 .14. Effect of reaction time on leaching of cobalt and lithium with 1 M hydroxylamine hydrochloride solution

2.4.1.4. Effect of Solid-to-Liquid Ratio (S/L)

Shin et al. reported in these experiments with the concentration of sulfuric acid to be 2 M, and pulp density to be 50 g/L.1 M hydroxylamine hydrochloride solution (T = 80 oC, S:L = 1 : 100) [4,19].

High pulp density is desirable to raise processing throughput. Yet a density higher than 50 g/L yields lower leaching efficiency, as illustrated in Fig. 2.15(a) for cobalt leaching and Fig. 2.15(b) for lithium. The leaching temperature was 75^{o}C with an agitation of 300 rpm. The leaching rate was fast in the initial stage regardless of the hydrogen peroxide concentration, whereas leaching efficiency depends upon the amount of hydrogen peroxide. A concentration of 15 vol. % was enough for the full leaching of both metal components. Because polyvinylidene fluoride (PVDF) binder does not dissolve in acid solution, it remains in the cake after filtration. Also, carbon does not dissolve in acid solution, and instead it floats on the solution; from filtration it is separated in the cake. The electrolyte lithium hexafluorophosphate ($LiPF_6$) decomposes into lithium fluoride and phosphor pentafluoride in the crushing process, and the lithium dissolves in the acid solution during leaching.

The organic solvents of propylene carbonate (PC) and diethyl carbonate (DEC) were evaporated in the crushing process. The concentrations of copper and aluminum in the leachate were 0.46 g/L and 0.79 g/L, respectively, and the amounts in the cake were less than 0.01 g [4].

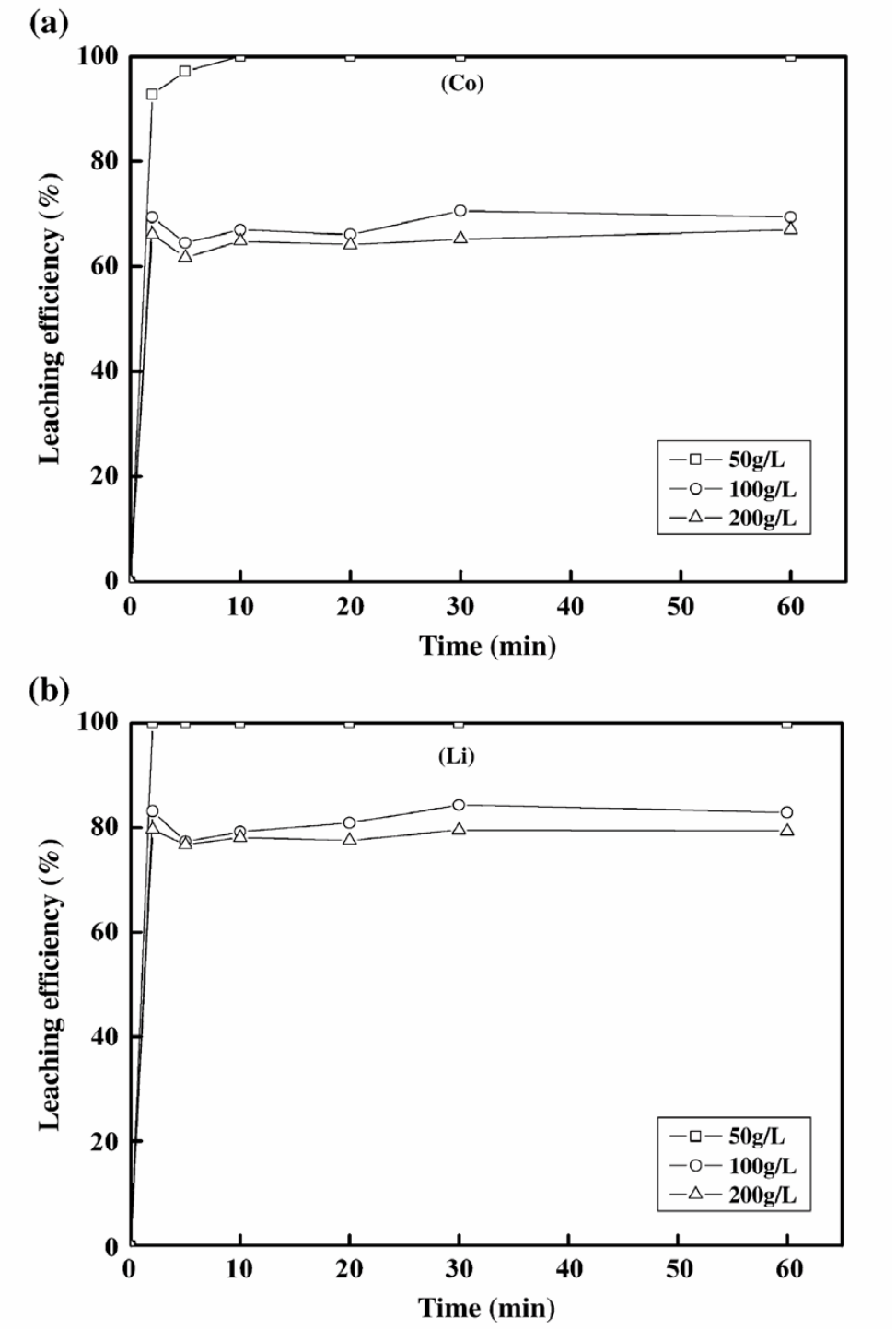

Figure 2.15. Effect of pulp density on cobalt (a) and lithium (b) leaching

2.5. Effect of Recovery Materials Process

2.5.1. Effect of Precipitate of Cobalt

Contestabile et al. studied the cobalt dissolved in the hydrochloric solution to be recovered as cobalt hydroxide Co(OH)2 by addition of one equivalent volume of a 4M NaOH solution [5]. The solubility product of cobalt hydroxide is about 10-16; consequently, its precipitation begins at a pH value of 6 and can be considered to be completed at a pH of 8. Ideally, one could obtain $Co(OH)_2$ precipitation by using an ammonia solution, i.e., by a weak base which forms a buffer solution at a pH of 9. Unfortunately, ammonia forms stable complexes with cobalt causing the partial dissolution of the hydroxide and thus, preventing from a quantitative recovery. Therefore, NaOH, which is a strong base and which allows to work with small volumes of solution, remains the best choice [30]. On an industrial scale, this step can be controlled by using an adequate pH sensor. The $Co(OH)_2$ precipitate can be easily separated from the solution by filtration, then to be recycled.

2.5.2. Effect of Precipitate of Lithium

Nan et al. referred to the recovery process given by Zhang et al., the raffinate was concentrated and treated with a saturated sodium carbonate solution to precipitate lithium carbonate at 100^oC [19,37]. The lithium carbonate was recovered after filtration and washing with hot water to remove the residual mother liquor. The results showed that about 80% lithium was recovered as a precipitate, which is similar to Zhang's recovery ratio. In addition, the analytical results showed that the contents of cobalt and copper in the precipitate were less than 0.96 and 0.001%, respectively.

2.6. Hydrometallurgy

Hydrometallurgy refers to production of metals or pure compounds with the help of reactions in aqueous and organic solutions. It is a process of beneficiation as well as extraction. Hydrometallurgical processing is generally carried out to the low grade ores which are not suitable for pyrometallurgical operations. Hydrometallurgical processing generally involves the following steps: leaching, purification of leach liquor, recovery of metallic values from leach liquor and reagent recovery.

2.6.1. Leaching

Leaching is the process of extracting minerals from a solid by dissolving it in a liquid. In leaching, usually the metallic values in an ore are selectively dissolved using a suitable liquid reagent. The selectivity in dissolution depends on the nature of the reagent while the rate of leaching depends on various factors including temperature, pressure, the solid/liquid ratio, the particle size, the composition and concentration of the reagent, leaching time and stirring rate. The leaching reagent should be inexpensive and it should be possible to regenerate it. For economical operation, it is also necessary that the reagent should be selective and of sufficient strength. It should dissolve the ore minerals rapidly without attacking the gangue minerals and thus being consumed unnecessarily. The choice of a leaching agent depends on the following factors:

1. Chemical and physical character of the material to be leached.
2. Cost of the reagent.
3. Corroding action of the reagent and the materials of construction required.
4. Selectivity of the leaching agent for the desired constituent to be leached.
5. Ability to be regenerated.

The common categories of leaching reagents are water, mineral acids, bases and aqueous salt solutions. Since hydrometallurgical processes are mainly concerned with the treatment of metal ions in solution, the first consideration should be the dissolution or leaching of the metal. For a successful leaching system there are a number of essential aspects of processing which must be fulfilled and there are a number of features which are desirable if costs are to be kept to a minimum.

Essential features

i) The valuable metal must be soluble in an economically usable solvent,
ii) The metal must be economically recoverable from solution, and
iii) Any impurity elements which are co-extracted during leaching must be capable of further separation from the solution.

Desirable features

i) The gangue minerals should not consume excessive amounts of solvent,
ii) The solvent should be recoverable (or capable of regeneration) for recycle,
iii) The feed material should be free of clay minerals, as these make separation of leach liquor from the treated solids difficult,

iv) The feed material should be permeable to the solution allowing direct contact between the solvent and the phase to be dissolved, and provide a high liquid/solid area for reaction for a given mass of material, and

v) The solvent should preferably be non-corrosive to materials used in plant equipment to minimize capital and maintenance costs, and should be non-toxic, to minimize any dangers to plant personnel.

The leach liquor is separated from solid residues by one or more of the various methods of materials separation, viz. settling, thickening, filtration, washing etc. Methods employed to recover the metallic values are evaporation, distillation, precipitation, cementation, electrolysis, ion exchange, solvent extraction etc. The leaching agent is generally recycled after purification.

2.6.2. Leaching Kinetics

Leaching is a heterogeneous reaction that takes place at the interface between a solid and liquid phase and sometimes also a gaseous phase. At the boundary between the two phases a diffusion layer is formed. In the case of a solid in an aqueous phase this layer consists of a stationary aqueous layer. The diffusion layer can be thinned by vigorous stirring but never be completely removed. Typical thickness of the diffusion layer in a well stirred system is in the range of 1-10 μm. The schematic representation of a mineral surface during leaching is shown in Fig. 2.16.

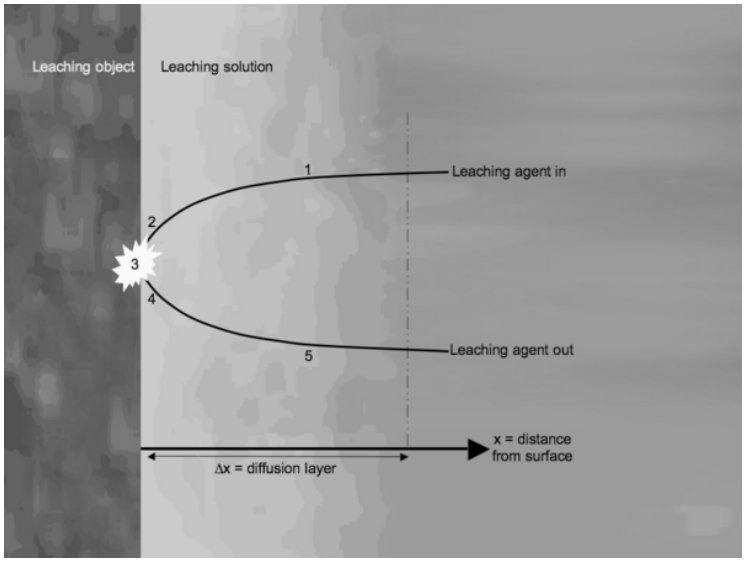

Fig. 2.16: Schematic representation of mineral surface during leaching

The kinetic step that determines the rate of leaching can be one or a combination of the followings:

1. Diffusion of reagent through the diffusion layer
2. Adsorption of reagent on surface
3. Reaction on the surface
4. Desorption of product from surface
5. Diffusion of product through the diffusion layer

The slowest step in the leaching reaction is the rate-controlling step. Depending on which process is rate-controlling, three different type reactions may be obtained, i.e., reaction controlled leaching, diffusion controlled leaching and intermediate controlled leaching whose are shown in Fig. 2.17.

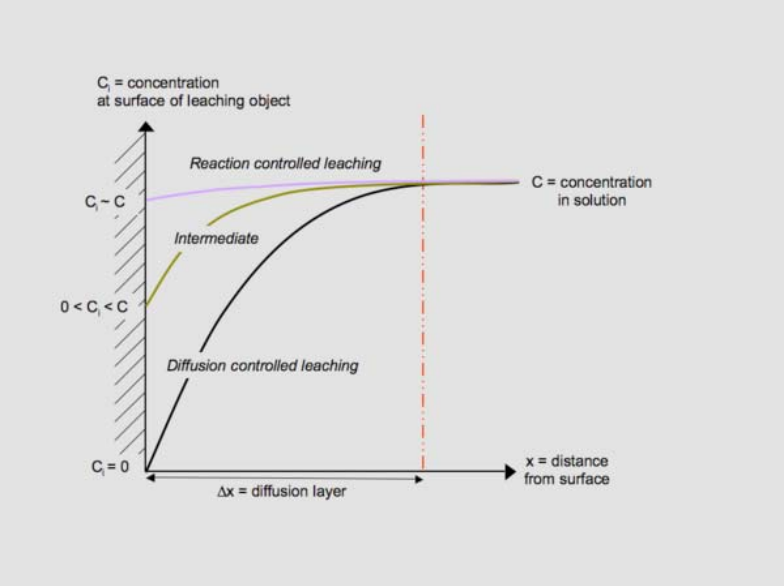

Fig. 2.17: Different rate controlling steps in leaching kinetics

In fluid particle reaction kinetics, in which a gas or liquid contact with a solid, the reactions may be represented as follows:

A (fluid) + bB (solid) = fluid products (2.6)

= solid products (2.7)

= fluid and solid products (2.8)

As shown in Fig. 2.18, solid particles may remain unchanged in size during reaction when they contain large amounts of impurities which remain as a nonflaking ash or if they form a firm product material by the reactions of Eq. 2.7 or Eq. 2.8. Particles shrink in size during reaction when a flaking ash or product material is formed or when pure B is used in the reaction of Eq. 2.6 [38]

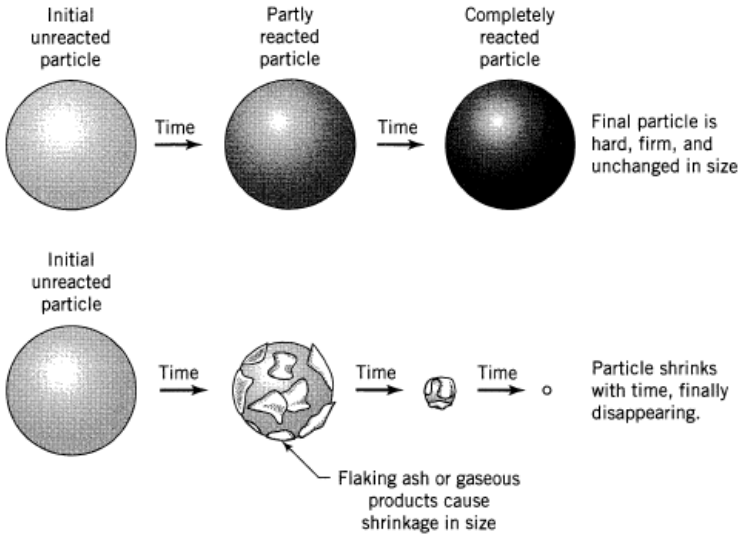

Fig. 2.18: Different sort of behavior of reacting solid particles

2.6.2.1. Kinetic model selection

For the noncatalytic reaction of particles with surrounding fluid, two simple idealized models, the progressive-conversion model and the shrinking unreacted-core model can be considered .

In Progressive conversion model (PCM) reactant liquid enters and reacts throughout the particle at all times, most likely at different rates at different locations within the particle. In Shrinking core model (SCM), reaction occurs first at the outer skin of the particle. The zone of reaction then moves into the solid, leaving behind completely converted material and inert solid. Thus, at any time there exists an unreacted core of material which shrinks in size during reaction. In real situation, it is usually found that unreacted solid material is surrounded by a layer of ash. Evidence from a wide variety of situations indicates that in most cases the shrinking-core model (SCM) approximates real particles more closely than does the progressive conversion model (PCM).

The following models are generally considered for the Shrinking core model.

1. Liquid film diffusion controlled
2. Chemical reaction controlled
3. Product layer diffusion controlled
4. Mixed kinetic mechanism

2.6.2.1.1. Liquid film diffusion controlled

The fraction of particle reacted at any time, t, in a liquid film diffusion control situation can be calculated from the following equation which apply to small particle moving in Stokes regime [38]

$$\frac{t}{\tau} = 1 - (1 - X)^{2/3}$$

Where X = $\frac{\text{Amount of reacted particle}}{\text{Total amount of partle}}$

The time for complete disappearance of particle, $\tau = \frac{\rho {R_O}^2}{2bCD}$

Where, ρ is the molar density of the solid particle,

Ro = Original particle size

b = Stoichiometric coefficient of the reaction

D = Diffusion coefficient of the leaching reagent

C = Concentration of the leaching reagent

2.6.2.1.2. Chemical reaction controlled

The fraction of solid particle reacted at any time, t, in a chemical reaction controlled process can be calculated from the following equation which applies to both small and large particle moving in Stokes regime, considering those particles as shrinking spheres and also to the constant size sphere particles.

$$\frac{t}{\tau} = 1 - (1 - X)^{1/3}$$

Again, the time for complete disappearance of particle, $\tau = \frac{\rho R_o}{bkC}$

Here, k = Rate constant of the reaction

2.6.2.1.3. Product layer diffusion controlled

Diffusion of the reagent or dissolved species through a solid reaction product at any time, t, can be calculated from the following equation

$$\frac{t}{\tau} = 1 - 3(1-X)^{2/3} + 2(1-X)$$

In this case,

$$\tau = \frac{\rho {R_o}^2}{6bCD}$$

2.6.2.1.4. Mixed kinetic mechanism

Mixed controlled process is the combination of surface reaction and diffusion. The fraction of particle reacted at any time t under mixed controlled process can be expressed as follows.

$$\frac{t}{\tau} = \left[1 - (1-X)^{1/3} + \frac{y}{6}\right](1-X)^{1/3} + 1 - 2(1-X)^{2/3}$$

2.6.3. Determination of activation energy

The energy that must be overcome for a chemical reaction to occur is called the activation energy. Activation energy can be thought of as the height of the potential barrier (sometimes called the energy barrier) separating two minima of potential energy (of the reactants and products of a reaction). For a chemical reaction to have a noticeable rate there should be a noticeable number of molecules with energy equal to or greater than the activation energy.

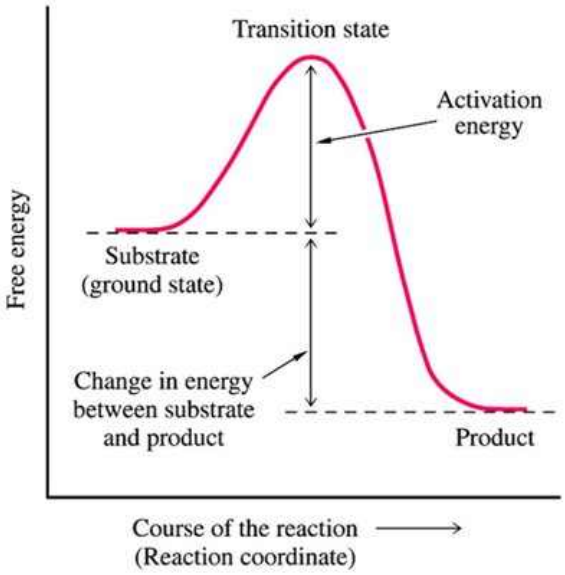

Fig. 2.19: Activation energy barrier for a reaction to occur

It is always possible to find out more than one set of configurational changes capable of providing a given transformation, called 'reaction paths.' However, because different transition configurations are involved, the activation energy is different. Only those with excess free energy equal to or greater than the activation energy will transform (Fig. 2.19). Those with insufficient free energy can transform by thermal activation [39].

The following effects of activation energy on reaction rate are generally considered:

1. Reactions with high activation energies are very temperature sensitive. Conversely, low activation energies imply lower temperature sensitivity of rate.
2. Temperature sensitivity of rate is more pronounced at lower temperature.
3. The preexponential factor in Arrhenius law has little effect on temperature sensitivity of reaction rate.

Chapter 3

EXPERIMENTAL

3.1. Battery Collection and Separation

Samples of spent batteries of all the commercially available types of Lithium ion batteries were collected from different sources. A wide range of brands like Nokia, Sony Ericson and Maxims were collected during the process. The samples, irrespective of the brands, were divided into the different models like M 660, V 83 etc. Some batteries were too badly damaged for physical separation of the components and were discarded. Batteries of M 660 and V 83 models were collected in sufficient quantity for this investigation. The potential voltage of all the batteries (M 660 & V 83) used in this study was 3.7V.

3.1.1. Weight measurement of the spent

The collected batteries were dismantled manually. The plastic cover of the batteries was removed by using a sharp cutting edge. It was then fixed in a vice to remove the metallic outside shell. The different component parts were carefully separated and weighed. The weight proportions of the different components (casing. paste, etc.) of five batteries in each type were estimated.

3.1.2. Characterization of Battery

The phases present in the paste on the cathode and anode of spent M 660 and V 83 type lithium ion batteries were determined by x-ray diffraction analysis. Identification of the constituents in the different component parts in the spent batteries and percentage of these constituents were determined by Atomic Absorption Spectroscopic analysis, and Optical Emission Spectroscopic (OES) analysis. Conventional methods of wet chemical analysis was used to determine the percentage of copper.

3.1.3. Identification of the battery components

The different component parts of both the types of battery were identified after manual dismantling of the battery. The different components were identified by physical appearance and information available in published literature. The batteries were found to be covered with plastic sheet. The separators, circuit and sealing agents were identified by physical appearance. The external metallic part, assumed to be of aluminium, was analysed by optical emission spectroscopy. The coating on anode, assumed to be graphite on the basis of available information was subjected to x-ray diffraction

analysis. The coating on the cathode, assumed to be lithium cobalt carbonate, was identified in x-ray diffraction analysis.

3.1.4. Total value metal percentage

The weighted average values of the metal contents of the whole battery in lithium ion spent types were also determined.

3.2. X-ray Diffraction analysis

X-ray diffraction analysis was performed in a Bruker D8 Advance X-ray Diffractometer. Sample weighing 1g to 3 g was mildly pressed in the sample holder. The excess sample was removed from the top of the sample holder as; powders falling out of a sample holder can contaminate the system.

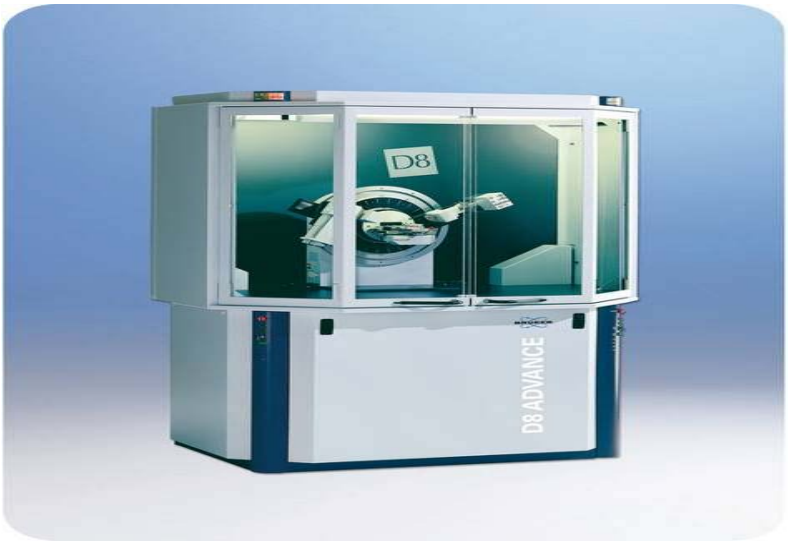

Fig. 3.1 D8 Advance X-ray Diffractometer

.

The operating conditions that were maintained during the experiments were:

Voltage and current: 40 kV and 30 mA

Water flow rate: 4.7 L/min

X-ray generator source: Cu anode

X-ray filter: Ni

Wavelength for Cu-Kα radiation: 1.54056 A^0

3.3. Optical Emission Spectroscopy analysis

The chemical analysis of the external metallic casing was performed by a Shimadzu PDA 7000 Optical Emission Spectrometer.

The general conditions that were maintained during the experiment on OES are:
Inside the machine temperature was = 400^{o}C
During stand by condition, Argon gas flow was = 1 lt/min
During working condition, Argon gas flow was= 10 lt/min

3.4. Hydrometallurgical Treatment of the cathode

Hydrometallurgy refers to production of metals or pure compounds with the help of reactions in aqueous and organic solutions. It is a process of beneficiation as well as extraction. Hydrometallurgical processing is generally carried on the low grade ores which are not suitable for pyrometallurgical operations. Hydrometallurgical processing generally involves the following steps: leaching, purification of leach liquor, recovery of metallic values from leach liquor and reagent recovery. Fig 3.2 and Fig.3.5 shows the process flow chat of hydrometallurgy route in sulfuric acid and hydrocholoric leaching media

3.4.1. Dissolution of electrode in N-methylpyrrolidone (NMP)

The active cathode was immersed N-methylpyrrolidone (NMP) which is a good solvent (solubility around 200 g/kg of solvent) at about 100^{0}C for an hour. This treatment allowed achieving the effective separation of the films from their support and thus the recovery of aluminum in their metallic form. The suspension of $LiCoO_2$ in NMP was filtered to separate the $LiCoO_2$ paste. The paste was dried in an oven to a constant weight at 110^{0}C and was used in all the leaching experiments.

3.4.2. Leaching in acid medium

The cathode paste was leached to dissolve lithium and cobalt. Both sulfuric acid and hydrochloric acid were used for leaching. Leaching in sulfuric acid was done in a beaker. The reaction was exothermic in nature and no external heating was required for this process. After leaching, the leach liquor was filtered and the solution was analyzed to determine the concentration of the dissolved elements. For the determination of lithium in the leach liquor, 1ml solution was taken in a 50 ml measuring cylinder and made 50 ml with water. For the analysis of cobalt, 5ml of solution was taken and a complex compound red color solution is made for its analyzed. Atomic flame photometry and UV –spectroscopy was used to determine the amount of lithium and cobalt in leach out solution in sulfuric acid media.

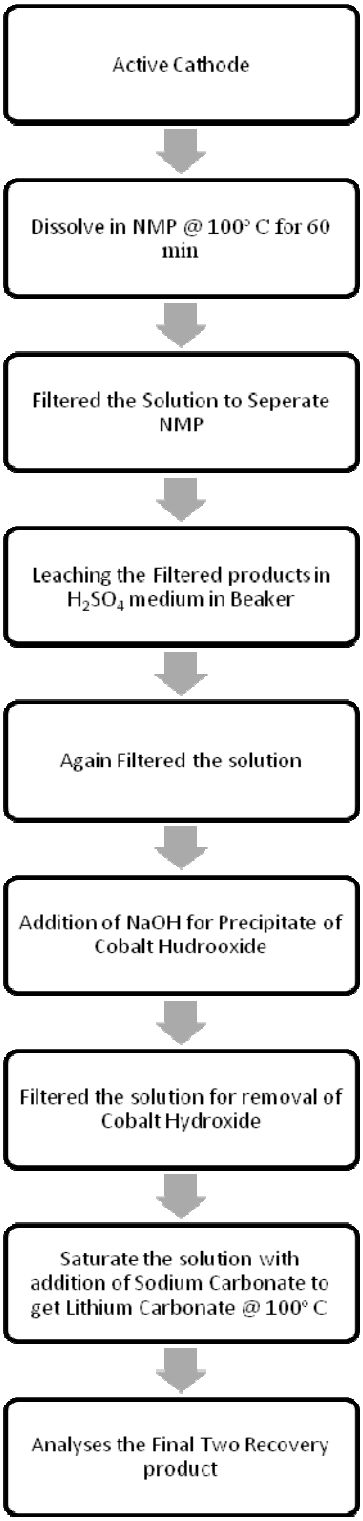

Fig. 3.2: Hydrometallurgical route of lithium and cobalt recovery from battery in sulfuric acid leaching media

Leaching in hydrochloric acid solutions was conducted in a 500-ml three necked round bottom flask with a mechanical stirrer, a temperature sensor and a refluxing condenser fitted to it (Fig. 3.3). Effects of concentration of hydrochloric acid, solid-liquid ratio, time of leaching, temperature and concentration of hydrogen peroxide in the leaching solution on the extent of dissolution of lithium and cobalt were studied. All leaching experiments were performed at a constant stirring speed of 400 rpm. The lithium and cobalt contents of the leach liquor were determined using an Atomic Absorption Spectroscopy.

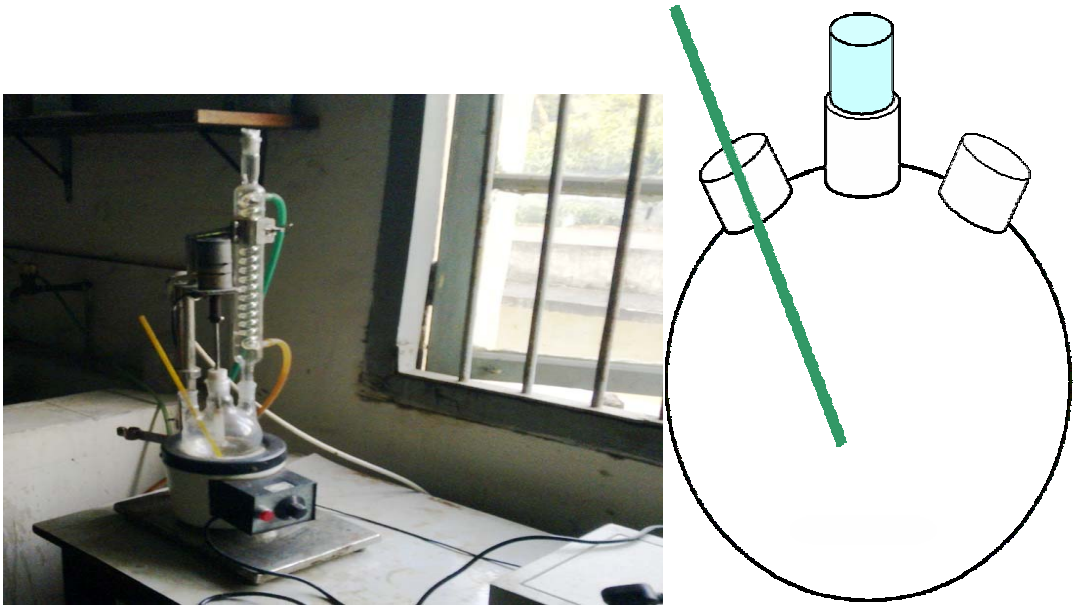

Fig.3.3: Experimental setup of the leaching

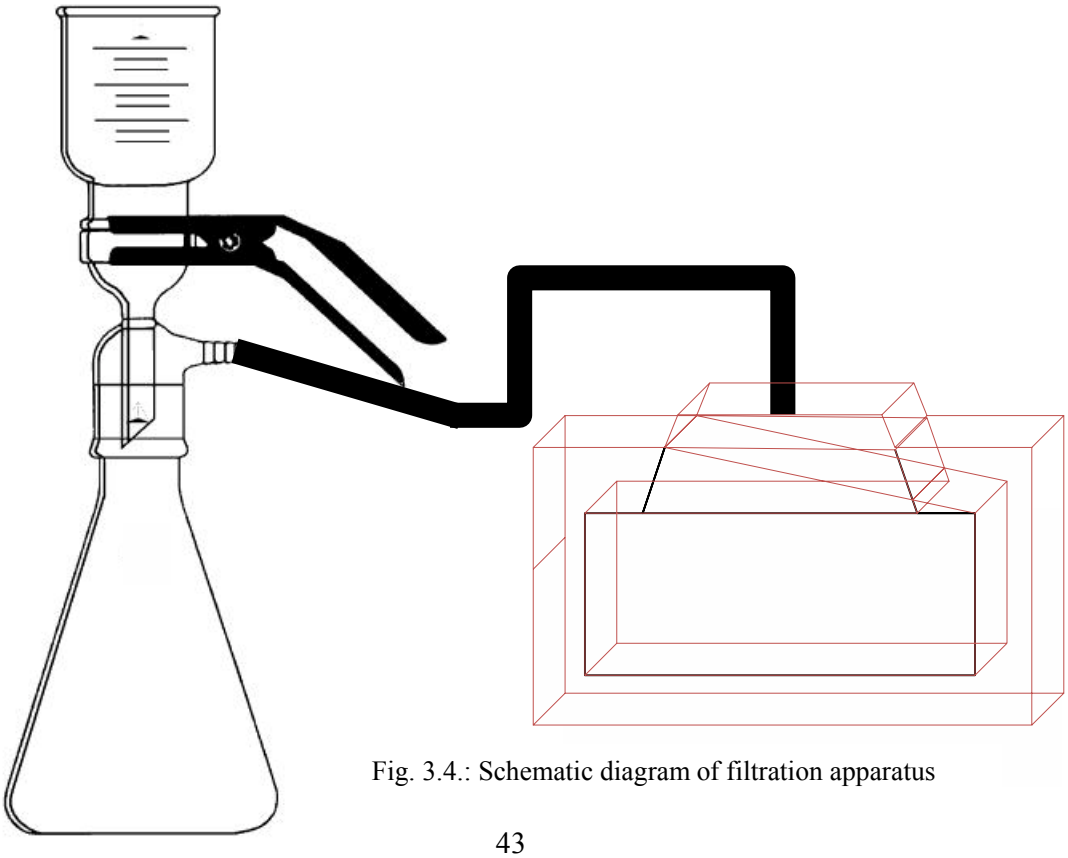

Fig. 3.4.: Schematic diagram of filtration apparatus

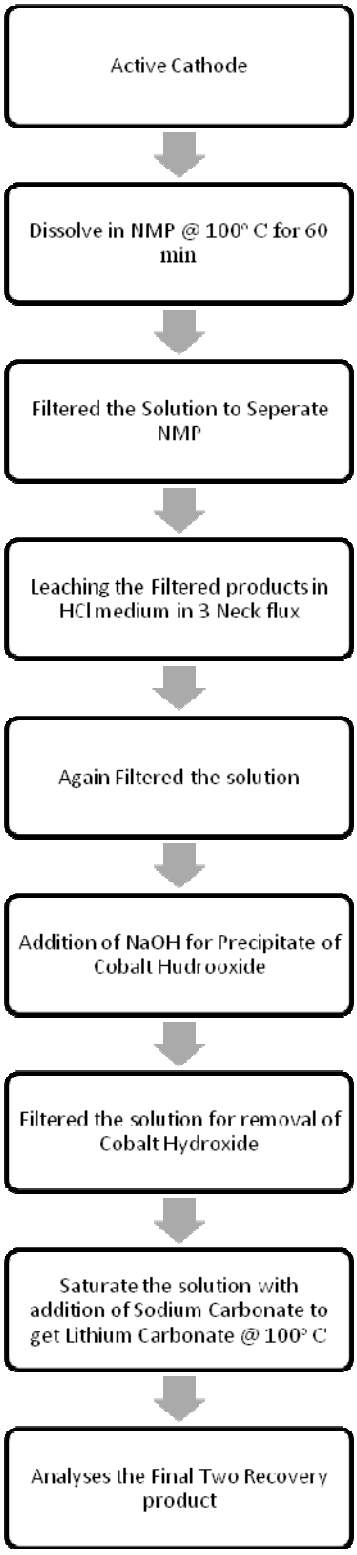

Fig.3.5: Hydrometallurgical route of lithium and cobalt recovery in HCl medium

3.4.3. Leaching Variables

During leaching in sulphuric acid, particle size was kept fixed; while sulfuric acid concentration, temperature, time, solid/liquid ratio and stirring speed were the variables within some predetermined range. The parameters studied and the conditions of these parameters during the leaching experiments are tabulated in Table 3.1.

Table 3.1: Experimental Design for Leaching (particle size were kept fixed) in Sulfuric Acid Solution

No. of Experiments	Parameters studied	Parameter Values	Constant Parameters
1	Concentration of leaching reagent (H_2SO_4)	0.5M	Room Temperature, Hydrogen peroxide concentration = 5 %, solid/liquid ratio = 1:20, Time = Instantly
2		1 M	
3		1.5 M	
4		2 M	
5		2.5 M	
6		3.0 M	
7	Concentration of Hydrogen peroxide	1%	Concentration of sulfuric acid 2M, Room Temperature, Solid/liquid ratio = 1:20 Time = Instantly
8		2%	
9		3%	
10		4%	
11		5%	
12	Solid/Liquid ratio	1:10	Concentration of sulfuric acid 2M, Hydrogen peroxide concentration = 3%, Room Temperature Time = Instantly
13		1:20	
14		1:30	
15		1:40	
16		1.50	

During leaching in hydrochloric acid solutions, particle size was kept fixed; while hydrochloric acid concentration, temperature, time and solid/liquid ratio were the variables within some predetermined range. The parameters studied and the conditions of these parameters during the leaching experiments are tabulated in Table 3.2

Table 3.2: Leaching experimental designs (Particle size were kept fixed) in Hydrochloric acid medium

No.of Experiments	**Parameters studied**	**Parameter Values**	**Constant Parameters**
1	Concentration of leaching reagent (HCl)	1M	Temperature 80^0C, stirring speed 400 rpm, solid/liquid ratio = 1:20, Time=60min
2		2M	
3		3 M	
4		4 M	
5	Temperature	40^oC	Concentration of acid 3M, stirring speed 400 rpm, solid/liquid ratio = 1:20, Time=60min
6		60^oC	
8		80^oC	
9		100^0 C	
10	Time	10 min	Concentration of acid 3M, Temperature 80^0C, stirring speed 400 rpm , solid/liquid ratio = 1:20
11		20 min	
12		40 min	
13		60 min	
14		80 min	
15	Solid/Liquid ratio	1:5	Concentration of acid 3M, Temperature 80^0C, stirring speed 400 rpm, Time=60min
16		1:10	
17		1:15	
18		1:20	
19	Concentration of Hydrogen Peroxide	1%	Concentration of acid 3M, S/L-1:20 Temperature 80^0C, stirring speed 400 rpm, Time=60min
20		2%	
21		3%	
22		4%	

3.4.3.1. Effect of acid concentration

The effect of concentration of acid on the extent of dissolution during leaching at a constant temperature for a predetermined period of time, fixed stirring speed and solid-liquid ratio was investigated. The optimum concentration for the maximum extraction of lithium and cobalt was determined. Extent of dissolution of both lithium and cobalt was plotted against sulphuric acid and hydrochloric acid concentration and the optimum concentration for the maximum dissolution was identified.

3.4.3.2. Effect of temperature

The effect of temperature on the extent of dissolution during leaching with a constant solid-liquid ratio, predetermined acid concentration, fixed period of time of leaching and fixed stirring speed was investigated. The particle size was not varied in any of these experiments. The temperatures investigated were 40, 60, 80 and 100^{o}C. The temperature for the maximum dissolution of lithium and cobalt was again determined from the plots of extent of dissolution of lithium versus temperature and extent of cobalt dissolution versus temperature respectively.

3.4.3.3. Effect of time

The effect of time on the extent of dissolution during leaching at a particular temperature with a constant solid-liquid ratio, predetermined acid concentration and fixed stirring speed was investigated. The periods of time under investigation were 20, 40, 60 and 80 minutes. The time at which maximum extraction of lithium and cobalt was obtained was identified. Two curves, showing the extent of dissolution versus time for both lithium and cobalt was plotted and analyzed for the determination of optimum time of leaching.

3.4.3.4. Effect of solid liquid ratio

The solid-liquid ratio was varied and the concentration of acid, temperature, time period of leaching and the stirring speed were kept constant during these leaching experiments. The solid/liquid ratio for the maximum dissolution of lithium and cobalt was identified from the dissolution versus solid-liquid ratio curves of lithium and cobalt.

3.5. UV-visible Spectrophotometer determination of Co (PP & PDC, BCSIR)

A Shimadzu UV-Visible Spectrophotometer–1601 was used for the determination of cobalt in the leach liquor. During measurement from an unknown solution by UV spectrophotometry, absorbance is determined from the machine and the corresponding concentration of the species is calculated from a calibration curve. The absorbance of solution was found near 415 nm against a reference.

Calibration flow chart for Cobalt:

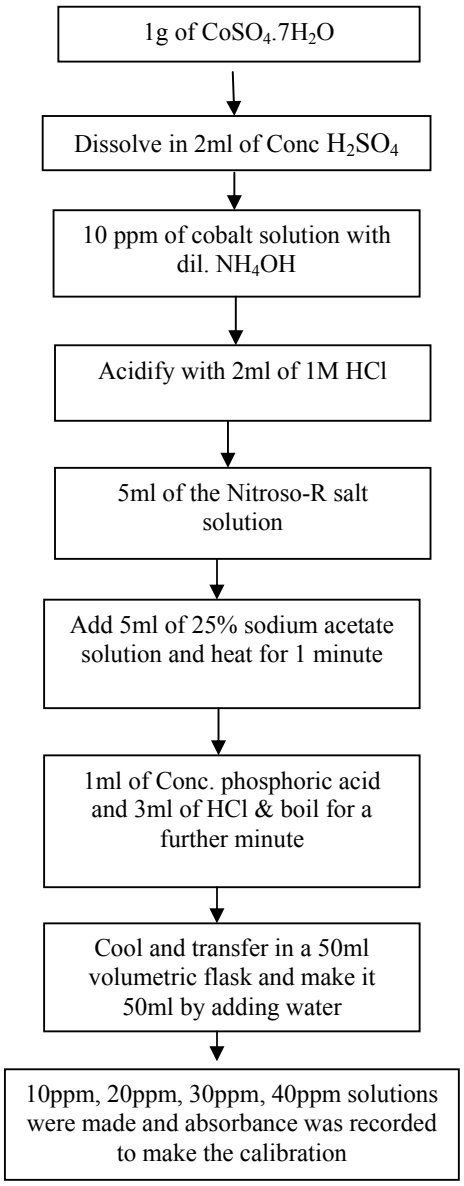

Fig.3.6: Calibration curve for cobalt estimation in UV- Spectroscopic

3.6. Flame Photometry Analysis of Lithium (PP & PDC, BCSIR)

The AFP-100 is used to determine Na, K, Ca and Li in plant material, food, beverages, and electrolytes in serum, body fluids, alkali and alkaline earth metal. An atom of a given element gives to a definite, characteristic line spectrum. It follows that there are different excitation state associated with different elements. The emission between the two values is converted to element concentration or mass Beer-Lambert Law.

Fig. 3.7: Atomic Flame Photometer

Sensitivity

Element	:	Na	K	Li	Ca
in ppm	:	0.5	0.5	0.5	15

Range

Element	:	Na	K	Li	Ca
in ppm	:	1-100	1-100	1-100	15-100
in mEq *	:	0-200	0-100	0-10	0-5

Linearity

Element	:	Na	K	Li	Ca
in %	:	---------- Better than 2% ----------			

Reproducibility

Element	:	Na	K	Li	Ca
in %	:	--------- 1% CV for 20 consecutive samples ----------			

Flame System	LPG and oil-free dry air
Detector	Photodiode
Power Requirement	90-260V, 47-63Hz, Max 65 VA

Calibration Curve

"Anal R" quality of Li_2CO_3 was weighed accurately and dissolved in minimum quantity of 1:1 HCl. Double distilled water was added to make it exactly 250ml. It was then diluted to 1:10 to get 10mg Li/100ml which is equivalent to 100ppm. From this 100 ppm standard solution five standard sample of 10ppm, 20ppm, 60ppm, 80ppm were made for calibration equipment for lithium sample.

Sample was aspirated through nebulizer and the absorbance was measured with a blank as a reference

3.7. Atomic absorption spectroscopic analysis of Lithium and Cobalt

Chemical analyses for leach liquor were performed with an Atomic Adsorption Spectroscopy (VARIAN AA240 FS).

Fig. 3.8 Atomic Absorption Spectroscopy (VARIAN AA240 FS)

Operating conditions:

Air acetylene flames for all elements were maintained.

For Cobalt estimation: Wavelength was = 204.7 nm; Lamp current was = 5.00 mA

For Lithium estimation : Wavelength was = 670.4 nm; Lamp current was = 5.00 mA

Sample was aspirated through nebulizer and the absorbance was measured with a blank as a reference. Calibration curve was obtained using 2 standard samples each time. In AAS analysis, samples had to be diluted many folds to keep the results in the analytical range.

3.8. Determination of activation energy

For kinetic study the particles were assumed to be perfectly homogeneous spherical solid phases and shrinking core model was selected to analyze the leaching mechanism. The experimental data was matched with the data of the following models:

1. Liquid film diffusion controlled

$$\frac{t}{\tau} = 1 - (1 - X)^{2/3}$$

2. Diffusion controlled through the product layer

$$\frac{t}{\tau} = 1 - 3(1 - X)^{2/3} + 2(1 - X)$$

3. Chemical reaction controlled

$$\frac{t}{\tau} = 1 - (1 - X)^{1/3}$$

where, τ = Time for complete disappearance of particles
and X = Fraction of reacted particles

3.8.1 Integral approach

In the integral form, t/τ versus time (t) were plotted. The reaction rate constants, k, at various temperatures for hydrochloric acid leaching were obtained from linearised plots of t/τ versus time (t). The rate constant, k was then plotted against temperature according to the Arrhenius type equation.

Arrhenius equation: $k = A \exp^{(-E/RT)}$

Therefore, $\ln k = \ln A - E/RT$

Here, k = Reaction rate constant
E = Activation energy
R = Universal gas constant
T = Reaction temperature
and A = Pre-exponential factor.

The apparent activation energy of the process is estimated from the Arrhenius type plot as Slope = -E/R

3.9. Lithium and Cobalt recovery from leaching solution

Separation of lithium and cobalt from sulfuric acid leach liquor of did not perfomed because the efficiency was near about 80 percent. Besides this, in case of commercial perpose sulfuric acid was costly. In addition to that, in sulfuric acid leaching parameter were limited. High solid liquid ration and more hydrogen per oxide required which made the process costly.

Considering in all respect, separation of lithium and cobalt from the hydrochloric acid leach liquor was performed by employing redox reaction. Direct addition of small additions of sodium hydroxide to the leach liquor gave no precipitate, because the leach liquor was excessively acidic. The pH of the solution had to be controlled by the addition of NaOH to effect precipitation of cobalt hydroxide. Therefore, precipitation of cobalt was recovered by addition one equivalent volume of 2M sodium hydroxide solution until changing the pH value.

Cobalt was precipitated as Cobalt hydroxide by the pH control method. The precipitation of $Co(OH)_2$ occurred at pH 12. pH was adjusted by adding required amount of NaOH.

After the recovery of cobalt as cobalt hydroxide, the resultant leach liquor was concentrated and treated with a saturated sodium carbonate solution to precipitate lithium as lithium carbonate. The precipitation process was performed at a temperature of approximately 100°C. The lithium carbonate was recovered by filtration and was washed with hot water to remove the residual liquor. These two recovery products were dried in oven.

3.9.1. Characterization of Recovered Products

The two products separated from the leach liquor were dried in an oven and subsequently subjected to x-ray diffraction analysis. The diffraction lines belonging to cobalt hydroxide and lithium carbonate were identified in the diffraction patterns. Some diffraction lines in both the patterns could not be identified.

Chapter 4

RESULTS AND DISCUSSIONS

4.1 Analysis of the Separated Parts in Spent

Dimension of the two types of lithium ion type batteries are shown in Table 4.1. All the other lithium ion type batteries are square in shape. Wide variations in dimensions of the different brands of the same type of battery were observed, data given in Table 4.1 are the typical values of the two types. Fig. 4.1 gives a view of the dismantled part of LIBS.

Table 4.1: Dimension of the typical lithium ion batteries

Battery type	Dimension (cm)
M 660	Length = 4.2 cm ,Width = 2.5 cm , Thickness = 1 m
V 83	Length = 4 cm , Width= 2.4 cm , Thickness= 0.8 cm

Weights of different components of the spent batteries were measured and the weight proportions were determined. The values reported for each of the components in this presentation are the average values of five randomly selected samples. These are shown in Table 4.2 and Table 4.3

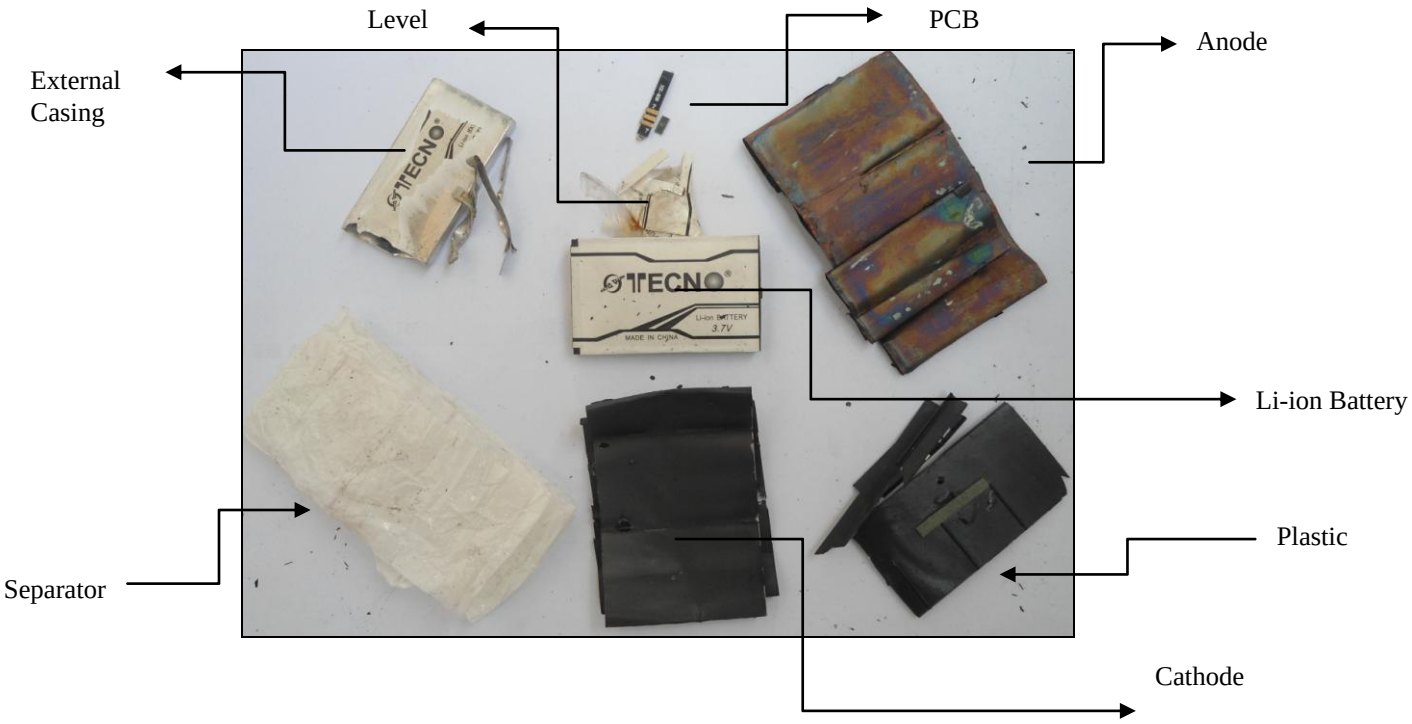

Fig. 4.1: A dismantled spent Lithium ion battery

Table 4.2: Percentage weight analysis of different parts in **M 660 Type** spent Lithium ion battery

SL.NO	Potential Voltage	Weight (gm)	Level for Branding (gm)	Ext. Casing (gm)	Chip of Circuit (gm)	Plastic Material (gm)	Cathode (gm)	Al-Foil (gm)	Anode (gm)	Cu-Foil (gm)
1	3.7V	29.599	0.504	4.821	0.399	3.574	10.551	1.107	7.284	0.869
2	3.7V	30.341	0.507	4.823	0.401	3.643	10.735	1.213	7.714	0.988
3	3.7V	30.807	0.497	5.063	0.387	3.663	10.953	1.113	7.936	1.092
4	3.7V	30.891	0.493	4.912	0.391	3.625	10.961	1.019	8.023	1.126
5	3.7V	31.065	0.529	4.826	0.397	3.630	11.354	1.158	8.163	1.195
Av. Wt	-	30.540	0.506	4.889	0.395	3.627	10.910	1.122	7.824	1.054
Wt%	- 0.75	100	1.66	16.01	1.29	11.88	35.73	3.64	25.60	3.45

Table 4.3: Percentage weight analysis of different parts in **V 83 Type** spent Lithium ion battery

SL.NO	Potential Voltage	Weight (gm)	Branding Level (gm)	External Casing (gm)	Chip of Circuit (gm)	Plastic Material (gm)	Cathode (gm)	Al-Foil (gm)	Anode (gm)	Cu-Foil (gm)
1	3.7V	23.787	0.499	3.206	0.379	3.174	7.899	0.967	5.785	0.869
2	3.7V	24.507	0.507	3.523	0.401	3.263	8.535	0.983	5.812	0.918
3	3.7V	24.610	0.493	3.363	0.385	3.463	8.853	0.967	5.892	0.927
4	3.7V	23.852	0.495	3.512	0.391	3.319	8.354	0.965	5.797	0.895
5	3.7V	24.879	0.519	3.626	0.397	3.256	8.836	1.053	5.906	0.956
Av. Wt		24.327	0.503	3.446	0.391	3.295	8.495	0.987	5.838	0.913
Wt (%)	-1.89	100	2.06	14.17	1.61	13.54	34.92	4.06	24	3.75

The weight percentage of the components in a battery of different types can also be expressed as a pie chart. This is shown in Fig. 4.2.

Data from Tables 4.4 and 4.5, show a comparison of weights of the different components parts of the two types of batteries. Variations in the weight proportions of the different component parts of the two types of batteries were noted. The weights of the different component parts of the same type of spent batteries were also found to vary. These variations in the weight of the whole battery and in the weight proportions of the different component parts of the spent batteries could be attributed to the difference in the physical condition of the battery when collected and mechanical loss and contamination during the manual dismantling of the batteries. The pie chart of M 660 and V 83 type batteries clearly indicate every proportion of spent batteries.

Table 4.4: Comparison of different components parts of the two types of spent batteries.

Components	M 660	V 83
Whole battery	**30.540 gram**	**24.327 gram**
Level for Branding	0.506	0.503
External Casing	**4.887**	**3.446**
Chip of Circuit	0.395	.391
Plastic Material	3.627	3.295
Cathode Electrode	**10.910**	**8.495**
Aluminum Foil (25µm)	1.122	0.987
Anode Electrode	**7.824**	**5.838**
Copper Foil (25µm)	1.054	0.913
Loss	0.215	0.458

Table 4.5: Comparison of weight proportions of different components parts of the two spent batteries

Components	M 660 (% wt)	V 83 (% wt)
Whole battery	100	100
Level for Branding	1.66	2.06
External Casing	16.01	14.17
Chip of Circuit	1.29	1.61
Plastic Material	11.88	13.54
Cathode Electrode	35.73	34.92
Aluminum Foil	3.64	4.06
Anode Electrode	25.60	24.0
Copper Foil	3.45	3.75
Loss	0.75	1.89

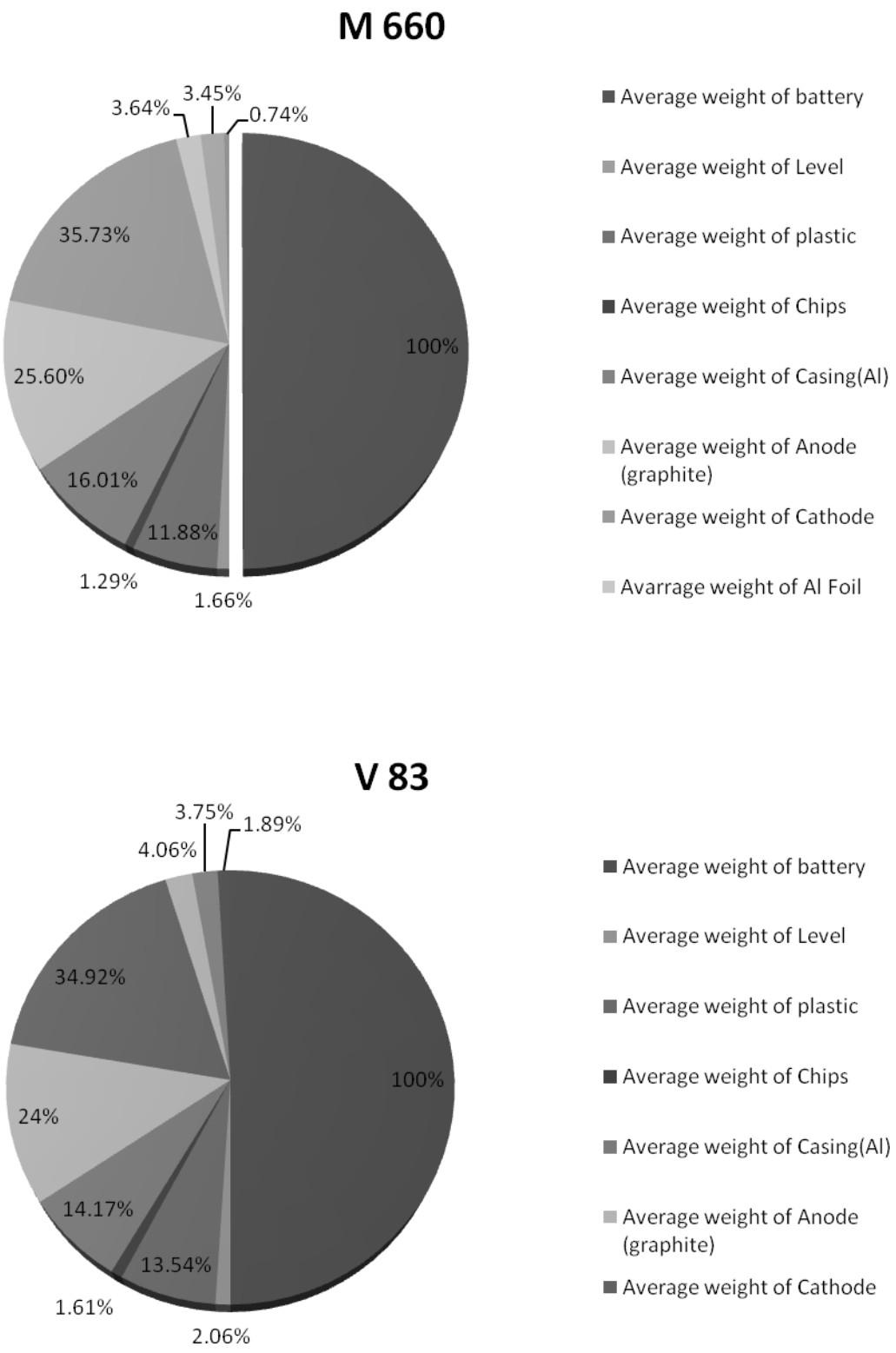

Fig. 4.2: Expression in pie chart of the spent battery components of M 660 and V 83.

4.2 Characterization of the Battery Components

4.2.1. Identification of the structural components

The chemical compositions of external casing of the two types of spent lithium ion batteries selected for this investigation were determined by optical emission spectroscopy and were essentially the same (Table 4.6). The material may be classified as commercially pure aluminum with the usual impurity elements. Materials that are used in the construction of the different component parts of the lithium ion battery are given in Table 4.7

Table 4.6: Optical emission spectroscopic analysis of the casing of spent Lithium ion battery

Elements	Na	**Si**	P	S	Cl	**Al**	Cr	Mn	**Fe**	Ni	Cu	V	Ti
Wt% (M 660)	-	**0.20**	-	-	-	**98.3**	0.02	0.72	**0.54**	0.08	0.06	0.01	0.04
Wt% (V 83)	-	**0.21**	-	-	-	**98.4**	0.03	0.70	**0.49**	0.04	0.07	0.01	0.03

Table 4.7: Materials Used in the Construction of the Different Component Parts (M660 and V83)

No.	**Component Parts**	**Materials**
1	External Case	Aluminum Alloy, Paper
2	Cathode	$LiCoO_2$
3	Anode	Graphite conductor
4	Electrolyte*	$LiClO_4$, $LiPF_6$
5	Electrolyte Solvent*	PC, DMC or DMC
6	Separators*	Plastics generally Polypropylene (PP), Polyethylene (PE)
7	Current Collector	Aluminum & Copper Foil
8	Current Joining*	Gold Plated Pad
9	Printed circuit board(PCB)	Component etc

* Materials have been identified on the basis of information available from published literatures [6].

4.2.2. Estimation of Aluminum in Aluminum Foil

The thickness of the aluminium foil in both the types of batteries under investigation was 25 µm. The amount of aluminum in the aluminum foil was determined by Atomic Absorption Spectroscopy (AAS). The amount of aluminum in the foil of M660 type battery was found to be 98.90% while the amount of aluminium in the foil of V83 type battery was found to be and 98.66%. Aluminum foil used as current collector is expected to be 100 percent pure. The presence of impurities in the aluminium foil of the spent batteries may be attributed to the physical contamination during the manual dismantling process. Aluminum could also have been contaminated by oxidation after the coating material was removed.

4.2.3. Estimation of Copper in Copper Foil

The thickness of copper foil in both the types of batteries was 25µm. The amount of copper in copper foil was determined by wet chemical analysis. In the M 660 type battery the amount of copper was found to be 99.06% and while the amount of copper in the V83 type battery was found to be 98.86%. In good agreement with the results of wet chemical analysis, the X-ray diffraction patterns (Fig.4.3) of the copper foils did not indicate the presence of impurities.

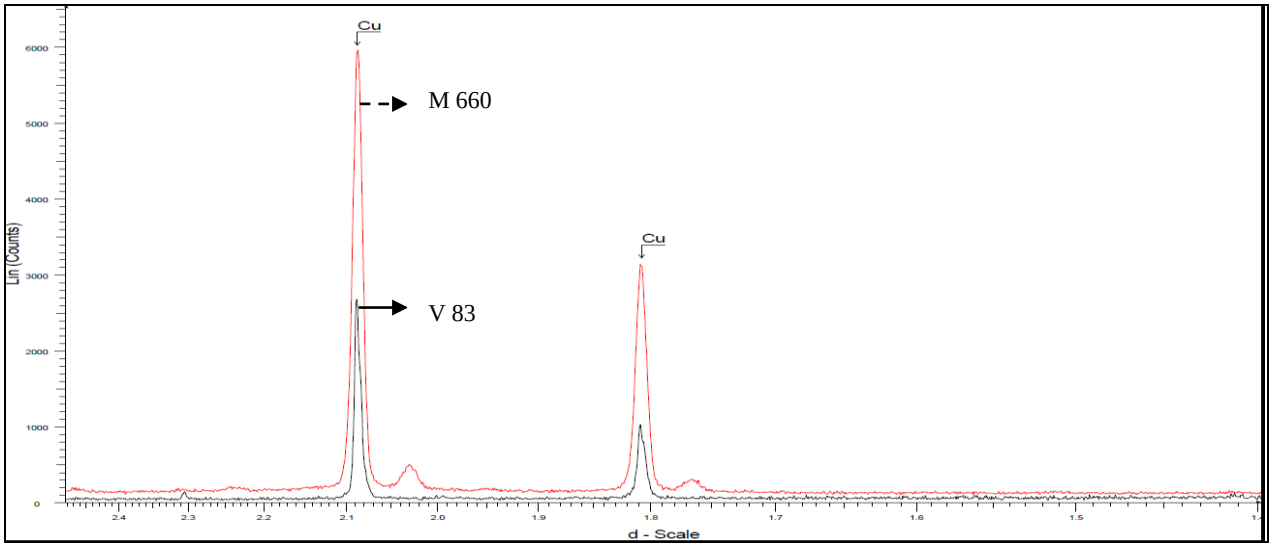

Fig.4.3: X-ray diffraction analysis of copper foil of M 660 and V83 Lithium ion Battery

4.2.4. Characterization of the Cathode

The composition of the paste on the cathode could not be determined by the x-ray fluorescence analysis as lithium was present as compound. The x-ray diffraction analysis, performed to identify the phases present in the paste, showed the presence of Li and Co in the form of $LiCoO_2$ as the major constituent (Fig.4.4 and Fig.4.5). The intensity (counts) of the intense diffraction lines in the pattern of M 660 battery was much higher than those in the V83 battery. The most intense peaks in the diffraction patterns of both the batteries occurred at almost the same angle, at near 19^0 and at 46^0. These peaks correspond to $LiCoO_2$. The patterns also contained some diffraction lines that could not be identified. These diffraction lines occurred at the same angles in the cathodic paste of both the batteries. In the figures, these lines have been marked as “U” and might be due to the binders or additives mixed with the active cathode material to facilitate its adhesion to the aluminum foil. It was thus inferred that Li and Co was present in the cathodes of lithium ion batteries in the form of lithium cobalt oxide.

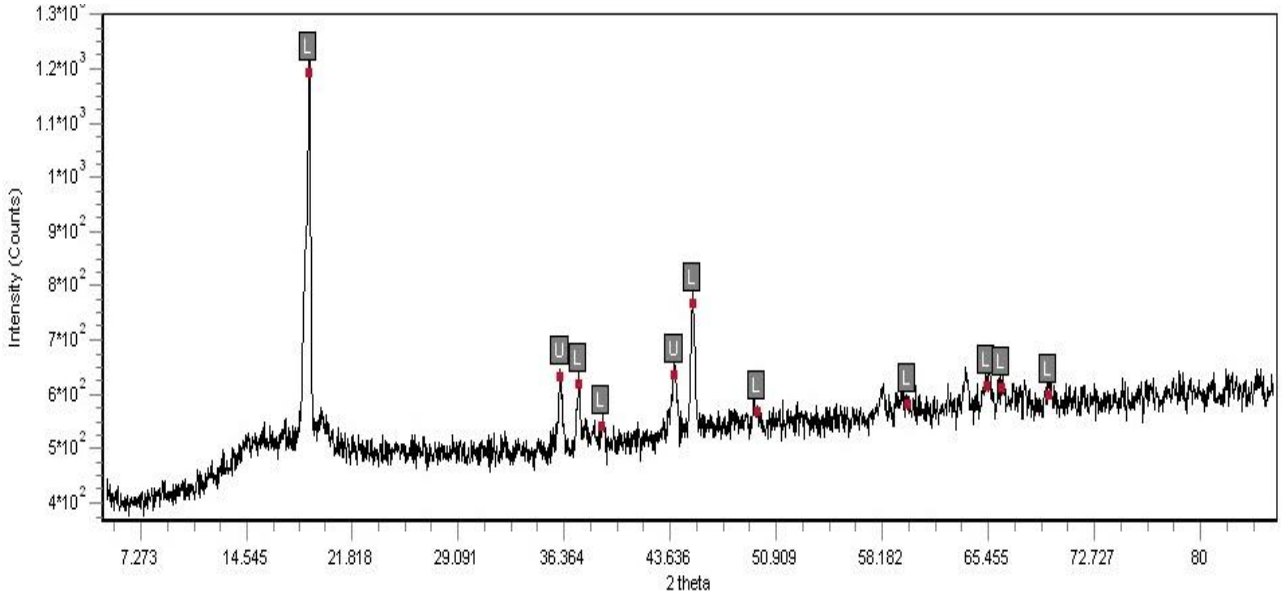

Fig. 4.4: X-ray diffraction analysis of cathode electrode of M 660 Lithium ion Battery

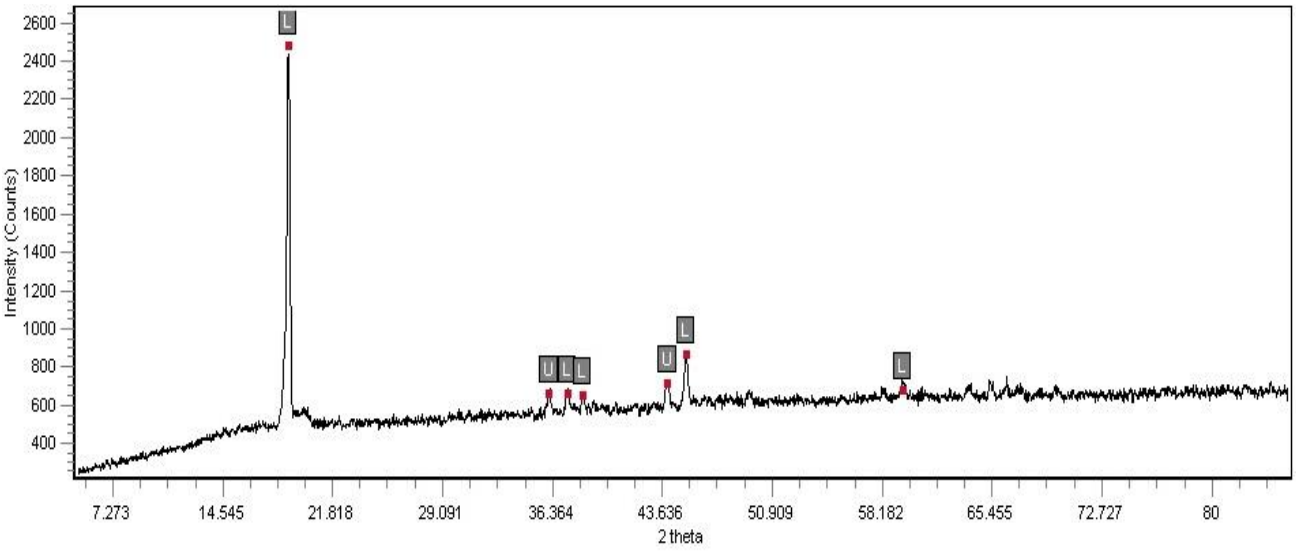

Fig.4.5: X--ray diffraction analysis of cathode electrode of V 83 Lithium ion Battery

4.2.5. Characterization of the Anode

The most intense peaks in the x-ray diffraction patterns recorded the material pasted on an anode of a spent lithium ion battery (Fig. 4.6) occurred at near 31.24^0 and at 51.56^0. These lines correspond to graphite. The diffraction lines that could not be identified has been marked as "U" and might be related to the additives or binders that were used to facilitate pasting of the active material on to the copper foil.

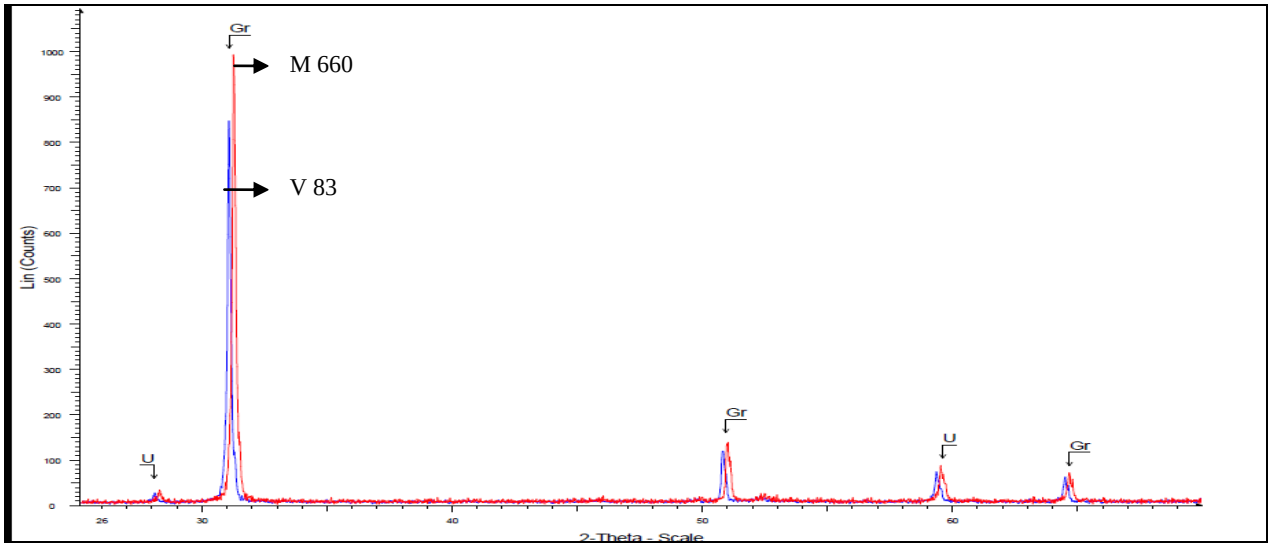

Fig. 4.6: X--ray diffraction analysis of anode electrode of M 660 and V83 Lithium ion battery

4.2.6 Total value metal percentage

The average values of the metal contents of spent lithium ion type batteries in are given in Table 4.8. Lithium was found to be around 2.50 percent and cobalt around 21.31percent of the total weight of the spent batteries. LIBs constituted aluminum around 18.76 percent and copper around 3.54 percent of the total weight. The remaining part is occupied by the carbon, PCB, plastics, adhesive and other minor elements.

Table 4.8: Average metal proportions in the spent M 660 & V 83 lithium ion batteries *

Types	**Spent Lithium ion Battery**							**Total value metals**			
	Total Weight (gm)	**Al casing (gm)**	**Al Foil (gm)**	**Amount of Al (gm)**	**Cu Foil (gm)**	**Amount of Li in Cathode (gm)**	**Amount of Co in Cathode (gm)**	**Total Al %**	**Total Li%**	**Total Cu %**	**Total Co %**
M 660	30.540	4.804	1.09	5.786	1.04	0.774	6.57	**19.29**	**2.53**	**3.41**	**21.51**
V 83	24.327	3.390	0.97	4.282	0.90	0.602	5.12	**17.92**	**2.47**	**3.69**	**21.05**
				Weighted Average				**18.64**	**2.51**	**3.53**	**21.31**

- Total metal values have been determined on as received battery lithium and cobalt was assume from weight percentage in received battery

4.3. Hydrometallurgical route for recovery of metals

4.3.1. Leaching

Cathode of the spent battery was leached in sulfuric acid and in hydrochloric acid. A small amount of hydrogen per oxide was added to sulfuric acid. Hydrogen per oxide acts as a reducing agent. The effect of temperature, time, hydrogen per oxide and solid/liquid ratios were determined in the leaching experiment. Thus, the variable parameters were acid concentration, hydrogen per oxide concentration and solid/liquid ratio for sulfuric acid. The variable parameters were acid concentration, time, hydrogen per oxide, temperature and solid/liquid ratio for hydrochloric acid.

Leaching was performed in a 500 ml round bottom flask fitted with a mechanical stirrer, thermometer and a refluxing condenser. The different variable parameters and their influence on leaching experiments are discussed in the following paragraphs.

4.3.1.1. Effect of sulfuric acid concentration

The effect of sulfuric acid concentration, in the range 0.5 to 3M, on the extent of dissolution of lithium and cobalt from the cathode of lithium ion battery was studied. The other parameters i.e., concentration of hydrogen peroxide (5%), stirring speed (400 rpm) and solid/liquid ratio (1:20) were kept constant during this study. It can be seen that the leaching rates increase gradually with the increase of initial sulfuric acid concentration. The increase in the amount of acid can increase the dissolution rate based on kinetics. Dissolution of lithium and cobalt were found to increase up to the sulfuric acid concentration of 2.5M. Above this concentration, the extent of dissolution same to some extent, may be for some Caro's acid formation at the higher concentrations of sulfuric acid.

$$H_2SO_4 + H_2O_2 \rightarrow H_2SO_5\,(\text{Caro's acid}) + H_2O$$

$$LiCoO_2 + H_2SO_5 + H_2O \rightarrow Li_2SO_4 + CoSO_4 + H_2O + O_2\uparrow$$

The percentage dissolution of lithium and cobalt versus sulfuric acid concentration is plotted in Fig. 4.7.

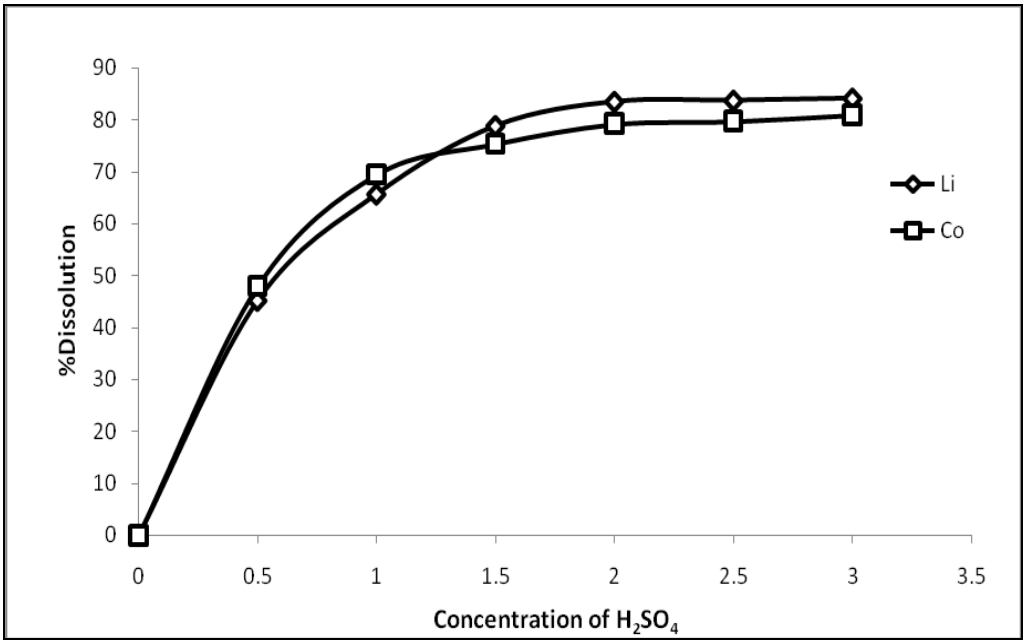

Fig. 4.7: Effect of H_2SO_4 concentration on lithium and cobalt dissolution percentage.
(Fixed Variable: Solid-liquid ratio = 1:20 gm/ml, H_2O_2 = 5% and Room Temperature)

Dissolution of lithium and cobalt into the leaching solution was a fast reaction. In 2.5M sulfuric acid, the dissolution of 84% lithium and 80% Cobalt was completed within only few minutes. Though the reaction was exothermic hence, temperature and time was not fixed. With the increasing retention time of the electrolyte in solution, the extent of dissolution did not increase significantly. At concentrations above 2.5M, the extent of dissolution did not increase furthermore. Hence, a sulfuric acid concentration of 2.5M was considered optimum for lithium and cobalt recovery from the spent LIBs cathode.

4.3.1.2. Effects of H_2O_2 concentration

Although, H_2O_2 is an oxidizing agent, in presence of a strong oxidizing agent, it acts as a strong reducing agent. Leaching without any H_2O_2 addition to the solution was rather slow. The dissolution of lithium and Cobalt reached only 60% in few minutes time with 1% addition of H_2O_2.

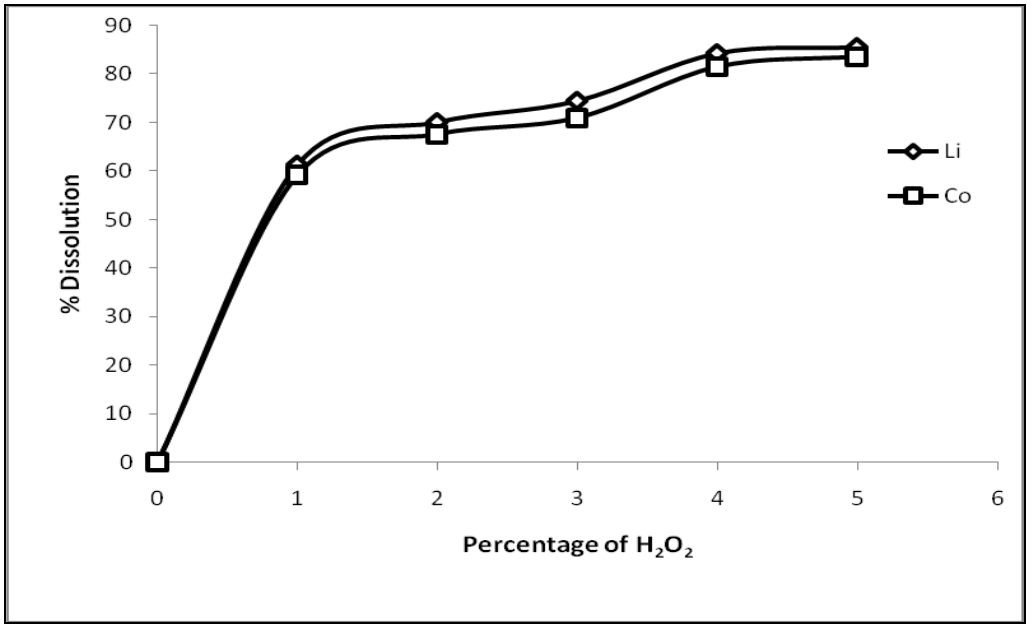

Fig. 4.8: Effect of H_2O_2 concentration on the dissolution of lithium and cobalt dissolution.
(Fixed Variable: Solid-liquid ratio = 1:20 gm/ml, H_2SO_4 = 2M and Room Temperature)

H_2O_2 concentration was varied keeping the other variables fixed. Increasing the H_2O_2 concentration increased the extent of dissolution of lithium up to 5% H_2O_2 (Fig. 4.8). Above 5% H_2O_2, the slope of extent of lithium dissolution did not change significantly. However, up to 5% H_2O_2 in the leach liquor, the dissolution of lithium was quite satisfactory, reaching 84% within only few minutes of time.

Dissolution of cobalt in the leach liquor without any hydrogen peroxide addition was also slow. In 2.5M sulfuric acid solution at room temperature a stirring speed of 400 rpm and a solid-liquid ratio of 1:20, dissolution of cobalt was not significant. Increasing the hydrogen peroxide concentration up to 5% increased the extent of dissolution of cobalt (Fig. 4.8). This behavior seems to be due to the reduction of Co^{3+} to Co^{2+}, which dissolves readily. The dissolution of cobalt increased up to 80% with 5% H_2O_2 within only few minutes time of leaching.

4.3.1.3. Effect of solid/liquid ratio

The ratio of solid to liquid was varied from 1:10 to 1:50 and other parameter was kept fixed. For lithium and cobalt the effect of solid/liquid ratio on the extent of dissolution was intense. Percentage dissolution of increased up to 84 % within few minutes due to an increase in the solid/liquid ratio from 1:10 to 1:30 . The percentage dissolution of lithium was found to decrease when the solid/liquid ratio was increased to 1:30 (Fig. 4.9).

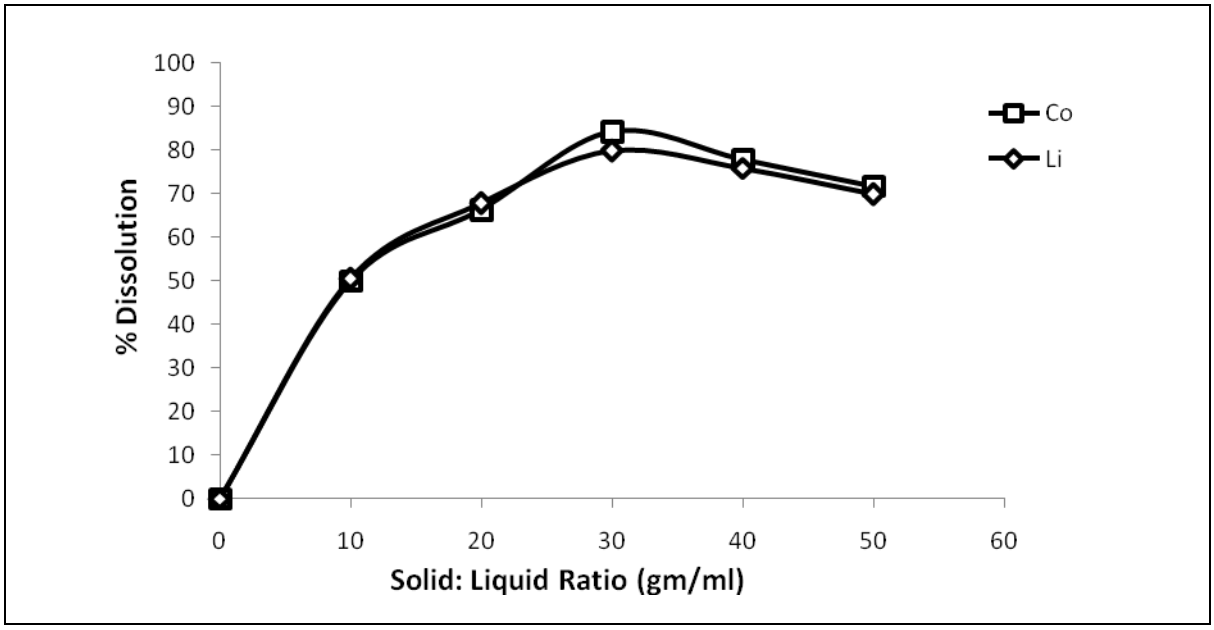

Fig. 4.9: Effect of solid/liquid ratio on the dissolution percentage on lithium and cobalt.

(Fixed Variable H_2SO_4 = 2M, H_2O_2 = 3% and Room Temperature)

The dissolution of cobalt increased with increasing the solid/liquid ratio in the leaching solution. The effect on cobalt dissolution with increasing the solid/liquid ratio up to 1:30 is shown in Fig. 4.9.

The maximum dissolution occurred at a solid/liquid ratio of 1:30. Under such conditions the dissolution of cobalt reached up to 80% within only few minutes and addition of 5% hydrogen per oxide. The other parameters, sulfuric acid concentration, temperature and stirring speed were kept constant during this experiment. Above 1:30 solid/liquid ratio could decrease the concentration of metal ion in leaching solution. But too high S/L ratio would lead to the increase of leaching solution volume, which is not favorable to subsequent separation.

4.3.1.4. Optimum leaching conditions for leaching with sulfuric acid

The optimum leaching conditions for the maximum recovery percentage of lithium and cobalt from the spent battery was taken to be:

Sulfuric acid concentration = 2.5M
Hydrogen per oxide concentration = 5%
Temperature = Room Temperature
Solid/Liquid ratio = 1:30
Without Stirring

Maximum Lithium dissolution = 84.25%
Maximum Cobalt dissolution = 79.83%
Time = Instantly.

4.3.1.5. Effect of Hydrochloric acid concentration

The effect of hydrochloric acid concentration, in the range 1 to 4M, on the extent of dissolution of lithium and cobalt from the cathode was studied. The other process parameters were kept fixed at temperature = 80^0C, stirring speed = 400 rpm, time = 60 min, solid/liquid ratio = 1:20 (gm/ml) and hydrogen peroxide concentration = 3%. Dissolution of lithium and cobalt was found to increase with an increase in the hydrochloric acid concentration of up to 3M. The percentage dissolution of lithium and cobalt versus concentration of HCl is plotted in Fig. 4.10

$$LiCoO_2 + HCl + H_2O \rightarrow Li_2SO_4 + CoSO_4 + H_2O + O_2$$

.

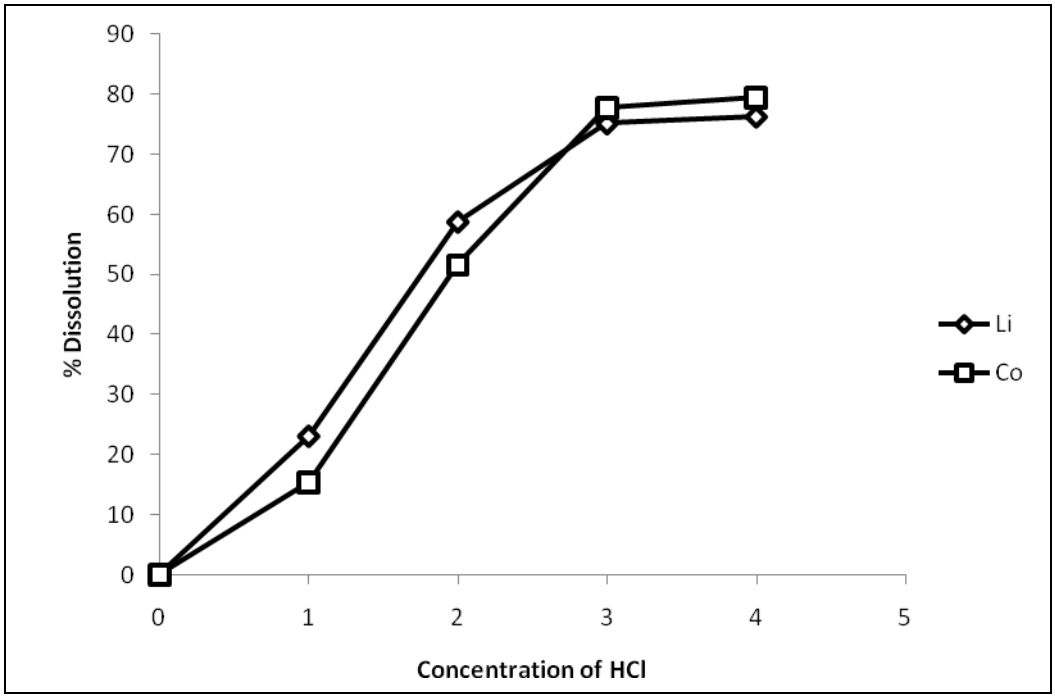

Fig. 4.10: Effect of HCl concentration on dissolution of Lithium and Cobalt
(Fixed Variable: Temp = 80^0C, S/L Ratio = 1.20 gm/ml, Stirring speed = 400 rpm, time = 60 min and H_2O_2 = 3 %.)

4.3.1.6. Effect of solid/liquid ratio in HCL medium

The ratio of solid to liquid was varied from 1:5 to 1:20 while the other parameters were fixed as: temperature = 80^0C, hydrochloric acid concentration = 3M, stirring speed = 400 rpm, time = 60 min and hydrogen peroxide concentration = 3%. The effect of solid/liquid ratio on the extent of dissolution

of lithium and cobalt was rather intense (Fig. 4.11). Extent of dissolution of lithium increased from about 30 percent at a solid-liquid ratio of 1:5 to 79% during leaching at a solid-liquid ratio of 1:15. The percentage dissolution of lithium was about 80% at a solid/liquid ratio of 1:20. The extent of dissolution of cobalt, at all solid-liquid ratios investigated, was slightly higher.

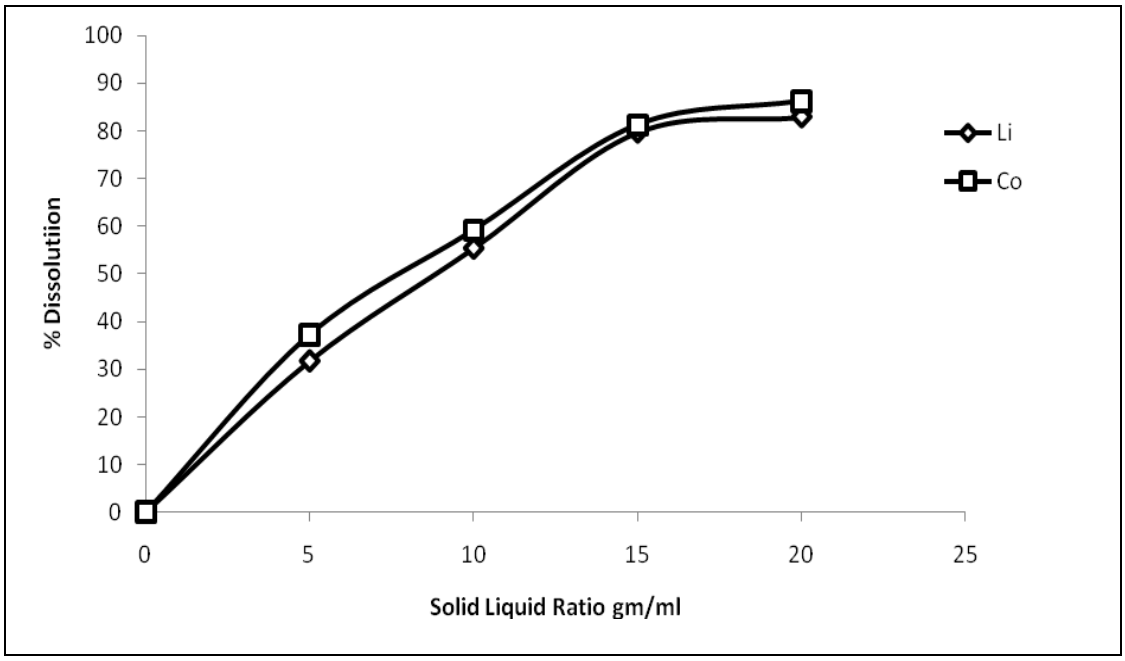

Fig. 4.11: Effect of solid/liquid ratio on the dissolution percentage on lithium and cobalt.
(Fixed Variable: Temp = 80^0C, HCl = 3M, Stirring = 400 rpm, time = 60 min and H_2O_2 = 3 %.)

4.3.1.7. Effect of temperature and time in HCL medium

Temperature was varied from 40°C to 100°C, while the other variables were kept fixed at: S/L ratio = 1:20, hydrochloric acid concentration = 3M, stirring speed = 400 rpm, time = 60 min and hydrogen peroxide concentration = 3 percent. The extent of dissolution of both Li and Co increased with an increase in the leaching temperature (Fig. 4.12). The increase in the rate of dissolution was not significant at temperatures above 80°C. Thus the optimum temperature for leaching of lithium and cobalt were taken to be 80°C. Moreover, at temperatures above 80°C, the cost of operation increases and hydrochloric acid poignantly evaporates resulting in the deterioration of the operation conditions.

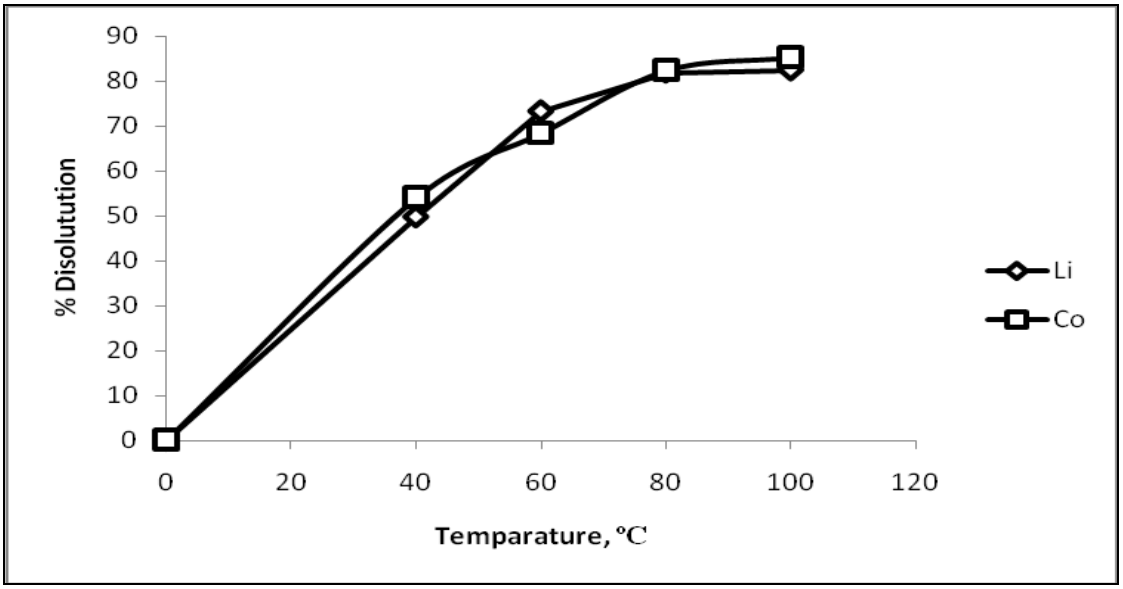

Fig. 4.12: Effect of temperatures on dissolution percentage of lithium and cobalt

(Fixed Variable: HCl = 3M, S/L Ratio = 1.20 gm/ml, Stirring = 400 rpm, time = 60 min and H_2O_2 = 3 %.)

Time of leaching was varied from 20 minute to 80 minute keeping the other variables in the leaching experiment fixed. The extent of dissolution increased with time of leaching (Fig. 4.13). A maximum dissolution of about 83.69% could be obtained within 60 minutes of leaching.

.

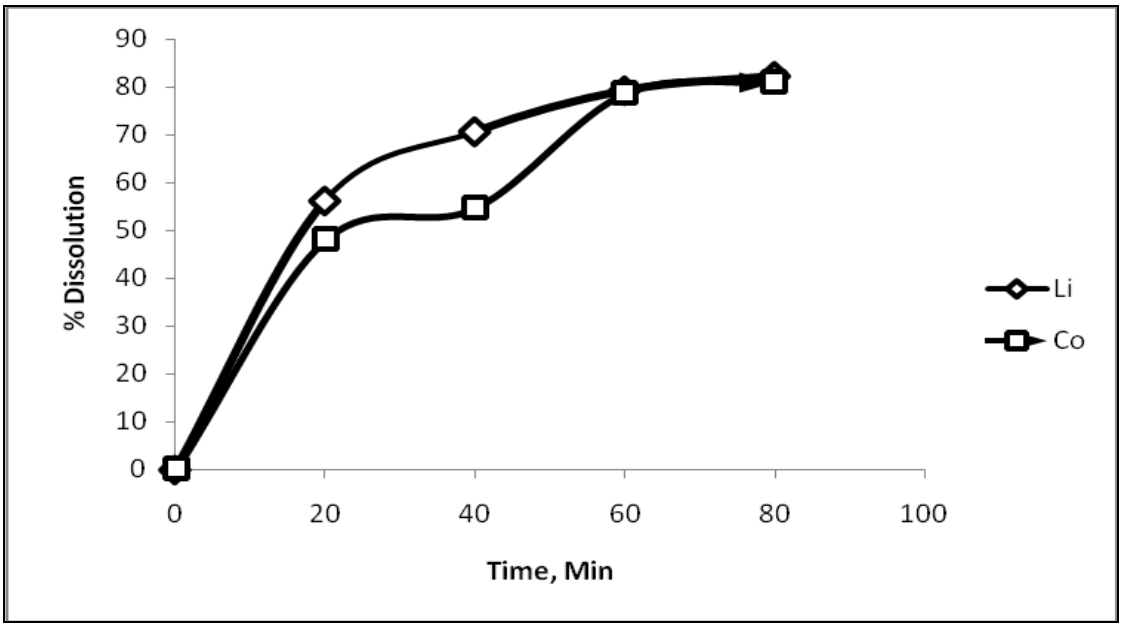

Fig. 4.13: Effect of time on dissolution percentage of lithium and cobalt

(Fixed Variable: Temp = 80^0C, HCl = 3M, S/L Ratio = 1.20 gm/ml, Stirring = 400 rpm, and H_2O_2 = 3 %.)

At all temperatures under investigation, the dissolution of lithium was fast at the initial stages of leaching. Later the dissolution increased gradually beyond 50 minutes of leaching time. It can also be seen that the rate of dissolution intensified greatly with an increase in temperature (Fig. 4.14). At 40^0C, the dissolution was only around 49% in 10 minutes which was increased to 70% at 80^0C in 10 minutes of leaching. The recovery was about 75% within only 40 minutes of leaching at 60^0C. The maximum recovery increased to 83.69% within 60 minutes of leaching at temperature 80^0C.

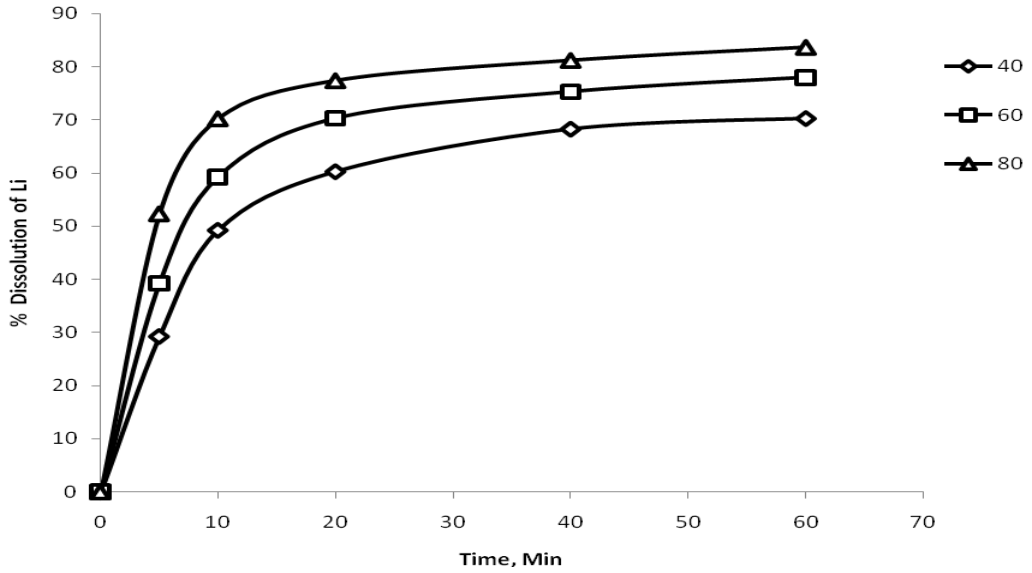

Fig. 4.14: Effect of time and temperatures on dissolution percentage of lithium
(Fixed Variable: HCl = 3M, S/L Ratio = 1.20 gm/ml, Stirring = 400 rpm and H_2O_2 = 3 %.)

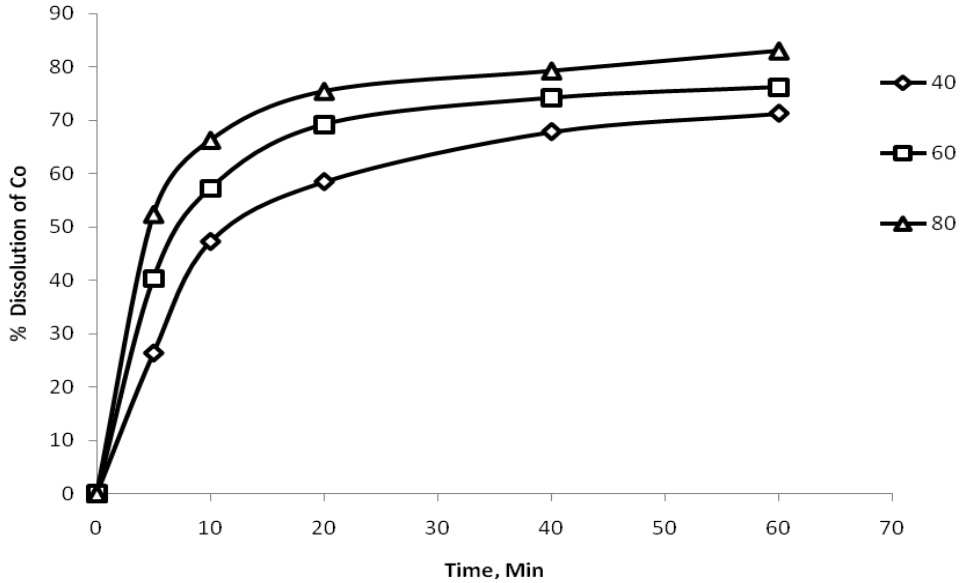

Fig. 4.15: Effect of time and temperatures on dissolution percentage of Cobalt
(Fixed Variable: HCl = 3M, S/L Ratio = 1.20 gm/ml, Stirring = 400 rpm and H_2O_2 = 3 %.)

The effect of temperature on the leaching of cobalt is shown in Fig. 4.15. The extent of dissolution of cobalt was increased with temperature for first 40 minutes at all temperatures under investigation. Later the dissolution was increased gradually slow up beyond 53 minutes of leaching time. At 40^0C, the dissolution was only around 47% in 10 minutes which was increased to 66% at 80^0C in 10 minutes of leaching. The recovery was about 74% within only 40 minutes of leaching at 60^0C. The maximum recovery increased to 83% within 60 minutes of leaching at temperature 80^0C.The optimum temperature for leaching of lithium and cobalt was taken to be 80^0C.

4.3.1.8. Effects of H_2O_2 concentration in HCl Medium

To investigate the effects of H_2O_2 concentration on the extent of dissolution, the concentration of H_2O_2 was varied from 0% to 4%. The other variables were kept fixed at: temperature = 80^0C, hydrochloric acid concentration = 3M, S/L ratio = 1:20, stirring speed = 400 rpm and time = 60 min). An increase in the H_2O_2 concentration increased the extent of dissolution of both lithium and cobalt (Fig. 4.16). This increase in dissolution of cobalt has been attributed to the reduction of Co^{3+} to Co^{2+} which dissolves readily. While the hydrogen peroxide helps the dissolution of cobalt, the dissolution of lithium is promoted because the two metals are contained in the same oxide compound. The optimum amount of H_2O_2 in the leach liquor was taken to be 3.5% for dissolution of lithium and cobalt.

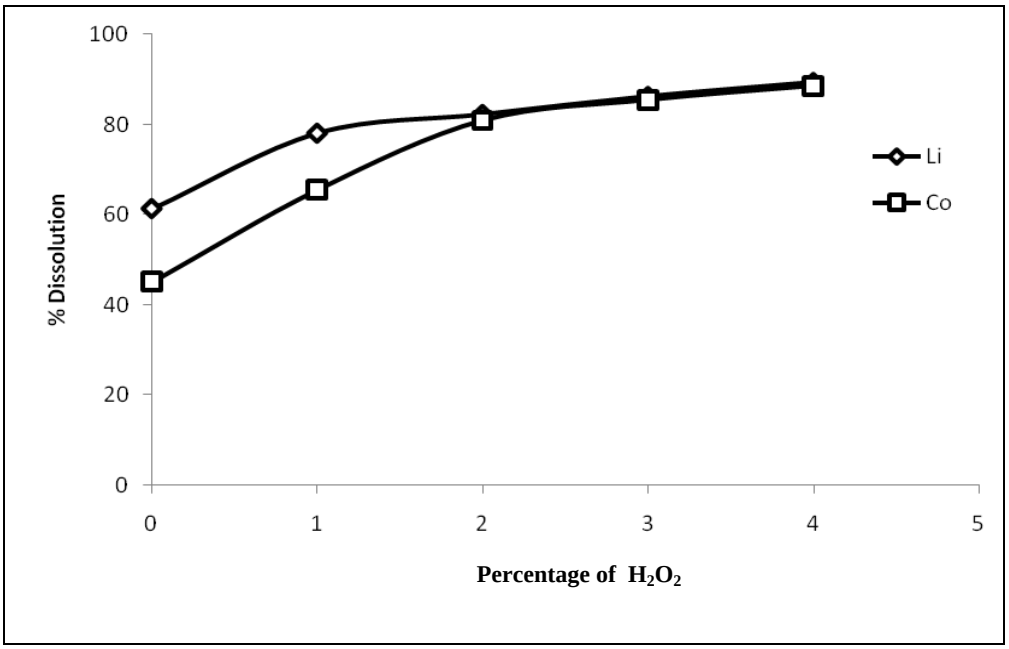

Fig. 4.16: Effect of H_2O_2 concentration on dissolution of Lithium and Cobalt

(Fixed Variable: Temp = 80^0C, HCl = 3M, S/L Ratio = 1.20 gm/ml, Stirring = 400 rpm and time = 60 min)

4.3.1.9. Optimum leaching conditions with hydrochloric acid

The optimum leaching conditions for the maximum recovery percentage of lithium and cobalt from the spent battery was taken to be:

Hydrochloric acid concentration = 3M
Solid –Liquid Ratio =1:20
Temperature = 80^0 C
Time = 60 min.
Stirring Speed = 400 rpm
Percentage of H_2O_2 = 3.5%

Maximum Lithium dissolution = 89.36%
Maximum Cobalt dissolution = 88.52%

4.3.2 Leaching kinetics

The rate controlling steps were determined from the effect of time and temperature on the dissolution of lithium and cobalt (Fig. 4.14 and Fig. 4.15). Three temperatures (40^0C, 60^0C and 80^0C) were considered for the kinetics analysis. After the selection of the appropriate kinetic model for lithium and cobalt dissolution, the activation energy was determined from lnK versus 1/T plot. The value of activation energy obtained again justified the appropriateness of the model which should conform to the data for activation energy in literature and previous studies.

Kinetic models

The particles were assumed to be perfectly homogeneous spherical solid phases and shrinking core model was selected to analyze the leaching solution. Three previously established models, i.e., liquid film diffusion controlled process, product layer diffusion controlled process and chemical reaction controlled process were considered for the initial selection of kinetics model to determine the mechanism of leaching for both lithium and cobalt. Each of these processes is discussed below.

1. Liquid film diffusion controlled

$$\frac{t}{\tau} = 1 - (1 - X)^{2/3} \quad \ldots\ldots\ldots\ldots\ldots\ldots\ldots\ldots\ldots\ldots \quad (1)$$

2. Diffusion controlled through the product layer

$$\frac{t}{\tau} = 1 - 3(1 - X)^{2/3} + 2(1 - X) \quad \ldots\ldots\ldots\ldots\ldots\ldots\ldots\ldots\ldots\ldots \quad (2)$$

3. Chemical reaction controlled

$$\frac{t}{\tau} = 1 - (1 - X)^{1/3} \quad \ldots\ldots\ldots\ldots\ldots\ldots\ldots\ldots\ldots\ldots \quad (3)$$

where, τ = Time for complete disappearance of particles

and X = Fraction of reacted particles

4.3.2.1. Liquid film diffusion controlled process

The time for different fraction of reacted particles of lithium and cobalt at 40^0C, 60^0C and 80^0C were calculated from Fig. 4.14 and Fig. 4.15. The data was then plotted according to the Eqn. 4.1 to verify if the reaction was a liquid film diffusion controlled process. The correlation coefficient values are also shown in the Fig. 4.17 and Fig. 4.18. It can be seen that the correlation is not high enough to suggest that liquid film diffusion controlled model was an appropriate model for leaching of lithium and cobalt in hydrochloric acid solution. At lower temperature, correlation coefficient values were much higher for both lithium and cobalt, but random coefficient values were observed at higher temperatures

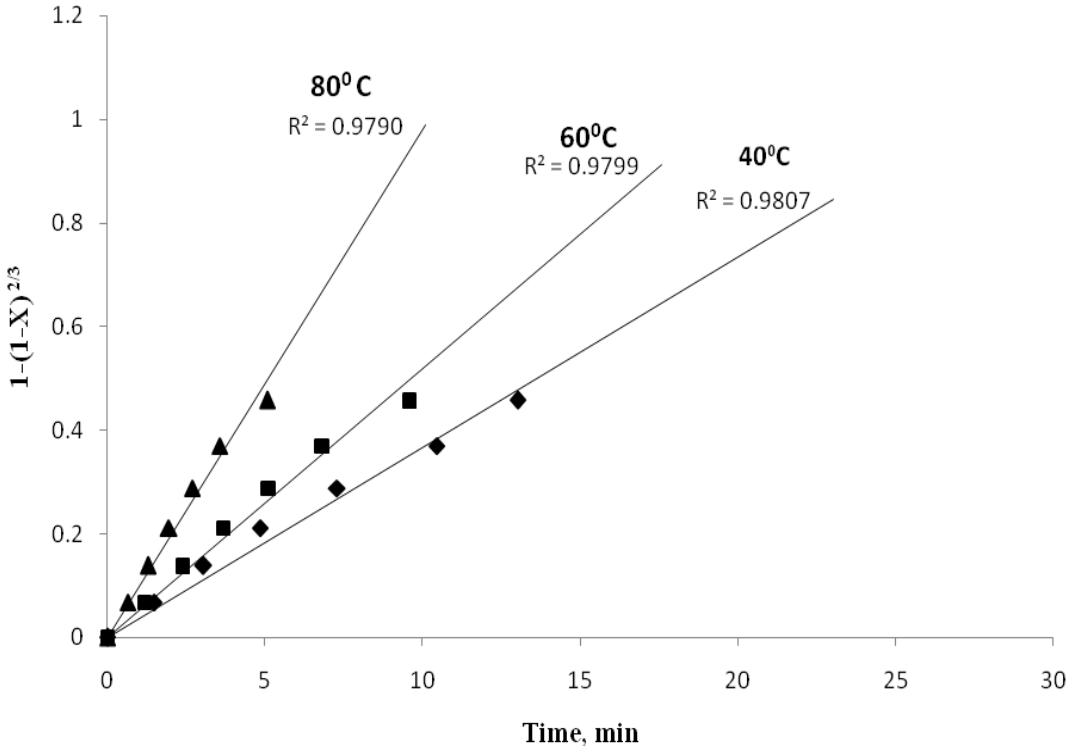

Fig. 4.17: Plot of $1 - (1 - X)^{2/3}$ versus time at various temperature for lithium

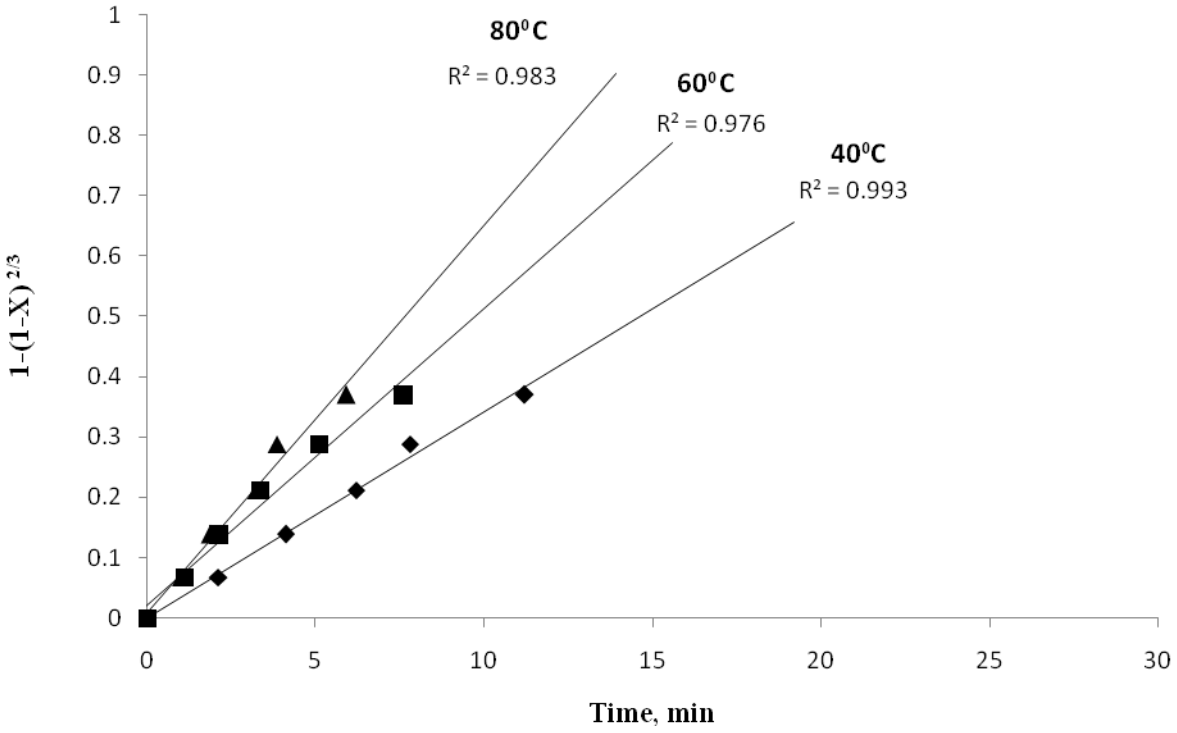

Fig. 4.18: Plot of $1-(1-X)^{2/3}$ versus time at various temperature for cobalt

4.3.2.2 Product layer diffusion controlled process

The right hand side of the Eqn. 4.2 was plotted against time to examine whether the leaching of lithium and cobalt were controlled by diffusion through the product layer (Fig. 4.19 and Fig. 4.20).

The correlation factor for the three temperature was very low and the curves also did not go thorough the zero point. This suggests that dissolution of lithium and cobalt is not product layer diffusion controlled process.

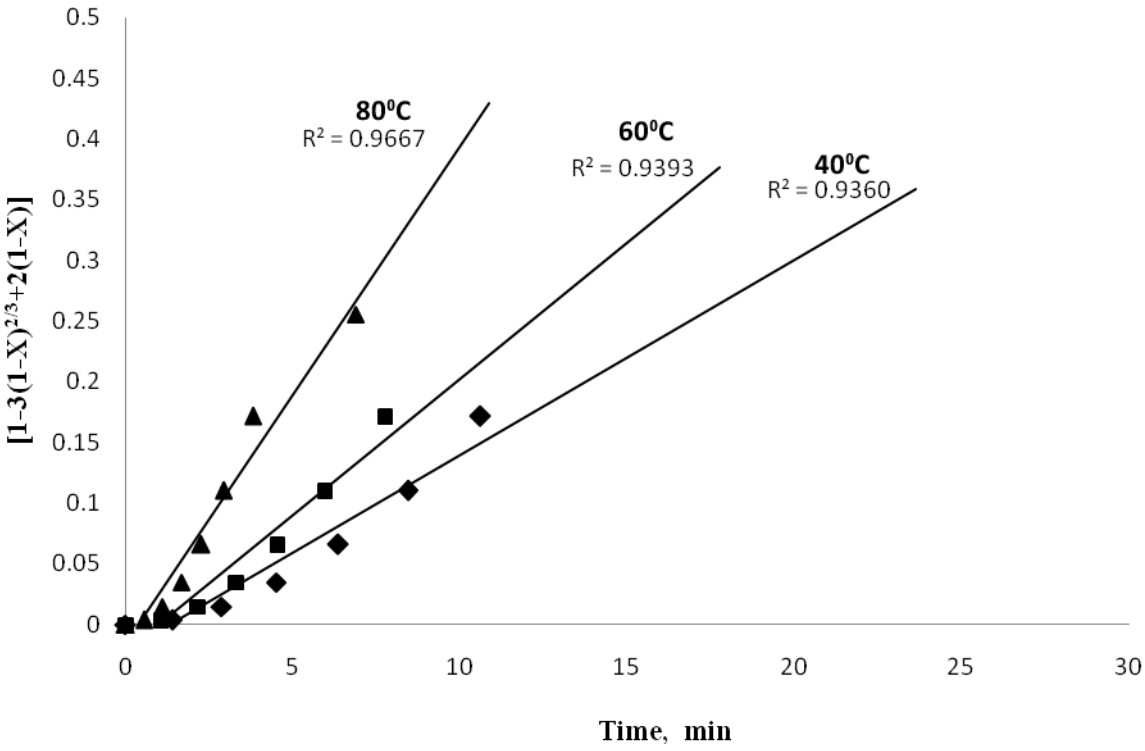

Fig. 4.19: Plot of $1 - 3(1 - X)^{2/3} + 2(1 - X)$ versus time at various temperature for lithium

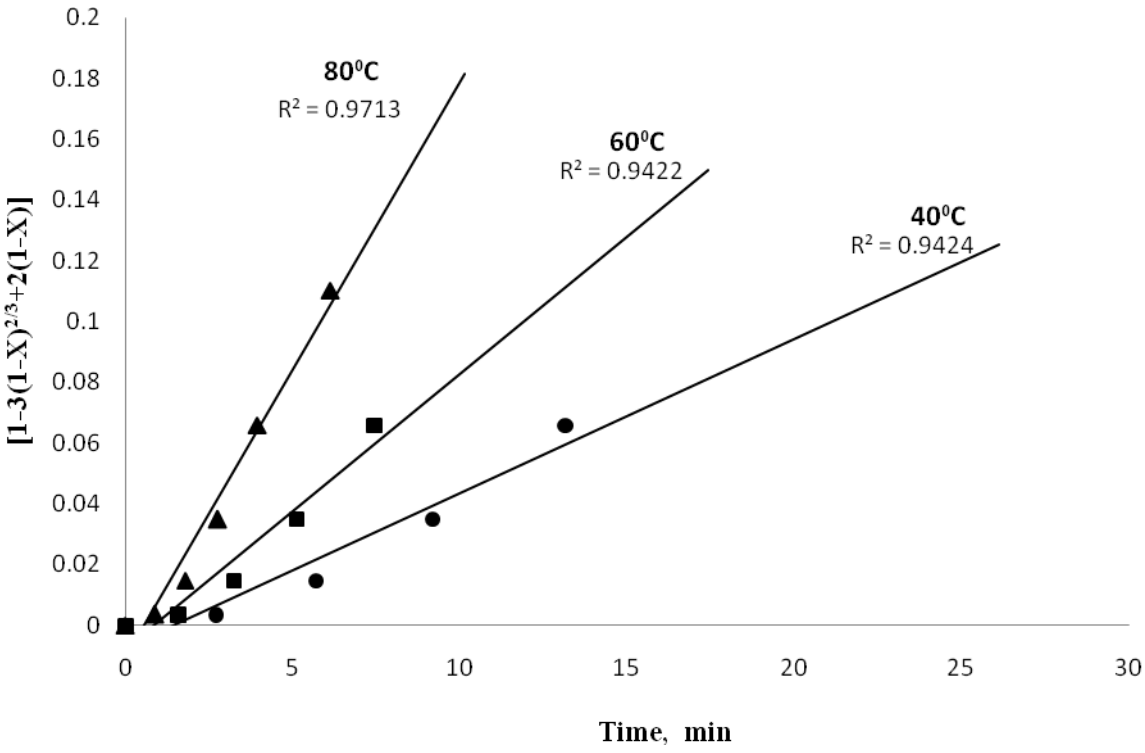

Fig. 4.20: Plot of $1 - 3(1 - X)^{2/3} + 2(1 - X)$ versus time at various temperature for cobalt

4.3.2.3. Chemical reaction controlled process

To examine if the reaction was a chemical reaction controlled process, the plot of [1 – (1 - X) $^{1/3}$] versus time is shown in Fig. 4.21 and Fig. 4.22 for lithium and cobalt respectively. The data yielded a very high correlation coefficient for all the temperatures for both lithium and cobalt. Also, the plotted lines at different temperatures passed through the zero point. The plot is therefore highly reliable for considering be the kinetic model for leaching of lithium and cobalt.

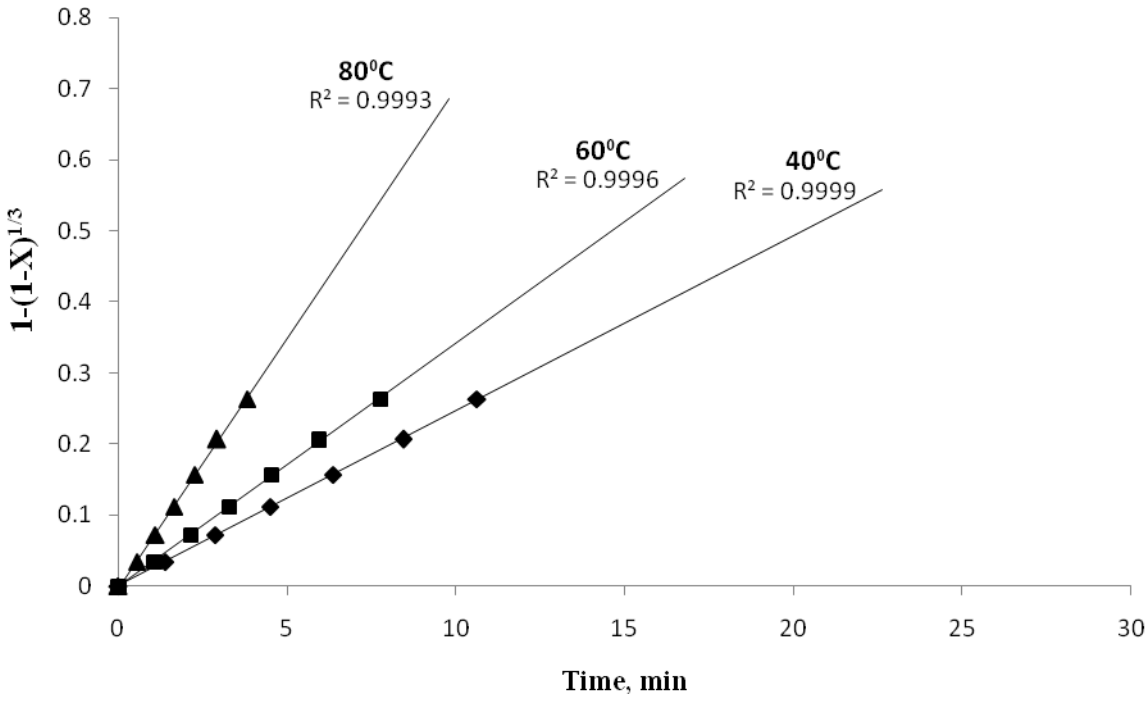

Fig. 4.21: Plot of $1-(1-X)^{1/3}$ versus time at various temperatures for lithium

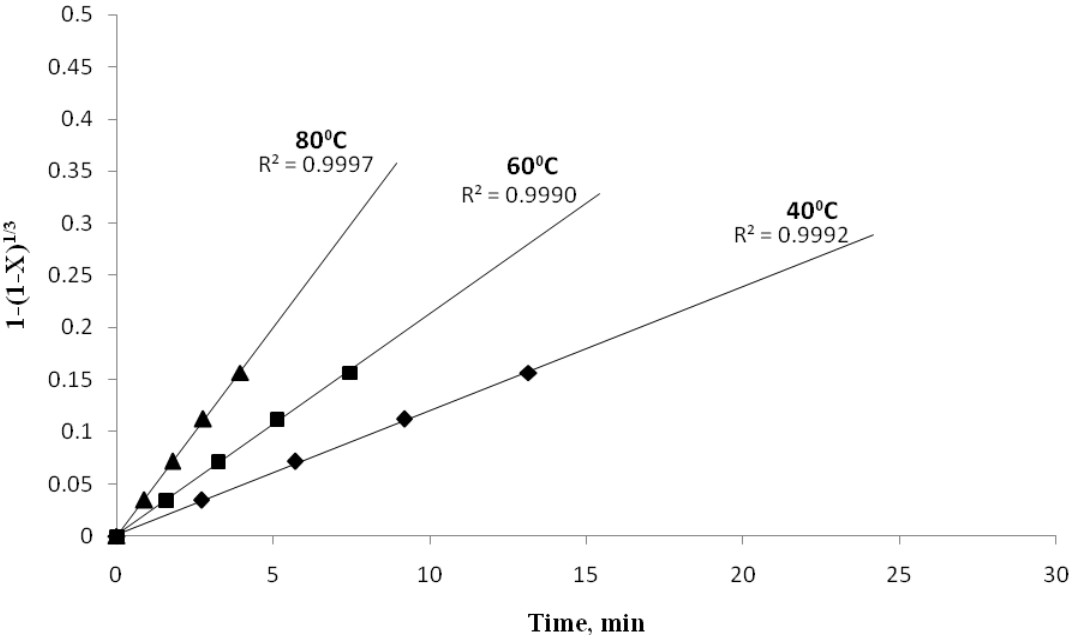

Fig. 4.22: Plot of $1-(1-X)^{1/3}$ versus time at various temperatures for cobalt

4.3.3. Activation energy determination

According to the integral approach reaction rate constants (k) of various temperatures were obtained from the slope of the linear plots from Fig. 4.21and Fig. 4.22 Then the values of reaction rate constants (K) were plotted according to the Arrhenius type equation [K = A exp (-E/RT)].

The plot of lnK vs. 1/T (K) was straight line. This is shown in Fig. 4.23 and Fig. 4.24.

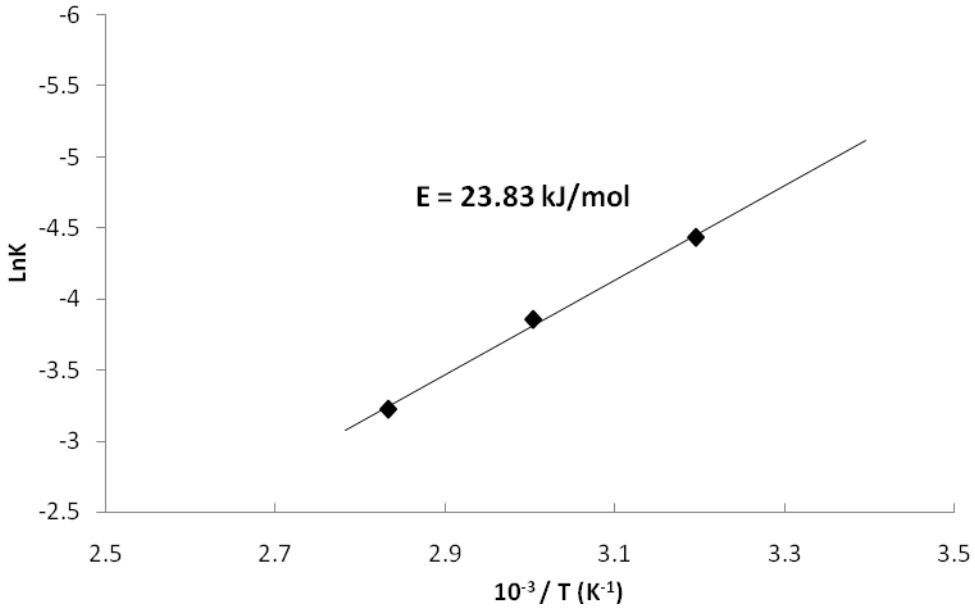

Fig. 4.23: Arrhenius type plot for lithium leaching kinetic data of Fig. 4.21

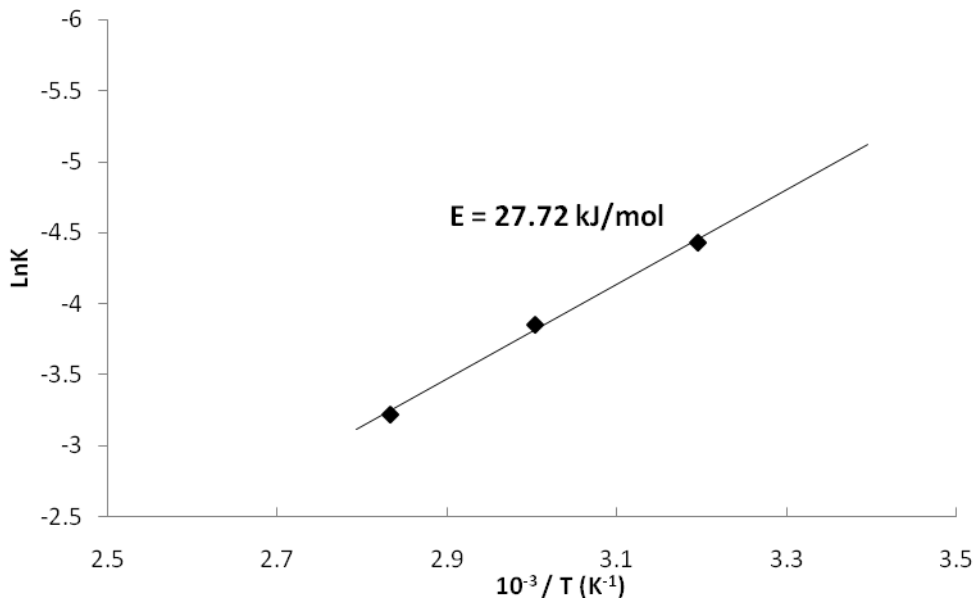

Fig. 4.24: Arrhenius type plot of kinetic data for cobalt leaching of Fig. 4.22

The apparent activation energy of the process is estimated from the Arrhenius type plot as

$$\text{Slope} = -E/R$$

The activation energy for lithium is therefore = **23.83 KJ/mol.**
And, the activation energy for cobalt is = **27.72 KJ/mol**

The typical activation energy for a diffusion controlled process is generally less than 40 KJ/mol and, the activation energy is generally more than 40 KJ/mol for a chemically controlled process [39]. As the activation energy for lithium is 23.83 KJ/mol and for cobalt is 27.71 KJ/mol, it seems that the it can be diffusion controlled process. However, activation energy alone does not precisely determine a fixed reaction kinetic model but only a lithium and cobalt guide to predict it [38]. From fig 4.21 and fig 4.22 it is highly reliable for considering be the chemically controlled process model for leaching of lithium and cobalt. Again from C.K. Lee and K.I Rhee it can be said that the dissolution of $LiCoO_2$ is controlling by surface chemical reaction [3]. Hence it can be ratiocinate that the chemically controlled process, as selected should be the appropriate method for lithium and cobalt leaching in hydrochloric acid.

4.4. Recovery of Value Metals from Leach Liquor

4.4.1. Recovery of Cobalt

Separation of lithium and cobalt from the leach liquor was effected by employing redox reaction. Direct addition of small additions of sodium hydroxide to the leach liquor gave no precipitate, because the leach liquor was excessively acidic. The pH of the solution had to be controlled by the addition of NaOH to effect precipitation of cobalt hydroxide. The extent of precipitation of cobalt hydroxide was found to increase with an increase in pH value (Fig. 4.25). Over 95 percentage of cobalt could be precipitated at a pH of about 12 leaving 93 percent of lithium in the leach liquor. The extent of recovery of lithium as indicated in this figure represents the percentage of lithium in the leach liquor after the separation of cobalt hydroxide. The figure indicates that the optimum value of pH for the precipitation of cobalt hydroxide could be taken to be 11-12. The $Co(OH)_2$ precipitate was separated by filtration.

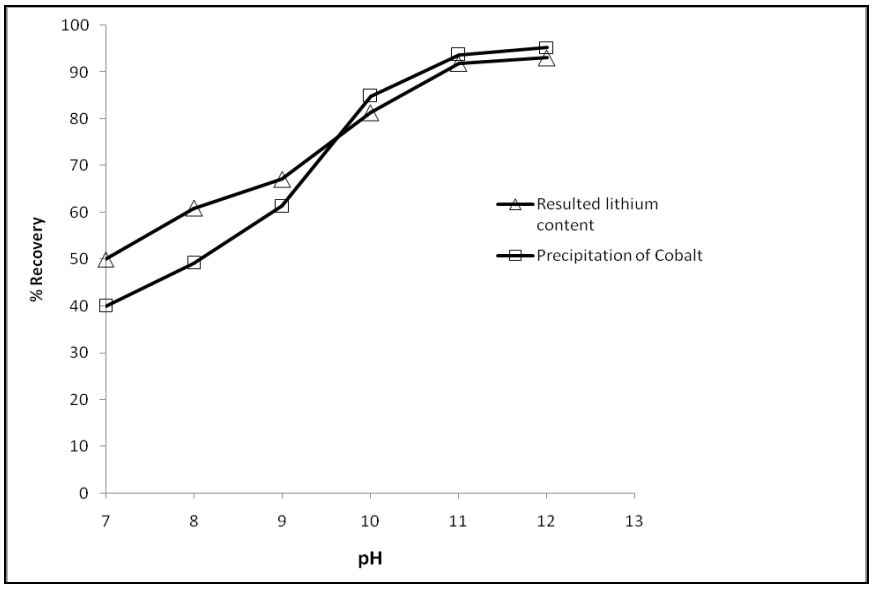

Fig. 4.25: Effect of pH on Precipitation of Cobalt and resulting Lithium content of Leach Liquor

4.4.2. Recovery of Lithium

After the separation of cobalt as cobalt hydroxide, the leach liquor was concentrated and treated with sodium carbonate solution to precipitate lithium as lithium carbonate. The precipitation process was performed at approximately 100°C. The lithium carbonate was separated by filtration and washed with hot water to remove the residual liquor.

4.4.3 Characterization of recovery products

The two recovery products were dried in oven to prepare for X-ray diffraction (XRD) analysis. The precipitation of lithium carbonate marked as "LC" and cobalt hydroxide was analyzed by X-ray diffraction (XRD) analysis which is shown below in Fig.4.26 and Fig.4.27 Some identical peak marked as "U" also found in analysis which might consider as impurities.

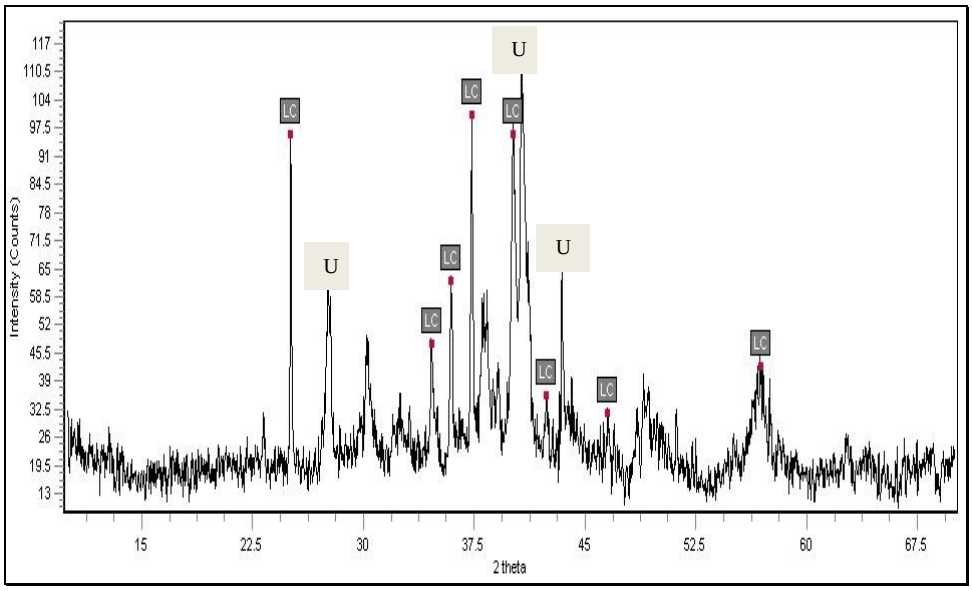

Fig. 4.26: X-ray diffraction analysis of recovery product (lithium carbonate) of Lithium ion Battery

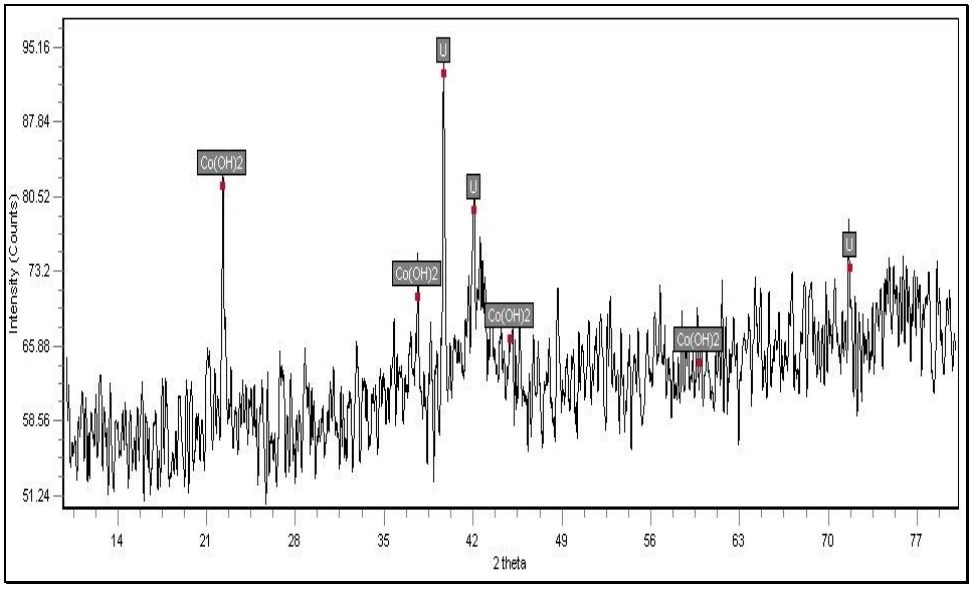

Fig. 4.27: X-ray diffraction analysis of recovery product (cobalt hydroxide) of Lithium ion Battery

4.4.4. Use of lithium carbonate and cobalt hydroxide

Li_2CO_3 is polymeric. It is an ionic compound. Lithium carbonate is soluble in water, and thus can be used either as a source of the lithium ion or the carbonate ion, but it is not that soluble, which is rare, given that lithium compounds typically have exceptional aqueous solubility. Lithium carbonate appears as a white powder in general.

Uses

Lithium carbonate is an important industrial chemical. It forms low-melting fluxes with silica and other materials. Glasses derived from lithium carbonate are useful in ovenware. Lithium carbonate is a common ingredient in both low-fire and high-fire ceramic glaze. Its alkaline properties are conducive to changing the state of metal oxide colorants in glaze particularly red iron oxide (Fe_2O_3). Cement sets more rapidly when prepared with lithium carbonate, and is useful for tile adhesives. When added to aluminum trifluoride, it forms LiF which gives a superior electrolyte for the processing of aluminum.[3] Lithium carbonate is used as an active material of carbon dioxide sensors.[4] It is also used in the manufacture of most lithium-ion battery cathodes, which are made of lithium cobalt oxid

Cobalt(II) hydroxide or **cobaltous hydroxide** is the chemical compound composed of cobalt and the ion with the formula $Co(OH)_2$. It occurs in two forms, either as a rose-red powder, which is the more stable of the two forms, or as bluish-green powder

Uses

It finds use as a drying agent for paints, varnishes and inks, in the preparation of other cobalt com pounds, as a catalyst and in the manufacture of battery electrodes.

Chapter 5

CONCLUSIONS

This work can be divided into several steps. (i) Characterization of spent lithium ion batteries. (ii) leaching of the cathode paste of the lithium ion batteries in sulfuric acid media without and in presence of hydrogen peroxide and in hydrochloric acid media and (iii) recovery of lithium and cobalt from the leach liquor. Also, the kinetics of leaching was investigated and the leaching parameters were optimized.

The characterization of spent lithium ion batteries yielded the following results:

- Pure aluminum and pure copper in the form of thin foils act as current collector in cathode and in anode respectively. Aluminum and copper constituted about 18.64 percent and 3.53 percent of the total weight of the battery.
- $LiCoO_2$ was found to be the prominent component of the active material of the cathode of lithium ion batteries, while graphite was the active material of the anode.
- Lithium and cobalt content was 23.82 percent of the total weight of the battery.

The leaching of the cathodic paste of spent lithium ion batteries yielded the following results:

- The optimum conditions for leaching of lithium and cobalt from the cathode active material of spent lithium ion battery was found to be hydrochloric acid concentration = 3M, solid-liquid ratio = 1: 20 (gm/ml), Temperature $=80^0$, time=60 minute, hydrogen peroxide = 3.5% and stirring speed = 400 rpm.
- A maximum of 89% $LiCoO_2$ could be leached at the optimised conditions.
- Over 95% cobalt could be precipitated from leach liquor at pH a value of 11-12, leaving 93 percent lithium in the leach liquor.

Kinetics of leaching of lithium and cobalt were studied. The experimental kinetic data were matched with those of standard models and the appropriate model for the reaction mechanism was identified.

The activation energy for the dissolution of the paste in HCl acid solution was determined. The following conclusions can be drawn from the kinetic study:

- Increasing temperature increased the rate of leaching of both lithium and cobalt up to $80^{o}C$.
- Chemical reaction controlled mechanism was found to be the rate controlling step for dissolution of both lithium and cobalt in leaching solution.
- Activation energy for dissolution of lithium and cobalt were found 23.83KJ/mol and 27.72 KJ/mol respectively, which validated the chemical reaction controlled process for lithium and cobalt.

Finally, the experiments on the recovery of metal values from the leaching solution yielded the following results:

1. Precipitation of cobalt and resultant lithium content of the solution increased rapidly with pH and a maximum precipitation of cobalt as cobalt hydroxide was obtained at a pH of 11. Over 95% cobalt could be precipitated at a pH of 12. Thus the optimum pH value for the precipitation of cobalt from the leach liquor could be taken to be 11-12.

2. A maximum of 93.07% of the lithium content of the leach liquor could be precipitated as lithium carbonate by treating the cobalt free leach liquor with a saturated solution of sodium carbonate.

5.1 Recommendation for Future Work

The primary aim of this work is to determine the optimum conditions for the extraction of metal values from spent lithium ion batteries. The academic interest of the work includes the study of the mechanism and kinetics of the various steps (leaching, chemical precipitation etc) involved in the process of recovery of metal values from spent lithium ion batteries

In future, research on the following aspects can be undertaken:

- The effect of reducing agents like oxalic acid, ascorbic acid, and other organic acid etc. on the extent of leaching may be investigated.
- Potentials of using mineral acids like hydrofluric acid, nitric acid etc. for the recovery of lithium and cobalt from the electrolyte paste may be investigated.
- Investigations on the suitability of using solvent extraction techniques for efficient and economic recovery of lithium and cobalt from the leach liquor using solvents like D2EHPA (di-2-ethyl-hexyl phosphoric acid), Cyanex – 272, PC-88A, etc. may be undertaken.
- A project can be undertaken to find out the potential of using the recovered lithium, cobalt and the aluminum component parts in a new type lithium ion battery manufacturing.
- A further study can be undertaken to investigate the feasibility of recycling the plastic component parts of the lithium ion battery.

REFERENCES

1. Dorella, G., M. B. Mansur “A study of the separation of cobalt from spent Li-ion battery residues”, Journal of Power Sources, 170, 210-215 (2007).
2. Xu, J., H.R. Thomas, R. W. Francis, K. R. Lum, J. Wang, B. Liang “ A review of processes and technologies for the recycling of lithium-ion secondary batteries” , Journal of Power Sources, 177, 512-527 (2008).
3. Lee, C.K., K.I. Rhee, “Reductive leaching of cathodic active materials from lithium ion battery wastes”, Hydrometallurgy, 68, 5 -10 (2003).
4. Shin, S.M., N. H. Kim, J. S. Sohn, D. H. Yang and Y. H. Kim, “Development of a metal recovery process from Li-ion battery wastes”, Hydrometallurgy, 79, 172-182, (2005).
5. Contestabile, M., S. Panoro and B. Scosati, “A labrotory scale of lithium ion battery recycling process” Journal of Power Sources, 92, 65-69 (2001).
6. Xia, Z., X. Xie, Y.Shi, Y. Lei, and F. Guo, “Recycling cobalt from spent lithium ion battery”, Front. Material Science China, 2, 281-285 (2008).
7. Wang, R.C.,, Y.C. Lin, and S. Wu, "A novel recovery process of metal values from the cathode active materials of the lithium-ion secondary batteries," Hydrometallurgy, 99, 194-201 (2009)
8. Linden, D., T.B. Reddy, “Handbook of batteries”, chapter eight, Mcgraw Hill Inc., 3rd edition, New York, 2002
9. Muchnick, D.J., D.M. Hurd, “Recycling of consumer dry cell batteries”, chapter four, Noyes data corp., New Jersy, 1993
10. Murphy, D.W., F. J. D. Salvo, J. N. Carides and J. V. Waszczak, ‘‘Topochemical reactions of rutile related structures with lithium,’’Materials Research Bulletin, 13(12), 1395-1402 (1978).
11. Whittingham, M.S. ‘‘Intercalation chemistry: an introduction,’ ’Intercalation Chem., 1-18 (1982).
12. Belharouak, I., Y.K. Sun, J. Liu, and K. Amine,‘‘Li($Ni_{1/3}Co_{1/3}Mn_{1/3}$)O_2 as a suitable cathode for high power applications,’’ Journal of Power Sources, 123(2), 247-252 (2003).
13. Padhi, A.K., K.S. Nanjundaswamy, C. Masquelier, S. Okada and J.B. Goodenough, ‘‘Effect of structure on the Fe^{3+}/Fe^{2+} redox couple in iron phosphates,’’ Journal of the Electrochemical Society, 144(5), 1609-1613 (1997).
14. Choi, S.H., J. Kim and Y.S. Yoon, ‘‘A TEM study of cycled nano-crystallin HT- $LiCoO_2$ cathodes for rechargeable lithium batteries,’’ Journal of Power Sources, 135(1-2), 286-290 (2004).

15. Fan, J. ‘‘Studies of 18650 cylindrical cells made with doped $LiNiO_2$ positive electrodes for military applications,’’ Journal of Power Sources, 138(1-2), 288-293 (2004).
16. Kang, S.H, K. Amine, ‘‘Synthesis and electrochemical properties of layer-structured$0.5Li(Ni_{0.5}Mn_{0.5})O_2$-$.5Li(Li_{1/3}Mn_{2/3})O_2$solid mixture,’’ Journal of Power Sources, 124(2), 533-537 (2003).
17. Takahashi, M., H. Ohtsuka, K. Akuto and Y. Sakurai, ‘‘Confirmation of long-term cyclability and high thermal stability of $LiFePO_4$ in prismatic lithium-ion cells,’’ Journal of the Electrochemical Society, 152(5), A899-A904 (2005).
18. Yoshio, M. and A. Kozawa, ‘‘Lithium-ion Secondary Battery - Materials and pplication,’’ Nikkan Kogyo Shinbunsya, 194, 185-189 (1996).
19. Zhang, P., T. Yokoyama, O. Itabashi, T.M. Suzuki and K. Inoue,‘‘Hydrometallurgical processfor recovery of metal values from spent lithium-ion secondary batteries,’’ Hydrometallurgy, 47(2-3),259-271 (1998).
20. Caballero, A., L. Hernan, J. Morales, E. Rodriguez Castellon and J.Santos, ‘‘Enhancing the electrochemical properties of LT-$LiCoO_2$ in lithium cells by doping with Mn,’’ Journal of Power Sources,128(2), 286-291 (2004).
21. Ceder, G., Y.M. Chiang, D.R. Sadoway, M.K. Aydinol, Y.I. Jang and B. Huang, ‘‘Identification of cathode materials for lithium batteries guided by first-principles calculations,’’ Nature (London), 392 (6677), 694-696 (1998).
22. Kobayashi, H., H. Shigemura, M. Tabuchi, H. Sakaebe, K. Ado, H.Kageyama, A. Hirano, R. Kanno, M. Wakita, S. Morimoto and S. Nasu,‘‘Electrochemical properties of hydrothermally obtained $LiCo_{1-x}Fe_xO_2$ as a positive electrode material for rechargeable lithium batteries,’’ Journal of the Electrochemical Society, 147(3), 960-969 (2000).
23. Wu, H.M., J.P. Tu, Y.F. Yuan, Y. Li, X. B. Zhao, G.S. Cao, ‘‘Structural, morphological and electrochemical characteristics ofspinel $LiMn_2O_4$ prepared by spray-drying method,’’ Scripta Materialia,52(6), 513-517 (2005).
24. Armstrong, A.R., Bruce and G. Peter, ‘‘Synthesis of layered $LiMnO_2$ as an electrode for rechargeable lithium batteries,’’ Nature (London),381(6582), 499-500 (1996).
25. Vitins, G. and K. West, ‘‘Lithium intercalation into layered $LiMnO_2$,’’ Journal of the Electrochemical Society, 144(8), 2587-2592 (1997).
26. Kubo, K., M. Fujiwara, S. Yamada, S. Arai and M. Kanda, ‘‘Synthesis and electrochemical properties for $LiNiO_2$ substituted by other elements,’’ Journal of Power Sources, 68(2), 553-557 (1997).
27. Song, S.W., G.V. Zhuang and P.N. Ross, ‘‘Surface Film Formation on $LiNi_{0.8}Co_{0.15}Al_{0.05}O_2$ Cathodes Using Attenuated Total Reflection IR Spectroscopy,’’ Journal of the Electrochemical Society, 151(8), A1162-A1167 (2004).

28. Capitaine, F., P. Gravereau and C. Delmas, ‘‘A new variety of $LiMnO_2$ with a layered structure,’’ Solid State Ionics, 89(3, 4), 197-202 (1996).
29. Tenorio, J.A.S., D.C. Oliveira and A.P. Chaves, ‘‘Carbon–zinc batteries treatment by ore processing methods, in: Proceedings of the Global Symposium on Recycling Waste Treatmentand Clean Technology,’’ REWAS 99 , 2, 1153-1160 (1999).
30. Lee, D. and M. Halmann, “Selective Separation of Nickel(II) by Dimethylglyoxime-Treated Polyurethane Foam, ‘Analytical Chemistry, 40, 214-217 (1976)
31. Castillo, S., F. Ansart, C. Laberty-Robert, J. Portal, ‘‘Advances in the recovering of spent lithium battery compounds,’’ Journal of Power Sources, 112(1), 247-254 (2002).
32. Saeki, S., J. Lee, Q. Zhang and F. Saito, ‘‘Co-grinding $LiCoO_2$ with PVC and water leaching of metal chlorides formed in ground product,’’ International Journal of Mineral Processing, 74(1), S373-S378 (2004).
33. Mantiano, D.P., G. Dorella, R.C.A. Elias and M.B. Mansur, ‘‘Analysis of a hydrometallurgical route to recover base metals from spent rechargeable batteries by liquid-liquid extraction with Cyanex 272,’’ Journal of Power Sources, 159(2), 1510-1518 (2006).
34. Cerruti, C., G.Curutchet and E. Donati, ‘‘Bio-dissolution of spent nickel-cadmium batteries using Thiobacillus ferrooxidans,’’
35. Moore, J.N. and S.N. Luoma, ‘‘Hazardous wastes from large-scale metal extraction. A case study, ‘Environmental Science and Technology, 24(9),1278-1284 (1990).
36. Mishra, D., D.J. Kim, D. Ralph, J.G. Ahn and Y.H. Rhee, ‘‘Bioleaching of metals of metals from spent lithium ion secondary batteries using Acidithiobacillus ferrooxidans,’’ Waste management, 28(2),332-338,(2008)
37. Nan, J.M., D. Han and X. Zuo, ‘‘Recovery of metal values from spent lithium-ion batteries with chemical deposition and solvent extraction,’’ Journal of Power Sources, 152, 278-284 (2005)
38. Levenspiel O., “Chemical reaction engineering”, 3rd edition, Chapter 25, John Wiley & Sons., New York, 1999.
39. Ray, Hem Shanker: Kinetics of Metallurgical Reactions, Oxford and IBH Publishing Co. Pvt. Ltd., 66 janapath, New Delhi, chap 1, 1993.